UNIVERSITAT POLITÈCNICA DE CATALUNYA

Programa de Doctorat:

AUTOMÀTICA, ROBÒTICA I VISIÓ

Tesi Doctoral

CONTRIBUTION TO RELIABLE CONTROL OF DYNAMIC SYSTEMS

Jean Carlo Salazar Cortes

Directors: Dr. Fatiha Nejjari Akhi-Elarab i Dr. Ramon Sarrate Estruch

Març 2018

Abstract

This thesis presents some contributions to the field of Health-Aware Control (HAC) of dynamic systems.

In the first part of this thesis, a review of the concepts and methodologies related to reliability versus degradation and fault tolerant control versus health-aware control is presented. Firstly, in an attempt to unify concepts, an overview of HAC, degradation, and reliability modeling including some of the most relevant theoretical and applied contributions is given.

Moreover, reliability modeling is formalized and exemplified using the structure function, Bayesian networks (BNs) and Dynamic Bayesian networks (DBNs) as modeling tools in reliability analysis. In addition, some Reliability Importance Measures (RIMs) are presented.

In particular, this thesis develops BNs models for overall system reliability analysis by using Bayesian inference techniques. Bayesian networks are powerful tools in system reliability assessment due to their flexibility in modeling the reliability structure of complex systems.

For the HAC scheme implementation, this thesis presents and discusses the integration of actuators health information by means of RIMs and degradation in Model Predictive Control (MPC) and Linear Quadratic Regulator algorithms.

In the proposed strategies, the cost function parameters are tuned using RIMs. The methodology is able to avoid the occurrence of catastrophic and incipient faults by monitoring the overall system reliability.

The proposed HAC strategies are applied to a Drinking Water Network (DWN) and a multirotor UAV system. Moreover, a third approach, which uses MPC and restricts the degradation of the system components is applied to a twin rotor system.

Finally, this thesis presents and discusses two reliability interpretations. These interpretations, namely *instantaneous* and *expected*, differ in the manner how reliability is evaluated and how its evolution along time is considered. This comparison is made within a HAC framework and studies the system reliability under both approaches.

Keywords: prognostics and health-management, health-aware control, reliability analysis, reliability importance measures, Bayesian networks, Dynamic Bayesian Networks, model predictive control, linear quadratic regulator, drinking water networks, octorotor

Resum

Aquesta tesi presenta algunes contribucions al camp del control basat en la salut dels components "Health-Aware Control"(HAC) de sistemes dinàmics.

A la primera part d'aquesta tesi, es presenta una revisió dels conceptes i meto-dologies relacionats amb la fiabilitat versus degradació, el control tolerant a fallades versus el HAC. En primer lloc, i per unificar els conceptes, s'introdueixen els conceptes de degradació i fiabilitat, models de fiabilitat i de HAC incloent algunes de les contribucions teòriques i aplicades més rellevants.

La tesi, a més, el modelatge de la fiabilitat es formalitza i exemplifica utilitzant la funció d'estructura del sistema, xarxes bayesianes (BN) i xarxes bayesianes dinàmiques (DBN) com a eines de modelat i anàlisi de la fiabilitat com també presenta algunes mesures d'importància de la fiabilitat (RIMs).

En particular, aquesta tesi desenvolupa models de BNs per a l'anàlisi de la fiabilitat del sistema a través de l'ús de tècniques d'inferència bayesiana. Les xarxes bayesianes són eines poderoses en l'avaluació de la fiabilitat del sistema gràcies a la seva flexibilitat en el modelat de la fiabilitat de sistemes complexos.

Per a la implementació de l'esquema de HAC, aquesta tesi presenta i discuteix la integració de la informació sobre la salut i degradació dels actuadors mitjançant les RIMs en algoritmes de control predictiu basat en models (MPC) i control lineal quadràtic (LQR).

En les estratègies proposades, els paràmetres de la funció de cost s'ajusten uti-litzant els RIMs. Aquestes tècniques de control fiable permetran millorar la disponibilitat i la seguretat dels sistemes evitant l'aparició de fallades a través de la incorporació d'aquesta informació de la salut dels components en l'algoritme de control.

Les estratègies de HAC proposades s'apliquen a una xarxa d'aigua potable (DWN) i a un sistema UAV multirrotor. A més, un tercer enfocament fent servir la degradació dels

actuadors com a restricció dins l'algoritme de control MPC s'aplica a un sistema aeri a dos graus de llibertat (TRMS).

Finalment, aquesta tesi també presenta i discuteix dues interpretacions de la fiabilitat. Aquestes interpretacions, nomenades *instantània* i *esperada*, difereixen en la forma en què s'avalua la fiabilitat i com es considera la seva evolució al llarg del temps. Aquesta comparació es realitza en el marc del control HAC i estudia la fiabilitat del sistema en tots dos enfocaments.

Resumen

Esta tesis presenta algunas contribuciones en el campo del control basado en la salud de los componentes "Health-Aware Control" (HAC) de sistemas dinámicos.

En la primera parte de esta tesis, se presenta una revisión de los conceptos y metodologías relacionados con la fiabilidad versus degradación, el control tolerante a fallos versus el HAC. En primer lugar, y para unificar los conceptos, se introducen los conceptos de degradación y fiabilidad, modelos de fiabilidad y de HAC incluyendo algunas de las contribuciones teóricas y aplicadas más relevantes.

La tesis, demás formaliza y ejemplifica el modelado de fiabilidad utilizando la función de estructura del sistema, redes bayesianas (BN) y redes bayesianas diná-micas (DBN) como herramientas de modelado y análisis de fiabilidad como también presenta algunas medidas de importancia de la fiabilidad (RIMs).

En particular, esta tesis desarrolla modelos de BNs para el análisis de la fiabilidad del sistema a través del uso de técnicas de inferencia bayesiana. Las redes bayesianas son herramientas poderosas en la evaluación de la fiabilidad del sistema gracias a su flexibilidad en el modelado de la fiabilidad de sistemas complejos.

Para la implementación del esquema de HAC, esta tesis presenta y discute la integración de la información sobre la salud y degradación de los actuadores mediante las RIMs en algoritmos de control predictivo basado en modelos (MPC) y del control cuadrático lineal (LQR).

En las estrategias propuestas, los parámetros de la función de coste se ajustan utilizando las RIMs. Estas técnicas de control fiable permitirán mejorar la disponibilidad y la seguridad de los sistemas evitando la aparición de fallos a través de la incorporación de la información de la salud de los componentes en el algoritmo de control.

Las estrategias de HAC propuestas se aplican a una red de agua potable (DWN) y a

un sistema UAV multirotor. Además, un tercer enfoque que usa la degradación de los actuadores como restricción en el algoritmo de control MPC se aplica a un sistema aéreo con dos grados de libertad (TRMS).

Finalmente, esta tesis también presenta y discute dos interpretaciones de la fiabilidad. Estas interpretaciones, llamadas *instantánea* y *esperada*, difieren en la forma en que se evalúa la fiabilidad y cómo se considera su evolución a lo largo del tiempo. Esta comparación se realiza en el marco del control HAC y estudia la fiabilidad del sistema en ambos enfoques.

Acknowledgements

This thesis was carried out at the Research Center for Supervision, Safety and Automatic Control (CS2AC) with the financial support of Ministerio de Economía y Competitividad from Spanish Government through the grant BES-2012-059571.

Firstly, I want to express my sincere gratitude to my supervisors, Prof. Fatiha Nejjari and Prof. Ramon Sarrate, I have learned a lot from them, and also I had an excellent environment for working, learning and communicating my ideas. I offer them my absolute thankfulness for their support and the confidence they have put on me, for their ideas, suggestions, and words of encouragement whenever I needed them.

I also want to thank Prof. Vicenç Puig and Prof. Joseba Quevedo for their support and for offering me the opportunity to carry out this thesis.

I would like to thank Prof. Louise Travé and Prof. Christophe Simon for the valuable time spent reading and reviewing this dissertation. I would also like to thank them, together with Prof. Teresa Escobet for accepting to be part of the thesis examination panel.

During the thesis, I have had the privilege of working at the Centre de Recherche en Automatique de Nancy, where I spent some months carrying out two research visits. My sincere thanks to Prof. Didier Theilliol and Prof. Philippe Weber for all the fruitful scientific discussions, their advice, and their constant good mood.

A Big Thanks to my family, who despite the distance, has given me their support and words of encouragement. A special thanks to my mother Julia, my wife Sofía for their continuous encouragement and care, and my sister Marisol for given me her support when I needed it the most.

I would also like to thank my fellows from CS2AC, who have contributed to making these years enjoyable. I especially estimate the break moments having a coffee or chocolate at the bar, the Xocomàtiques, and the excursions to the mountain. A special recognition to the administrative staff for their support, their professionalism helped me to make my development as a Ph.D. student much easier. Moltes gràcies!

Contents

List of Figures

List of Tables

List of acronyms and notation

Acronyms

AFTC	Active Fault-Tolerant Control
AFTM	Accelerated Failure Time Model
AHM	Additive Hazard model
ANN	Artificial Neural Network
CBM	Condition-Based Maintenance
cdf	Cumulative distribution function
CIF	Critical Importance Factor
CPT	Conditional Probability Table
DBN	Dynamic Bayesian Network
DFR	Decreasing-Failure-Rate
DIF	Diagnostic Importance Factor
DWN	Drinking Water Network
FDI	Fault Detection and Isolation
FEM	Finite Element Method
FFNN	Feedforward Neural Network
FTC	Fault-Tolerant Control
FV	Fussell-Vesely importance measure
HAC	Health-Aware Control
HMM	Hidden Markov Models
IFR	Increasing-Failure-Rate
ISE	Integrated Square Error
JCAR	Joint Cumulative Actuator Reliabilities index
LMI	Linear Matrix Inequalities
LP	Linear Programing
LRM	Logistic Regression Model

MC	Markov chain
MIF	Marginal Importance Factor
MPC	Model Predictive Control
MTBF	Mean Time Between Failures
MTTF	Mean Time To Failure
MTTR	Mean Time To Repair
NLMPC	Nonlinear Model Predictive Control
pdf	Probability density function
PFTC	Passive Fault-Tolerant Control
PHM	Prognostics and Health Management
PrHM	Proportional Hazard model
PIM	Proportional Intensity Model
QP	Quadratic Programing
RAW	Reliability Achievement Worth
RIM	Reliability Importance Measure
RAW	Reliability Reduction Worth
$R_{S\text{cum}}$	Cumulative system reliability for the instantaneous reliability interpretation
$R_{S\text{cum}}^{k_f}$	Cumulative system reliability for the expected reliability interpretation
RUL	Remaining Useful Life
SIM	Structural Importance Measure
SOM	Self-Organizing Map
SSI	Stress-Strength Interference model
SVM	Support Vector Machine
TRMS	Twin-Rotor MIMO System
UAV	Unmanned Aerial Vehicles
Ucum	Cumulative control effort
WPHM	Weibull Proportional Hazard Model

Notation

I_β	Identity matrix of size $\beta \times \beta$
$[\Lambda]_\beta$	Block column matrix composed by $\beta \times 1$ blocks of matrices Λ

$T_{\beta}^{\mathit{\Lambda}}$	Block lower triangular matrix composed by $\beta \times \beta$ blocks of matrices $\mathit{\Lambda}$
β	Shaper parameter (Weibull and Gamma distribution)
h_0	Baseline failure rate
B_{mr}	Viscous friction coefficient of the main propeller
$\underline{u}_i$	Lower bound of the control input for the i actuator
$\overline{u}_i$	Upper bound of the control input for the i actuator
B_{tr}	Viscous friction coefficient of the tail propeller
Dn	Component/system state is down or failed
ε	Weighting parameter of cost function objectives
η	Scale parameter (Weibull distributions)
k_{fvn}	Aerodynamic force coefficient of the main rotor for negative ω_v
Γ	Complete Gamma function $\Gamma(\beta) = (\beta - 1)!$ (Gamma distribution)
γ	Column vector of regression coefficients
H_c	Control horizon
H_p	Prediction horizon
$[\Lambda]_{\beta}^{T}$	Block row matrix composed by $1 \times \beta$ blocks of matrices Λ
$\boldsymbol{\alpha}$	Diagonal weighting matrix of elements α_i
$\boldsymbol{\delta}$	Diagonal weighting matrix of elements δ_i
$\boldsymbol{\rho}$	Diagonal weighting matrix of elements ρ_i
$\tilde{\boldsymbol{\alpha}}$	Diagonal weight matrix of elements $\boldsymbol{\alpha}$
$\tilde{\boldsymbol{\delta}}$	Diagonal weight matrix of elements $\boldsymbol{\delta}$
$\tilde{\boldsymbol{\rho}}$	Diagonal weight matrix of elements $\boldsymbol{\rho}$
Y_{ref}	Output set point
I_B	Variable representing the Birnbaum measure
I_{β}	Identity matrix of size $\beta \times \beta$
T_{β}^{Λ}	Block lower triangular matrix composed by $\beta \times \beta$ blocks of matrices Λ
I_{CIF}	Variable representing Critical Importance Factor
I_{DIF}	Variable representing Diagnostic Importance Factor
I_{DIF}^{c}	Variable representing DIF using minimal cut sets
I_{DIF}^{p}	Variable representing DIF using minimal path sets
I_{RAW}	Variable representing Reliability Achievement Worth
I_{RRW}	Variable representing Reliability Reduction Worth

J_{mr}	Moment of inertia main DC motor
J_{tr}	Moment of inertia in tail motor
k_1	Input constant of the tail motor
k_2	Input constant of the main motor
$k_{ah/v}\varphi_{h/v}$	Physical constant
k_{chn}	Cable force coefficient for negative θ_h
k_{chp}	Cable force coefficient for positive θ_v
k_{fhn}	Aerodynamic force coefficient of the tail rotor for negative ω_h
k_{fhp}	Aerodynamic force coefficient of the tail rotor for positive ω_h
k_{fvp}	Aerodynamic force coefficient of the main rotor for positive ω_v
k_g	Gyroscopic constant
k_m	Positive constant
k_{oh}	Horizontal friction coefficient of the beam subsystem
k_{ov}	Vertical friction coefficient of the beam subsystem
k_t	Positive constant
k_{th}	Drag friction coefficient of the tail propeller
k_{tv}	Drag friction coefficient
λ_i	Failure rate of the ith component
$L_{ah/av}$	Armature inductance of tail / main motor
λ	Exponential and Gamma distribution parameter, failure rate and inverse scale respectively
$[\Lambda]_\beta$	Block column matrix composed by $\beta \times 1$ blocks of matrices Λ
$[\Lambda]_{\alpha\times\beta}$	Block matrix composed by $\alpha \times \beta$ blocks of matrices Λ
l_b	Length of counter-weight beam
l_{cb}	Distance between the counterweight and the joint
l_m	Length of main part of the beam
l_t	Length of tail part of the beam
$(\cdot)^{-1}$	Inverse of matrix
$(\cdot)^T$	Transpose of matrix
m_b	Mass of the counter-weight beam
m_{cb}	Mass of the counter-weight
C_k	kth minimal cut set

T_M	Mission time
m_m	Mass of main part of the beam
m_{ms}	Mass of the main shield
P_s	sth minimal path set
m_{mr}	Mass of the main DC motor
m_t	Mass of the tail part of the beam
m_{ts}	Mass of the tail shield
μ	Location parameter (Lognormal distribution)
Ω_h	Angular velocity of the TRMS around the vertical axis
ω_h	Rotational velocity of the tail rotor
Ω_v	Angular velocity of the TRMS around the horizontal axis
ω_v	Rotational velocity of the main rotor
Φ	*cdf* for the standard normal distribution (Lognormal distribution)
p_i	Probability of being up
q_i	Probability of being down
Pr(A)	Probability of event A
$\psi(\cdot)$	Covariate function
$R_{ah/av}$	Armature resistance of tail / main motor
R_i	Reliability of the ith component
r_{ms}	Radius of the main shield
θ_h	Revolutions per minute
$R_s(T_M)$	System reliability at the end of the mission
R_s	Reliability of the system
r_{ts}	Radius of the tail shield
T_s	Sampling time
σ	Scale parameter (Lognormal distribution)
$\Phi(\cdot)$	Structure function
S	Random variable representing the state of the system
T	Lifetime of a device
θ_v^0	Equilibrium pitch angle corresponding to $u_v = 0.2753V$
θ_h	Yaw angle of the beam
θ_v	Pitch angle of the beam

t	Time
m_{tr}	Mass of the tail DC motor
u_h	Input voltage of the tail motor
Up	Component/system state is up or functioning
u_v	Input voltage of the main motor
$\boldsymbol{z}$	Row vector of covariates
$Z(t)$	Degradation process
Z_{th}	Degradation failure threshold

Chapter 1

Introduction

1.1 Background and motivation

1.1.1 Degradation vs. Reliability

The degradation of physical components in engineering systems is generally inevitable, in view of factors such as wear due to usage, aging of the materials and hostile environmental conditions. In particular, the degradation of actuators in a closed-loop control system can lead to poor performance and sometimes to a loss of controllability when the level of degradation increases and the actuator reduces its capabilities such as speed response, force, pressure, strength, etc; or becomes prone to faults when its degradation level reaches or goes beyond a certain safe level, known also as failure threshold or critical value [185].

There exist two types of degradation: natural and forced degradation. On the one hand, natural degradation is an age- or time-dependent internal process where components gradually degrade, leading to their failure or breakdown. On the other hand, the forced degradation is artificially induced by an external agent, where component loading gradually increases in response to an increased demand [16, p. 32, 37, 52]. Such degradation can be characterized into three categories: binary, degradation with a finite number of levels, and degradation with an infinite number of levels [105].

The health of system components is of primordial importance for the safety and reliability of the controlled system. Reliability prediction based on degradation modeling can be an efficient method to estimate the health for some highly reliable components or systems where observations of failures are uncommon. Thus, to avoid failures it is important to enhance system safety by taking into consideration the degradation of components health in the controller design [73, 124].

As fault and failure concepts are used in different fields such as reliability, safety, and fault-tolerant systems, in different technological areas, their terminological use is not uniform. In this thesis, the definition given by [60] is used.

Definition 1.1. Fault: A fault is an impermissible deviation of at least one characteristic property (feature) of the system from the acceptable, usual, standard condition.

Definition 1.2. Failure: A failure is a permanent interruption of a system ability to perform a required function under specified operating conditions.

Recently, the interest of the research on performance degradation in control system design has increased [22, 41, 126, 189]. If the design objective is still to maintain the original system performance, this may force the remaining components to work beyond their normal service level to compensate for the handicaps caused by the degraded ones. Therefore, the trade-off between achievable performance and available actuator capability and their importance for the reliability of the system should be carefully considered in all control designs [146].

System components can experience physical degradation during their operation, and the severity of such degradation is related to the total operating life of the component. In this context, it may be interesting to design controllers that can exploit the available knowledge of the degradation dynamics to maintain adequate performance and extend the useful life of the components.

Some assumptions are usually taken into account in order to model the degradation of a component. For instance, in [56, 74, 75, 143–146] it is assumed that the degradation is proportional to the control effort of actuators and it modifies the failure rate of each actuator. More accurate assumptions can also be taken, for instance in [139, 141] the degradation is assumed to be dependent not only on the load but also on the time and environmental conditions. Constraints could be imposed to ensure that the cumulative degradation will be acceptable at the end of the maintenance horizon [124].

Higher levels of availability and reliability are important objectives for the design of most modern engineering systems and recently, a growing interest to model the reliability of complex industrial systems by means of Bayesian Networks (BN) has appeared [174] and some works on BN and system safety have been developed [178, 180, 181].

This can be performed by redistributing the control effort among the available components or actuators to alleviate the work load and the stress factors on the equipment with worst conditions to avoid their break down. For this purpose, an appropriate policy should be developed to redistribute this effort until maintenance actions can be taken. Such policy could be defined in terms of remaining useful life, reliability, degradation, structure importance, aging, among others [10, 74].

The application of BNs to reliability started at the end of 90's. In [163] the authors present the advantages of BNs in comparison with Reliability Block Diagrams (RBD). In [15] the authors propose to model a fault tree using a BN.

Reliability is the ability of a system to operate successfully long enough to complete its assigned mission under stated conditions. It can be modeled as an exponential function [43, 182], a Weibull function [9, 67] or a Gamma function [84, 95, 112], among others.

Reliability can also be expressed as a stochastic process [117]. For example, it is common to use Markov Chains (MC) to model the reliability of components [118]. Unfortunately, in practice the complexity of the system leads to a combinatorial explosion of states resulting in a MC with a very large size. The reliability information obtained with the MC is propagated to the system using a Dynamic Bayesian Network (DBN) which includes temporal information to calculate the impact of the component reliability on the system reliability [10].

The research in this field was mainly focused on improving the maintenance methodologies. However, the growing importance of maintenance has generated an increasing interest in the development and implementation of optimal maintenance strategies for improving system reliability, preventing the occurrence of system failures, and reducing maintenance costs of deteriorated systems [171].

The maintenance has been done traditionally based on one of two conceptions; preventive maintenance or corrective maintenance. Preventative maintenance performs regularly scheduled maintenance actions to maintain system in good conditions and avoid failures during service. Corrective maintenance leaves the system in operation until it fails and then takes restorative maintenance actions. In contrast, both of them have drawbacks. On one hand, preventive maintenance is expensive and the life cycle of system and components is not maximized. On the other hand, the corrective maintenance maximizes the life cycle of components but it has risks of damage to other components when failures occur. Whichever of the approach that is taken, unanticipated failures result in downtime of the system, and therefore there will always be a reactive maintenance needed.

As a result, the system downtime will be as long as the necessary spare parts and personnel be available and the time necessary to carry out the maintenance task. Condition-Based Maintenance (CBM) has appeared as a new maintenance methodology which involves the real-time analysis of system condition or system health state and based on this information the maintenance tasks are performed.

By contrast to preventive and corrective maintenance approaches, CBM has the potential for minimizing system failures incidents, reducing scheduled maintenance tasks, maximization of the life cycle of components, and increment of system availability. The technical capabilities to infer system and components condition in real-time from measurements of the process are critical to the success of a CBM implementation.

The use of new technologies in the production systems allows to improve products quality, reduce costs and increase productivity. However, new technologies usually involve a high level of complexity and this complexity may result in more failure-prone systems. Fault-tolerant control (FTC) has emerged as a response to this problem [23]. Therefore, it is also possible to implement fault tolerant control (FTC) techniques whose objective is to allow system functioning in spite of having faulty components such as actuators or sensors [190]. Nevertheless, it would be interesting not to wait until a failure occurs but to anticipate and prevent them from happening, especially to avoid incipient faults which are difficult to detect. The detection of incipient faults is an open field of research due to the fact that some detection methods such as observers or parity equations tend to track the system even when there is a fault [39]. To achieve such an objective a Prognostics and Health Management (PHM) strategy is commonly used.

The problematic of fault tolerant in systems has been widely treated by several authors. Now days it is possible to talk about Fault Detection and Isolation (FDI) as a field of research addressed to the problem of detection and localization of faults. In FTC and FDI research, works such as [13, 23, 44, 60–62] are obligatory reference due to the progress they have made.

In recent years, HAC has been emerging as a new technique to handle this problem. It consists in taking predictive actions to prevent a failure occurrence, instead of FTC that takes actions after fault occurrence.

Hence, this problem can be addressed taking into account the system to improve the system safety. HAC can extend the life time of the entire system or components and avoid failures until the next maintenance task.

1.1.2 Prognostics and Health Management

Prognostics and Health-Management (PHM) involves the application of three concepts: diagnostics, prognostics and health management. The first one identifies the state of the system during its functioning, providing an accurate fault detection and isolation capability with low false alarm rate [122].

PHM provides system health information based on the evaluation of its reliability and/or its remaining useful life (RUL) which allows to make prediction of the advent of future failures or faults. In other words, PHM is a methodology which aims at the monitoring of the system health which can be evaluated by the system reliability or the system RUL. Moreover, PHM strategies also allow the reduction of the inspection and maintenance efforts due to its continuous monitoring nature [40].

Figure 1.1 shows a generic architecture for PHM. It is based on three steps or stages, observation, analysis, and decision-making [36, 122]. The observation step consists in data acquisition, processing, collection or storage. The analysis step processes the acquired data and extracts of them the diagnostics, and prognostics information. In this step, the monitoring of the system is performed based on the data acquired in the previous step. Next, the appropriate decisions about logistics actions, maintenance, mission or control reconfiguration are taken based on the information provided by the previous data analysis.

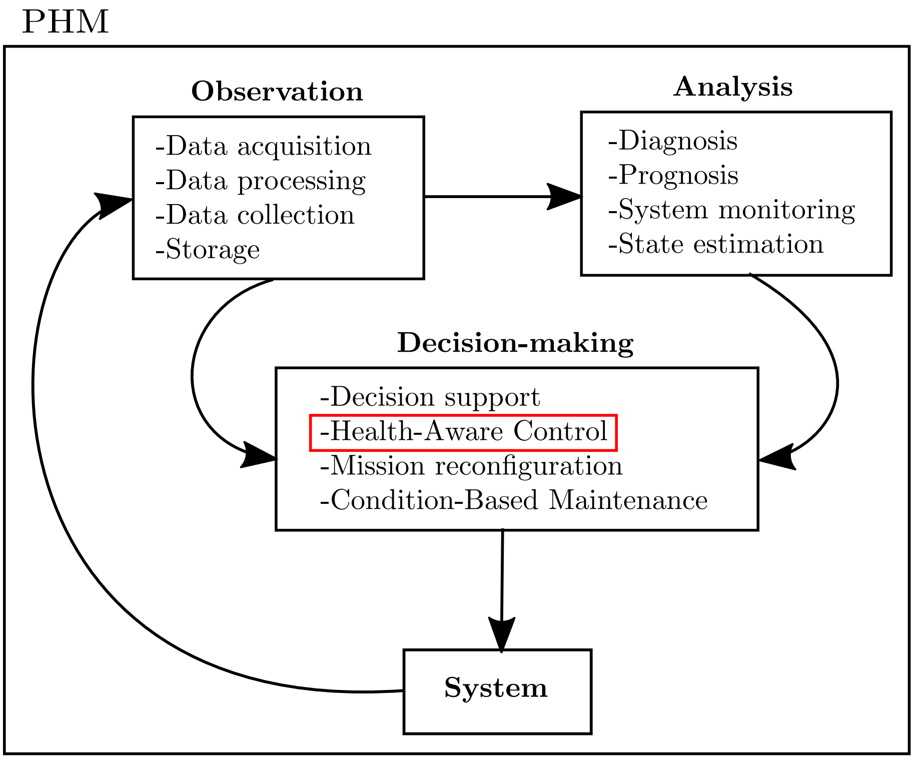

FIGURE 1.1: PHM architecture.

In the analysis step various methods and algorithms are used in order to estimate the remaining useful life of the asset. This process constitutes the diagnosis and prognostics. In literature, there is a certain consensus about the classification of these methodologies, for instance, in [4] they are classified into four categories, such as physical based, data-driven, hybrid and experimental based.

The next step is the decision-making, where the proper actions are taken based on the state of the asset or system. Among the decision that could be taken are the mission reconfiguration, perform or schedule a CBM or reconfigure the control inputs. To reconfigure the system control inputs, a Health-Aware Control (HAC) methodologies should be implemented. An HAC is a control methodology that based on the diagnosis and prognostics information is able to reconfigure the control efforts in order to extend the life cycle of the system and maintain a minimum level of control performance.

The concept and framework of PHM have been developed based mainly on maintenance methodologies [40]. Basically, PHM tries to give a solution to two problems. On one hand, it determines the time period to perform the maintenance tasks which produces the less impact to the system operation integrity. And, on the other hand, it estimates the RUL of the system and based on this information the decision-making module takes the appropriate action, which could be, for example, to continue operating or perform an immediate shut-down for maintenance.

The first gives an estimation if it is possible to reduce the maintenance needed by optimizing the maintenance intervals, and at the same time, it aims at avoiding unplanned maintenance shut-downs and their associated costs as well as improving safety and reducing environmental impacts.

The second one estimates how changes in operational variables such as speed, load, stress, can be applied in the next maintenance operation as well as the information about if the system has a high probability of safe operation for the intended mission.

This thesis will study how the information about system health can be used by the control algorithm in order to extend the useful life of the system, leading to the proposed HAC methodology (red rectangle in Figure 1.1). This technique uses proper online prognostics information of the system to modify the control actions or to change the mission objective in order to maintain a high level of system health. An HAC prevents the occurrence of incipient faults control loop.

Health-Aware Control (HAC) uses the information proportioned by the observation or analysis steps to perform the proper actions in order to main the system under control and mitigate the decrease of system health. HAC is part of the PHM structure conforming the Decision-making step and combines the control theory and prognostics. In this thesis, the prognostics if based on the reliability assessment of the system.

The HAC objective is achieved by modifying the controller in such a way that the system health is part of the control objectives. Therefore, the control actions will be computed to fulfill the control objectives and also to mitigate the degradation of the system, which extends its useful life compared to schemes without HAC methodologies and facilitates the implementation of CBM strategies.

To mitigate the system reliability degradation, minimize operational costs and prevent failures occurrence, actuator health monitoring should be considered. In some cases the control effort can be redistributed among the available actuators to alleviate the work load and the stress factors on equipments with worst conditions avoiding in this manner their breakdown.

1.2 Thesis Objectives

The main objective of this thesis is to study and develop a methodology for the design of a Health-Aware Control strategy that takes into account the system and actuators reliabilities degradation in order to extend its useful life cycle.

Therefore, this thesis aims at going further in the research of making dynamic systems to safer and more reliable. The proposed HAC methodology should provide major benefits such as reducing maintenance costs, avoiding incipient and catastrophic failures and increasing equipment uptime.

This thesis proposes a methodology to perform the system health evaluation, computation, and characterization and develop a methodology which allows the integration of those health techniques in the control algorithms design.

The specific objectives involved in this thesis can be summarized as following:

1. To study the degradation and the reliability models for dynamic systems:

   In this case a study of state of the art in degradation and reliability models used for dynamical systems is developed.

2. To investigate and study the relation between control actions and degradation of system actuators:

   The purpose here is to identify the relationship between the control action and the degradation of the actuators system).

3. To develop and design a health-aware control strategy that takes into account the health information of the system and its components:

   Design a HAC scheme that achieves some given performance specifications taking into account the degradation/reliability information of the system and/or actuators.

4. To study the performance of designed the control strategy:

The objective is to study the impact of including degradation and reliability of the system in the controller algorithm in terms of tracking error, efficiency, among others.

5. Applications of the proposed Health-Aware Control methodology on different dynamic systems:

   For the purpose of testing and validating the proposed methods and algorithms, different case studies have been used: unmanned aerial vehicle, water distribution network systems and twin rotor system. It is expected then, to illustrate with these applications the objectives outlined before.

1.3 Case studies

As stayed by objective 5, the purpose of these applications is to illustrate the contributions of this thesis. They will be used to study different approaches for control, degradation and reliability modeling and assessment, and to compare results. In the following, the systems are outlined and the expected results are stated.

The proposed HAC strategy will be implemented in a Drinking Water Network (DWN) system, an octorotor system and a Twin Rotor MIMO system. The proposed approach will integrate information about actuators health into the control design contributing to a controller which achieves the control objective with a high overall system reliability. The objective is to deal, from an availability point of view, with a closed-loop system combining a deterministic part related to the system dynamics and a stochastic part related to the actuator and system reliability. The main contribution of this application is the integration of the reliability assessment computed online using a DBN in the Model Predictive Control (MPC) algorithm. The resulting scheme will provide control performance while preserving system reliability.

These applications are justified by the fact that having a system in a good condition is a must to avoid failure impacts or economic waste. For instance in the multirotor field, a system which is able to operate in a safe way, i.e. avoiding unanticipated failures, can prevent injuries and damage to operators and people in its surrounding and also to the environment. Regarding a DWN, it is critical to have a healthy system an interruption of its operation can leads to economic losses and consumer complaints.

Therefore, there are two important objectives, one is related to the reduction of economic costs and the other is the safety of the system for the people, the environment and the system itself.

In the UAV application, the aim is to modify the control inputs or change the mission objective, using system reliability information that will be provided by a proper on-line prognostic tool. It is expected to have an increment of the operation time of the system [136, 144].

Unmanned aerial vehicles (UAVs) are well-suited to a wide range of mission scenarios, such as search, rescue, vigilance, and inspection, among others. However, the overall mission performance can be strongly influenced by vehicle sensors and actuators failures or degradations. Moreover, for this kind of systems, it could be more appropriate to avoid the fault occurrence than tolerate them.

The emergence of complex and autonomous systems, such as automated industrial processes, modern aircraft, unmanned aerial vehicles, among others, is driving the development and implementation of new control technologies that are aimed to accommodate incipient failures and maintain a stable system operation for the duration of the emergency. The primary motivation for this application has emerged over the need for improved reliability and performance for safety critical systems, particularly in aerospace-related applications.

An over-actuated system can be defined as a system which has more control inputs than regulated outputs. These systems are interesting in many control applications, especially where multiple actuators performing the same action are desirable for safety reasons, fault-tolerant policies or energy consumption optimization. Moreover, the presence of multiple inputs introduces a certain degree of redundancy, meaning that there exist an entire family of input functions and possibly of state trajectories that are compatible with a prescribed reference for the output [28, 186]. By contrast, an under-actuated system is defined as a system whose number of control inputs is lower than the number of controlled outputs [42, p. 18].

In particular, multirotors UAVs are under-actuated systems, but they present redundancy in the actuators and have the potential to improve safety and reliability. Several control techniques have been applied to multirotors, such as Model Predictive Control (MPC) [2, 94, 129], PID [131] and LQR [3, 100]. Some control techniques have been used to design HAC strategies, i.e. with MPC [143] or control allocation [72].

Another application including actuator degradation information to illustrate the proposed HAC approach has been performed on a Twin Rotor MIMO system. The approach consists in considering not only the degradation constraints but also the control input weighting factors, in the MPC cost function, as a tool to design a reliable control.

1.4 Thesis outline

The thesis is organized into two parts:

Part I presents a review of the fundamental concepts on which this thesis is based, resulting in a literature review of degradation modeling, reliability modeling and control techniques. It is made up of four chapters:

- **Chapter 2** presents a literature review on PHM and HAC approaches.
- **Chapter 3** is dedicated to degradation and reliability modeling approaches that exists in the literature.
- **Chapter 4** presents the reliability assessment methods including: Markov chains, the structure function, Bayesian and, dynamic Bayesian networks. The component and system reliability modeling is illustrated through a DWN example.
- **Chapter 5** recalls the background theory about Model Predictive Control and Linear-Quadratic Regulator.

Part II presents the results that constitute a contribution to the state of the art on Health Aware Control (HAC). It is made up of two chapters:

- **Chapter 6** presents the integration of the system health information into the HAC approach proposed in this thesis.
- **Chapter 7** presents a study about two reliability interpretation approaches: the instantaneous reliability and the expected reliability.

Finally, the thesis is concluded by:

- **Chapter 8** which summarizes the main conclusions and briefly suggests some possible lines for future research arising from this work.

1.5 List of publications

The publications resulting of this thesis are listed below:

- Journals

  J. C. Salazar, P. Weber, F. Nejjari, R. Sarrate, and D. Theilliol. "System reliability aware Model Predictive Control framework". In: *Reliability Engineering & System*

Safety 167 (2017). Special Section: Applications of Probabilistic Graphical Models in Dependability, Diagnosis and Prognosis, pages 663 –672.

J. C. Salazar, A. Sanjuan, F. Nejjari, and R. Sarrate. “Health-Aware and Fault-Tolerant control of an octorotor UAV system based on actuator reliability”. In: *To be submitted to International Journal of Applied Mathematics and Computer Science* (2018).

J. C. Salazar, R. Sarrate, and F. Nejjari. “Health-Aware Control: A selective review and survey of current development”. In: *To be submitted to Annual Reviews in Control* (2018).

- Book chapter

J. C. Salazar, P. Weber, F. Nejjari, D. Theilliol, and R. Sarrate. “MPC Framework for System Reliability Optimization”. In: *Advanced and Intelligent Computations in Diagnosis and Control*. Ed. by Z. Kowalczuk. Advances in Intelligent Systems and Computing 386. Springer International Publishing, 2015, pages 161–177.

- International conferences

J. C. Salazar, R. Sarrate, and F. Nejjari. “Upper bound system reliability assessment for health-aware control of complex systems”. In: *Proceedings of the 4th European Conference of the Prognostics and Health Management Society (PHME 2018)*. Utrecht, The Netherlands, 2018.

J. C. Salazar, R. Sarrate, F. Nejjari, P. Weber, and D. Theilliol. “Reliability computation within an MPC health-aware framework”. In: *Proceedings of the 20th World Congress of the International Federation of Automatic Control (IFAC 2017)*. Toulouse, France, 2017, pages 12230–12235.

J. C. Salazar, A. Sanjuan, F. Nejjari, and R. Sarrate. “Health-Aware Control of an octorotor UAV system based on actuator reliability”. In: *Proceedings of the 4th International Conference on Control, Decision and Information Technologies (CoDIT’17)*. Barcelona, Spain, 2017.

J. C. Salazar, F. Nejjari, R. Sarrate, P. Weber, and D. Theilliol. “Reliability importance measures for a health-aware control of drinking water networks”. In: *Proceedings of the 3rd Conference on Control and Fault-Tolerant Systems (SysTol’16)*. Barcelona, Spain, 2016, pages 572–578.

J. C. Salazar, P. Weber, R. Sarrate, D. Theilliol, and F. Nejjari. “MPC design based on a DBN reliability model: Application to drinking water networks”. In: *Proceedings of the 9th IFAC Symposium on Fault Detection, Supervision and Safety for Technical Processes (SAFEPROCESS 2015)*. Vol. 48. 21. Paris, France: IFAC, 2015, pages 688–

693.

J. C. Salazar, P. Weber, F. Nejjari, D. Theilliol, and R. Sarrate. "MPC Framework for System Reliability Optimization". In: *Proceedings of the 12th Diagnosis of Processes and Systems (DPS 2015)*. Ustka, Poland, 2015, pages 386.

J. C. Salazar, F. Nejjari, and R. Sarrate. "Reliable control of a twin rotor MIMO system using actuator health monitoring". In: *Proceedings of the 22nd Mediterranean Conference of Control and Automation (MED'14)*. Palermo, Italy, 2014, pages 481–486.

- Collaboration

  A. Soldevila, J. Cayero, J. C. Salazar, D. Rotondo, and V. Puig. "Control of a quadruple tank process using a mixed economic and standard MPC". in: *Actas de las XXXV Jornadas de Automática*. Valencia, Spain, 2014.First place on the CEA contest 2014.

1.5.1 Research stays

During the development of this thesis, two research stays were made in the Centre de Recherche en Automatique de Nancy at the Université de Lorraine with a duration of 4 months each one. The first one, from May to July 2014 where the work was concerned to the topic of reliable control of complex systems, the study of the mathematical modeling of the degradation/reliability using Bayesian approaches, and the investigation of the integration of this modeling in the control algorithm.

And the second one, from May to July 2015 where the work was concerned with the topic of reliable control of complex systems, the study of reliability importance measures, the study of the integration of degradation/reliability model in the control algorithm, and also some ideas on the integration of reliability with linear matrix inequalities to compute the controller feedback gain were defined.

Part I

Fundamentals

Chapter 2

Prognostics and Health Management

This chapter presents the concept of Prognostics and Health Management and offers a review of PHM methodologies based on the control techniques used to implement an HAC approach.

2.1 Introduction

In industrial processes or dynamical systems health status of its components such as actuators or sensors is of primary concern as its failure will lead to immediate system shutdown or loss of performance in terms of economical cost or productivity. A well-managed system that minimizes the risk of failure is therefore desirable in many applications. The capability to accurately predict the health of system components (and consequently the system health itself) is the key to ensuring their dependability, availability, reliability, safety, and security.

A system is said to be dependable when it is trustworthy enough to have confidence on the service that it gives. For a system to be dependable, it must be available and ready for use when is needed; reliable, when it is able to provide continuity of service while it is in use; safe, when it does not have a catastrophic consequence on the environment; and secure, when it is able to preserve confidentiality [147].

Thus, the concern about preserving the health of complex system has led to the development of different techniques such as Fault-Tolerant Control (FTC) and Prognostics and Health Management (PHM).

Briefly, those control techniques which have the capacity to maintain the overall system stability and a satisfactory performance in presence of faults are called FTC. This means that a closed-loop system is fault tolerant if it is able to tolerate component malfunctions while maintaining a desirable performance and stability properties.

FTC techniques can be classified into three groups:

- Hardware redundancies techniques:

  The hardware redundancy techniques try to achieve fault tolerance by taking advantage of the hardware redundancy in the system. Their main advantage is its simplicity but it implies a cost of redundant hardware and maintenance.

- Analytical redundancy techniques: Passive Fault Tolerant Control (PFTC):

  The passive FTC techniques are control laws that take into account the fault appearance as a system perturbation. Therefore, within defined margins, the control law has built-in fault-tolerant capabilities, allowing the system to face fault occurrence, thanks to its robustness against a class of faults.

  The advantage of this approach is that it needs neither fault diagnosis nor controller reconfiguration, but as it needs to take in consideration all possible faults of a system during the design stage it provides limited fault tolerance capabilities, thus it cannot be guaranteed that unconsidered faults can be handled. Moreover, it entails a loss of performance with respect to the nominal case.

- Analytical redundancy techniques: Active Fault Tolerant Control (AFTC):

  The active FTC techniques readjust the control law based on the information provided by the faults diagnosis module. With this information, some automatic adjustments in the control law are done after the fault occurrence attempting to meet the control objectives with the minimum performance degradation.

Discussions on FTC are beyond the scope of this thesis and interested readers are referred to [13, 190] and the references therein which review the developments made in this area.

PHM is a methodology aimed at handling the *"System Health"* understood as system reliability, remaining useful life (RUL), system degradation, etc, and based on a real-time monitoring and incipient fault detection.

The main difference between both methodologies is that while FTC is applied when the fault has occurred, PMH is applied during the whole system functioning and its aim is to avoid or at least to delay the fault occurrence.

In other words, FTC techniques do not provide an active reconfiguration of the control law given the health component state. In so far, as the application of PHM and the development of on-line prognostics techniques have evolved, a new type of FTC called Proactive FTC, which has two primary objectives: damage avoidance while ensuring primary mission success [160].

Proactive Fault-Tolerant Control is also called Health-Aware Control (HAC), and its functioning is as follows: given proper on-line prognostic information of the system, the HAC modifies the controller actions or reschedules the mission profile in order to preserve a high level of system health.

HAC technique evaluates the health system while performing control over the system in a non-faulty situation. Moreover, it avoids faulty scenarios by mitigating the health degradation via appropriate control actions considering health indicators in the control objectives. This is done by constantly evaluating the system health indicators and making corrections through the control actions based on those indicators.

A review on methodologies which combine the use of reliability and control theories, their origins, and their applications, based on a bibliography search related to the topics involved in HAC will be presented.

Remark in Figure 2.1 the persistent increase in the works related to the topics of reliability and control, including fault-tolerant and health-aware techniques from 2000 to 2016.

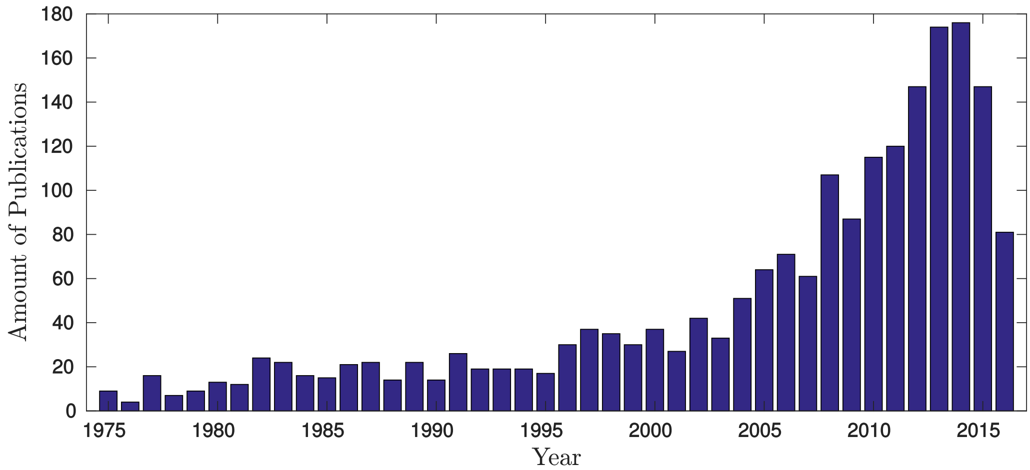

FIGURE 2.1: Amount of Publications Evolution.

Therefore, it is clear that the interest on this field has been increasing. Those works are classified in the following fields: Engineering, Computer Sciences and Mathematics, Material Sciences, Chemical Engineering and Multidisciplinary as it is shown in Figure 2.2.

Furthermore, it is worth to highlight the work that some research communities are doing in this field encouraging the development of new work and promoting different conferences and journals. To mention just a few, there is the Prognostics and Health Management Society, which supports a conference each year and maintains a journal. Also, the IEEE Reliability Society, which supports a conference and a journal on these topics.

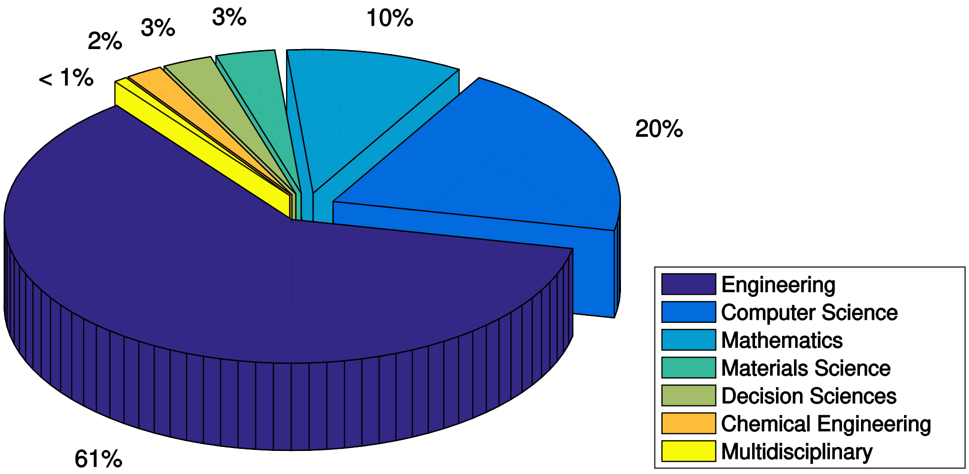

FIGURE 2.2: Related works by fields.

In addition, these topics are being addressed in reputed conferences, such as the Mediterranean Control Conference (MED), the IFAC Symposium on Fault Detection, Supervision and Safety on Technical Process (SAFEPROCESS), the International Conference on Control and Fault-Tolerant Systems (Systol), the International Science Conference Diagnostics of Processes and Systems (DPS), the International Conference on Control, Decision and Information technologies (CoDIT), and the World Congress of the International Federation of Automatic Control among others.

2.2 Prognostics and Health Management

The prognostics information is useful because it supplies the decision maker with adequate information about the expected time to system or components failure and allows to take the suitable actions to deal with them. Assessing the health of a system provides information that can be used to meet several critical goals: (1) providing advance warning of failures; (2) minimizing unscheduled maintenance, extending maintenance cycles, and maintaining effectiveness through timely repair actions; (3) reducing the life-cycle cost of equipment by decreasing inspection costs, downtime, and inventory; and (4) improving qualification and assisting in the design and logistical support of fielded and future systems [121]. In this sense, PHM is an emerging engineering discipline that links studies of system failure to system life cycle management [36].

The main aim of PHM is to improve safety and reduce maintenance cost. To achieve this objective some tasks, such as system monitoring, failure prognostics, and RUL computation, can be involved. Based on that, some actions like logistics requirements, maintenance performance, components replacement or controller reconfiguration, among others, should be taken in order to *manage* the health of the system.

The steps involved in a PHM strategy are observation, analysis, and decision making (see Figure 2.3). Observation is the step where the data is acquired and processed. The second step consists in analyzing the data and extracting information of it, such as health state, RUL, to perform diagnosis and prognostics. And, the third step consists in taking the convenient action based on the analyzed data to extend the useful life of the system or components.

- PHM
  - Observation
    - Data acquisition
    - Data processing
  - Analysis
    - Health assessment
    - Diagnosis
    - Prognostics
  - Decision making
    - Condition-Based Maintenance
    - Logistic actions
    - Health-Aware Control

FIGURE 2.3: Steps involved in a PHM strategy.

PHM concept has its origins in system engineering and considers aspects such as quality, reliability, and maintenance which are used to provide indications of anomalies and make predictions of future failures [40].

Research on PHM methodologies motivated by the benefits it brings has been increased considerably in the last decade. For instance, a literature review on prognostics can be found in [122], and a particular review of data-driven methods for PHM can be found in [165], a PHM review in manufacturing process can be found in [170]. A review on machinery PHM implementing Condition-Based Maintenance (CBM) which summarizes the recent research with emphasis on models, algorithms and technologies for data processing and maintenance decision-making is presented in [64].

In [48] a diagnosis and prognostic approach for power electronic drives and electric machines (AC/DC, DC/DC and DC/AC systems) is presented. This approach incorporates a low cost monitoring of the power electronics such as power MOSFETs and IGBTs. The proposed HAC strategy consists in reducing the performance of the control accomplishing the mission with reduced performance.

Prognostics strategies can be implemented using different techniques. A classification of them can be found in [4, 36]. The one given in [4] is presented in Figure 2.4, which considers four categories: physical-based, data-driven, hybrid and experimental-based techniques. These categories are explained in detail below primarily based in [4, 36, 64].

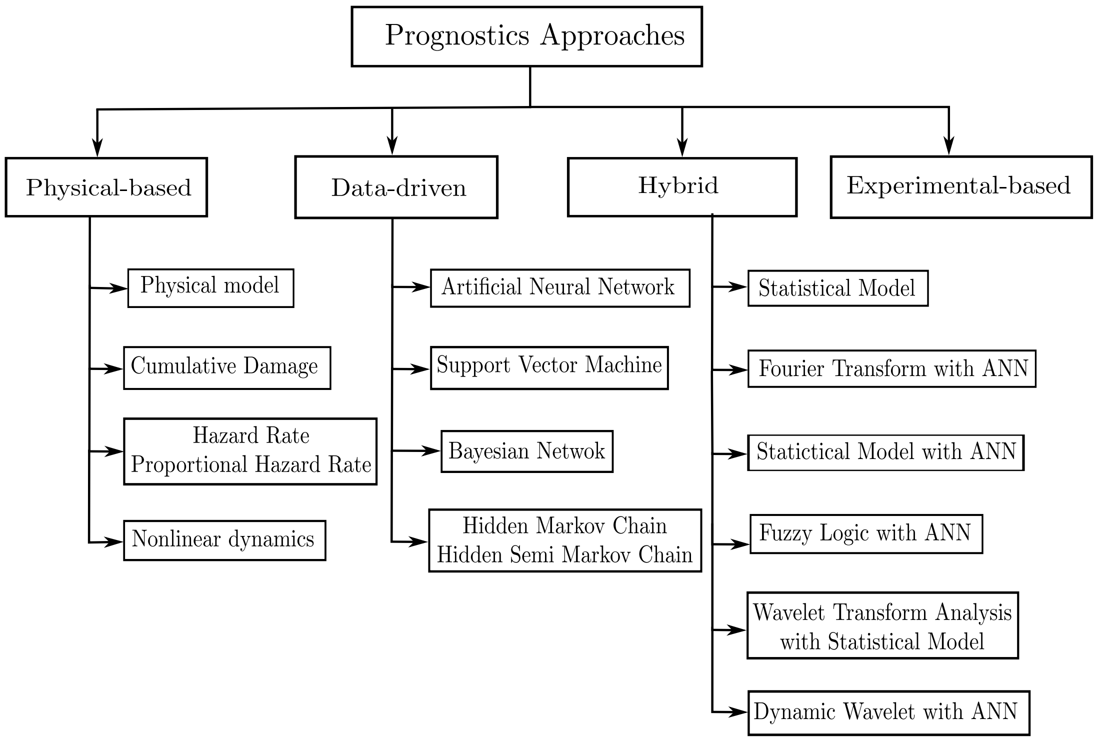

FIGURE 2.4: Prognostics approaches

Physical-based methodologies

In the physical-based approach, the first principles are used to obtain accurate theoretical models specific for a particular type of component. In this category, there are the following approaches: physical model, cumulative damage, hazard rate and proportional hazard rate, nonlinear dynamics.

The physical models are used to describe the physics of the system and failure modes, such as crack propagation, wear corrosion among others. These models combine system-specific mechanical knowledge, defect growth equations, and condition monitoring to provide better prognostics output. These methodologies are more accurate than data-driven ones due that they contain a functional mapping of the system parameters.

Using an explicit model of the system and residual generation methods such as Kalman filter, parameter estimation (or system identification) and parity relations, it is possible to obtain signals, called residuals, which are indicative of fault presence in the system. The residuals are used to implement fault detection, isolation and identification techniques.

Model-based approaches can be more effective than other model-free approaches. However, a correct and accurate model is needed, and an explicit mathematical model may not be feasible for complex systems [64].

There are some applications of physical models, for instance in [90], the authors used the Paris' law to model spur gear crack growth from an analysis of the stress and strain fields based on gear tooth load, geometry and material properties. In [116], the authors presented RUL computation approach based on a crack growth model and implemented using observers and intensity stress measures. In [87], RUL estimation approach for gears based on fatigue teeth crack, gear dynamics, and fracture models was proposed.

Physics-based prognostics have been applied to systems in which their degradation phenomenon can be mathematically modeled such as in a gearbox prognostic module [17]. Physical modeling and parametric identification techniques have been applied with fault detection an failure prediction algorithms in order to predict the system time-to-failure. The faults and failure modes are traced back to physically meaningful system parameters, providing valuable diagnostic and prognostic information.

In [102], a residual-based failure prognostic technique applied to a hydraulic system was proposed. The remaining system useful life is estimated based on residual signals, a bond graph model of the system dynamics, and the degradation model, which allows the prediction of the future health state of the system.

Physical-based prognostics approaches are very effective and descriptive because system degradation modeling is based on laws of nature. Remark that the accuracy and precision depend on model fidelity [166]. There are some disadvantages and limitations of this approach such as: developing a high fidelity model for RUL estimation is very costly, time-consuming, and computationally costly and sometimes it cannot be obtained. Also, it will be component/system specific which limits its use to other similar cases. Hence, sometimes the data-driven approach is preferably used [36].

Data-driven methodologies

Data-driven methods are based on the fact that condition monitoring data and the extracted features vary with the development of either the initiation and propagation process or the degradation process. These methods are useful when a large quantity of noisy data needs to be transformed into a logical information to estimate the RUL whose accuracy depends on the quantity and quality of the data.

The data-driven prognostics methodology is based on statistical and learning techniques, most of which come from the theory of pattern recognition. Such approaches incorporate conventional numerical algorithms, like linear regression or Kalman filters, as well as algorithms commonly found in the machine learning and data mining communities. The recent algorithms include Artificial Neural Networks (ANNs), decision trees, and Support Vector Machines (SVMs).

An ANN is a computational model that mimics the human neural system structure. It consists of simple processing elements connected in a complex arrangement which allows the model to approximate a non-linear function with multiple inputs and multiple outputs. A processing element involves a node and a weight. By a training process, the ANN learns the function by adjusting its weights with observations of inputs and outputs [64]. There are different neural network types. The Feedforward Neural Network (FFNN) is one of the most popularly applied in machine fault diagnosis. For instance, in [134] the authors proposed a condition-based health monitoring approach for rotating machinery using ANNs, where the neural network is trained to contain the knowledge of a detailed finite-element model whose results are integrated with system measurements to produce accurate machine fault diagnostics and component stress predictions.

The use of ANN for prognostics has two types of applications, one is a nonlinear function approximation to predict system failure features and biases by estimating and classifying, the other involves feedback connections to model dynamic processes of system degradation for RUL assessment [29].

In [188], the use of a Self-Organizing Map (SOM) neural network for multivariable trending of fault development to estimate the RUL of a bearing system was proposed. In [149] a diagnosis approach based on Bayesian networks incorporating failure probability information, instrument uncertainty, and the predictions of false indication. They extend such ideas to perform prognostics and model the evolution over time using a DBN.

Hidden Markov model (HMM) is also an appropriate model for the joint analysis of event and condition monitoring data. An HMM consists of two stochastic processes: a Markov chain with finite number of states describing an underlying mechanism and an observation process depending on the hidden state. Particularly, the approaches of this category do not require assumptions or empirical estimations of physical parameters. They are adequate to process noisy data, such as that provided by measurements of input/output. Nevertheless, they require a large amount of data to be accurate [64].

Hybrid methodologies

In some cases, the use of a determined prognostics approach is not enough to characterize the system parameters which makes it difficult to predict with a single method. Hence, the application of several methodologies used in conjunction produces more accurate results [6]. Such approach takes data from all the sensors required by various methodologies, performs stipulated steps and gives optimum RUL estimate through the fusion of all estimates.

The statistical model-based approach requires the formulation of a model using parameters of the considered system. The RUL is obtained by using data gathered over a period of time as an input to the model.

In [76], RUL estimation methodology for aircraft components based on usage monitoring data was proposed. The authors used Monte Carlo simulations based on a desired component reliability to prognosticate the component loads and fatigue lifetime values.

Fourier transform can also be used to extract useful data from monitored signals. That extracted data can be used as input in an ANN and compute the RUL estimation. For example, in [83], the authors proposed to monitor the vibration signals of a rotating bearing and perform a spectral analysis using Fourier transform to separate useful time-frequency features. They proposed a 2-layer neural network: one for diagnosis with three situations (normal condition, unbalance failure and other failures) and another to estimate the RUL of the bearing.

Cheng and Pecht [25] presented a case study for RUL estimation using fusion approach for ceramic capacitors. This method fuses data-driven methods and physics of failure methods to predict the remaining useful life of electronic products. This fusion provides the advantage and overcome the limitations of the data-driven methods and the physics of failure methods to provide better predictions. A fusion approach is also proposed in Goebel, Eklund, et al. [50], where a model from first principles of the physics of fault initiation and propagation, and data from controlled condition experiments are used to develop an empirical model of condition-based fault propagation rate for aircraft engine bearings.

Experimental-based methodologies

In the experience-based approach, probabilistic or stochastic models of the degradation process or the life cycle of components is used by taking into account the data and the knowledge acquired in the practice or collected in experiments [70].

The experiments can be performed in several manners; they can be by using one parameter or multivariate methods. The selection of the most method depends on the problem and the number of parameters to be considered. In the experiments, the time to failure has been considered as function of of load, frequency of load and other relevant parameters. With methods such as finite element method (FEM), the possibilities of performing theoretically stresses calculation have dramatically increased. As experiments are often costly, an effort has been made to develop these types of methods [4].

In [157] a study of three prognostic approaches was presented. The comparison of these approaches is based on experimental data from 17 ball bearing. The estimation of the remaining useful life of the test bearing is performed by algorithms trained with experimental data.

The research in experimental approaches is leading to the development of new measurement equipment to collect the experimental parameters and then formulate theoretical models based on data [4].

The application fields based on this approach include: energy engineering, experimental mechanics, engineering materials, fluid mechanics, steel structures, chemical processing, among others. The experimental test rigs are typically designed in research laboratories to simulate real operating conditions for the component or system in question usually to verify theoretical models.

This approach is used to validate other methods. For instance, in [21] the authors validated the performance of an adaptive neuro-fuzzy inference systems predictor using experimental data obtained from the planetary gear carrier plate of a UH-60 helicopter. In [101], it is proposed to use experimental data from the accelerated life of bearings to verify a method based on data driven and model based approaches.

2.3 Reliability and Control: historical review

In the literature, some authors have used the term of "reliable control" to indistinctly name to a health-aware control, control with redundancy, FTC, etc. As an attempt to disambiguate the meaning of reliable control and health-aware control concepts, a review of the uses given to those concepts in the literature is presented.

The beginning of reliable control concept can be found in [152], where the author proposed the use of redundant controllers to enhance the reliability of the control system based upon a decentralized control scheme. In this case, the *reliability* concept is associated with the control structure composed by 2 or more independent controllers. Such structure guarantees stability under controller failures and perturbations in the plant interconnection structure. The concept reliable comes from the fact of having redundancy improves the control system availability in case of failure of one control module.

Next, in [169], the authors used the term *reliable* to define a pair of controllers which are able to stabilize and regulate the system, either working together or separately in case of a failure of one of them. They referred to this approach as *reliable stabilization problem* and *reliable regulation*, respectively. Again, the concept of reliability is linked with the ability of the controller to continue functioning in the presence of failures on itself.

Later in [11], the authors proposed a methodology to fusion system theory and reliability. It involved including the structural reliability of system components (computed by a Markov model) into a gain scheduling control law. Such methodology was referred to as a *reliable control system design*. In this work, the reliability of the components is taken into account to influence the control system design. The resulting control law depends on the system structure, the structural dynamics, and the system dynamics. The solution to the optimal control problem defines the boundary between reliable (stabilizable) designs and unreliable designs. Note that the authors use the concept of reliability to denote a system which stability can be ensured.

In [26], the authors propose a *reliable control system* to enhance the reliability of the controller using a multiple parallel controller structure composed of a main feedback controller in addition to a redundant adaptive controller whose outputs summation guarantees zero tracking error between the set-point input and the plant output in the case of failure of the main controller and/or changes in plant parameters. This approach basically incorporates fault tolerance and robust control characteristics to the system by adding a redundant controllers.

In [167] the authors presented a methodology for the design of *reliable* centralized and decentralized control systems. The authors meant by *reliable* in this case that the proposed methodology guarantees stability and H_∞ performance not only when all control components are operative, but also under sensor or actuator outages in the centralized case, or control channel outages in the decentralized case. In other words, they use the concept of *reliable control* to designed the effects of a FTC methodology.

In [74] and [72], the authors propose a methodology of fault-tolerant control design incorporating actuator health (actuator reliability) for stability and tracking control problem was proposed. The fault-tolerant controller which the control objective with a high overall system reliability improving the dependability of the system by keeping the set of actuators available as long as possible. The proposed approach attempts to diminish the use of those actuators with the highest impact on the system reliability. Such impact is computed based on a reliability analysis of the system structure assumed to be a parallel one.

An attempt to delineate the relationship between reliability and FTC can be found in [180, 181], where the authors propose a reliability analysis of fault-tolerant control systems using Markov models and present some of the software tools for assessing the reliability. They define the concept of *coverage* as a parameter that reflects the ability of a system to automatically recover from the occurrence of a fault and claim that enhancing the coverage is the key to enhanced the system reliability.

As it has been presented, the concepts of reliable control and FTC have many aspects in common. Both are intended to enhance the reliability, safety, and ensure system operation, among others. For instance, reliable control aims at enhancing the control system by improving its reliability, i.e., by having a redundant control architecture as a backup strategy in the case of control module failure. Furthermore, FTC aims at enhancing the system reliability by reconfiguring the control action in order to compensate system components faults, such as sensor, actuators or deviation of parameters.

On the other hand, Health-Aware Control (HAC) is a concept that combines the health monitoring and prognostics with the control theory. This means that techniques to perform condition monitoring, prognostics and control are integrated in order to develop an HAC scheme. Figure 2.5 represents the different techniques involved in HAC scheme found in the literature.

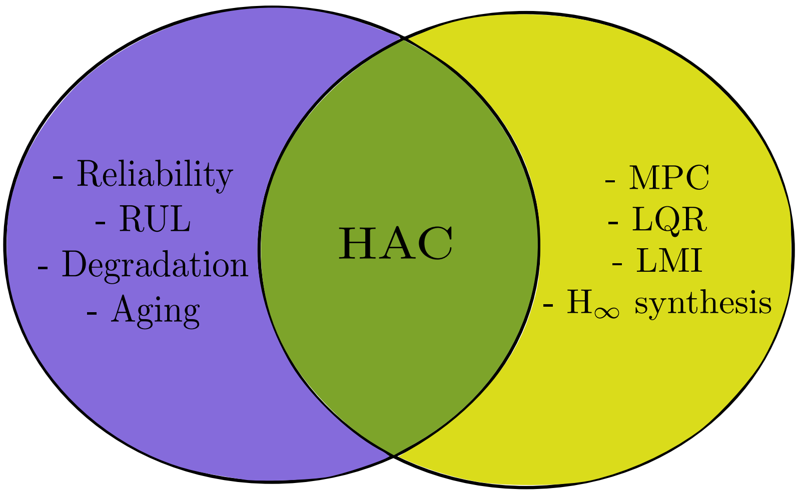

FIGURE 2.5: Control theory and health monitoring merge.

The main difference between FTC and HAC is that, on the one hand, FTC is concerned with the control of a system where a component is in a faulty state. This situation implies that the controller is able to adapt the system behavior once the fault is detected, isolated and estimated. On the other hand, the HAC uses the information provided by the prognostics and health monitoring module about the component or system health to modify the controller in order to fulfill the control objectives and also extend the availability and useful life of the system.

In other words, an HAC strategy adjusts the controller when the system is in a nonfaulty situation and redistribute the control efforts based on the prognostics module, which estimates the component and system aging under the specific operating condition. Whereas, the FTC adjust or modifies the control input one the fault has occurred.

2.4 HAC classification

Although HAC is currently an incipient field of research, there are some contributions that combine control and reliability theories, as it has been presented along this chapter, and most of them are known as *reliable control*.

However, since at that time prognostics was not a developed field, the HAC approach was not sufficiently developed, and a lot of emphasis was put on diagnosing the fault and developing control reconfiguration and accommodation techniques which led to the development of FTC techniques.

Table 2.1 presents a list of the control approaches used in combination with reliability methods to develop FTC schemes in addition to system monitoring. For instance, in [124] the authors propose to model the degradation process in terms of asset usage and then use it to redistribute the control effort in a two-tank system by means of an MPC algorithm which solves a quadratic optimization problem and a linear optimization problem [125].

TABLE 2.1: Existing Control design methodologies in HAC

Control designing approaches	References
MPC	Grosso, Ocampo, et al. [54], Pereira, Galvao, et al. [124, 125], Robles, Puig, et al. [133], Salazar, Nejjari, et al. [136, 137], and Salazar, Weber, et al. [143, 144]
LMI, robust control, H_∞, LQR	Chamseddine, Theilliol, et al. [20], Dardinier-Maron, Hamelin, et al. [31], Gokdere, Chiu, et al. [51], Guenab, Theilliol, et al. [56], Guenab, Weber, et al. [58], Khelassi, Jiang, et al. [72], Khelassi, Theilliol, et al. [73–75], Langeron, Grall, et al. [82], Oca and Puig [113], Tang, Kacprzynski, et al. [159], Weber, Boussaid, et al. [175], and Weber, Simon, et al. [178]
PID	Escobet, Puig, et al. [38], Nguyen, Dieulle, et al. [109–111], Tang, Kacprzynski, et al. [160], and Wang, Tomovic, et al. [173]

Robust control approaches are used for instance in [58], where the objective is to maintain stability and performance of the system near to the desired performance in the presence of system component faults, and in certain circumstances reduce the performance requirements to achieve the objective. In [75] and [74], the authors propose the integration of reliability and reconfigurability analysis in an FTC system for a tank system and aircraft model, respectively. These works have in common the use of components reliability as indexes to perform the control reconfiguration after the occurrence of failures.

In [73], the authors propose an FTC system based on a feedback controller which guarantees the highest system reliability. This controller is synthesized using linear matrix inequalities (LMIs) and incorporating a reliability indicator, this reliability indicator is the well known Birnbaum measure which indicates those system components whose reliability are critical for the reliability of the system. Note that in the mentioned works, the asset reliabilities are modeled using the exponential distribution function.

In [72], the authors propose a reconfigurable control allocation problem applied to an over-actuated system in which the redistribution factor is defined in terms of the actuator reliabilities modeled by using the Weibull distribution function. Then, the control allocation problem consists in assigning more control effort to those actuators whose reliabilities are higher and to relieve those actuators whose reliabilities are lower.

In [10] and [9], a control allocation problem is solved by incorporating reliability importance measures to redistribute the control effort among the available actuators of a hydraulic system. The reliability is modeled using a Weibull distribution function and it is computed by a Dynamic Bayesian Network (DBN).

Table 2.2 present a list of application made in this topic. For instance, in [124] a PHM scheme using MPC is presented. An application using a tank level over-actuated system is presented. The main idea is to manage the actuators degradation over the maintenance horizon to achieve the control goals using MPC.

In [113] an approach to design a reliable admissible model matching (AMM) fault tolerant control (FTC) for LPV systems is proposed. The main idea is to reconfigure the controller on-line taking into account changes due to the faults, maintaining a certain actuators reliability level in spite of the faults.

In [91] the authors present a reliable robust tracking controller against actuator faults and control surface impairment for aircraft bases in on a mixed linear-quadratic (LQ)/ H_∞ performance indexes and multiobjective optimization using linear matrix inequalities (LMIs). In such work, the concept *reliable* is used to mean *trustworthy* due to the fact that authors proposed a control approach with fault tolerance capabilities under actuators outages.

TABLE 2.2: Application examples of HAC

Applications	References
Aircraft	Chamseddine, Theilliol, et al. [20], Khelassi, Jiang, et al. [72], Khelassi, Theilliol, et al. [73, 74], LI, Zhao, et al. [88], Oca and Puig [113], Salazar, Nejjari, et al. [137], Theilliol, Weber, et al. [162], and Weber, Boussaid, et al. [175]
Tank level systems	Abdel-Geliel, Badreddin, et al. [1], Bicking, Weber, et al. [9], Dardinier-Maron, Hamelin, et al. [31], Grosso, Ocampo, et al. [54], Guenab, Weber, et al. [58], Khelassi, Theilliol, et al. [75], Nguyen, Dieulle, et al. [109–111], Pereira, Galvao, et al. [124, 125], Robles, Puig, et al. [133], Salazar, Nejjari, et al. [136, 137], Salazar, Weber, et al. [143, 144], and Weber, Simon, et al. [178]
Electromechanics systems	Escobet, Puig, et al. [38], Ginart, Barlas, et al. [48], Gokdere, Chiu, et al. [51], Lee, Kim, et al. [85], and Tang, Kacprzynski, et al. [159]

In [75] the authors propose the integration of reliability evaluation in a fault-tolerant control system and illustrate with a flight control application. The controller is analyzed with respect to reliability requirements and its controllability defined through its Gramian. The admissible solution is proposed according to reliability evaluation based on energy consumption under degraded functional conditions.

In [132] the authors present an overview of modeling and control strategies including fault-tolerant capabilities for wind turbines and wave energy devices. In these systems, the reliability improvement is achieved by a significant reduction of periods of null or very low power production.

2.5 Conclusions

In this chapter, a literature review on Prognostics and Health Management, particularly in the historical development of Health-Aware Control methodologies has been presented. Besides the attempts to address the problem of HAC, a list of applications and control techniques used were given.

Approaches to include the system health information in the controller design has been proposed, but it is still an open research field to explore. The problem of how to include the health information in a systematic way in the controller design should be further investigated.

The interaction between prognostics and control establishes a new feedback loop. To understand the effects of this loop in the whole performance of the system, a mathematical formulation of the problem should be considered. Due to the combined discrete-event/continuous nature of the reconfiguration/accommodation actions and the control loop, respectively, techniques coming from hybrid system theory could be applied.

The appropriate health indicator to be used for reconfiguring/accommodating the controller is also a key issue. Some methodologies for the designer should be given in order to facilitate the design of the HAC reconfiguration/accommodation strategy.

Furthermore, model-based prognostic approaches accuracy depends on the availability of an accurate model and data. Data-driven methods are preferred in the case of quick estimations with lower accuracy. Nevertheless, physics-based approaches seem to be the most adequate when prognostics accuracy is needed and the data is limited.

Chapter 3

Background on reliability

In this chapter, a review of degradation and reliability concepts and their modeling approaches is presented. The research in degradation and reliability has been a topic of relevant interest since they provide an estimation of span life for systems and components. Therefore, a review of the most relevant of both, theoretical and applied contributions found in the literature is given.

In Section 3.1, an introduction to reliability and degradation is given, and the most used probability distributions are described. Then, in Section 3.2, an explanation about covariates and how they can be modeled and integrated into the probability distributions is presented (Section 3.2.1). After, in Section 3.2.2, some models to fit degradation data, such as fitting data to probability distribution or using regressors, are presented.

3.1 Reliability and degradation

Reliability analysis of dynamical systems helps to prevent failures which could be costly and sometimes disastrous. In complex systems or in safety-critical systems, it is imperative to identify the key component of the system and prevent the system failure. Generally, this is done by implementing Conditioned-Based Maintenance (CBM) methods, where decisions are supported by the reliability analysis information.

In the literature, authors refer indistinctly to the concepts of reliability, degradation, deterioration, etc. In general terms, *reliability* leads to the concept of dependability, successful operation or performance, and the absence of failures, whereas unreliability (lack of reliability) leads to the opposite [14]. Thus, it is convenient now to give a clear definition of these concepts.

Definition 3.1. *Reliability* is the probability that an asset will perform its functioning correctly for a specified period of time and under specified operating conditions [14].

Whereas, degradation can be defined as:

Definition 3.2. *Degradation* is the the reduction in performance, reliability and lifespan of assets [52].

Degradation can be viewed as a damage that the system accumulates over time and eventually leads to a failure when the accumulated damage reaches a failure threshold.

The condition of a component can be characterized according to the degree of detail given to the degradation process [105]. It could be characterized as binary condition (see Figure 3.1(a)), being equal to 1 if the component is in its working state, i.e., the component performance is satisfactory or acceptable, and 0 for the opposite situation, where the component is in the faulty state. In this characterization, the component starts in the working state and changes to the failed one after a period of time (failure time). This is represented as a random variable because the time instant of change from working to failed is uncertain. An example of characterization is an electric bulb where its state changes from working to failed in a very short time which can be assumed to be instantaneous.

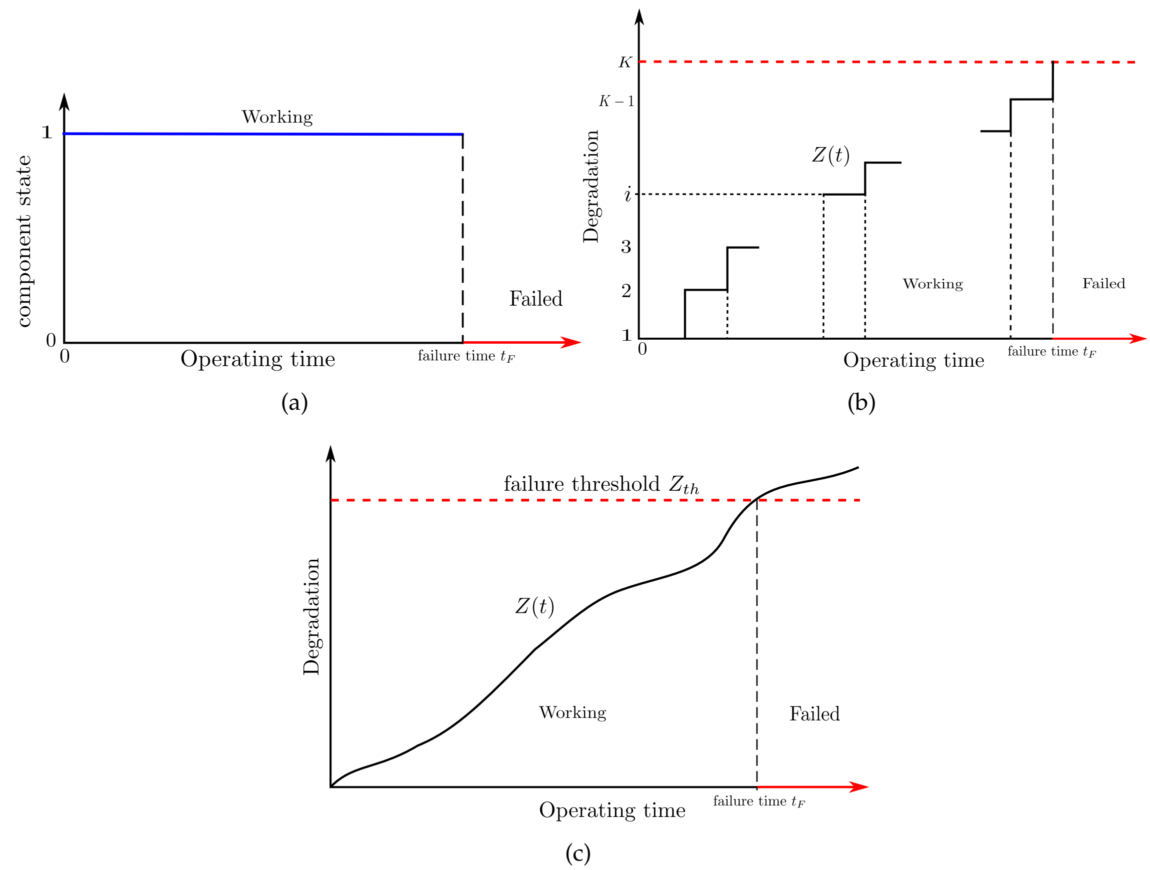

FIGURE 3.1: Component condition characterization: (a) binary states, (b) multi-state with finite states, (c) multi-state with infinite states.

Also, it could be characterized with a finite number of states (see Figure 3.1(b)) where the condition of the component can assume any value from the set $\{1, 2, \ldots, K\}$ with:

- 1 corresponding to component performance being fully acceptable, i.e., the component is in the good working state.
- i, $1 < i < K$ corresponding to component performance being partially acceptable, i.e., component is in a working state with a higher value of i implying a higher level of degradation and,
- K corresponding to component performance being unacceptable, i.e, the component is in a faulty state.

The time to failure of the component is given by $t_F = \inf\{t : Z(t) = K\}$. An example of this characterization consider the wear in a tire, where no wear corresponds to state 1 and complete wear corresponds to state K.

And finally, it could be characterized with an infinite number of levels (see Figure 3.1(c)) being an extension of the above case with $K = \infty$. Here a higher value implies a higher degradation, and the component failure time is given by $t_F = \inf\{t : Z(t) = Z_{th}\}$.

Remark that, when the level of degradation reaches the threshold Z_{th} the asset failure occurrence increases. As a consequence, a failure is often a result of the effect of degradation.

From these two definitions, remark that reliability declines when assets degrade or deteriorate. The failure threshold provides a link between degradation and assets failure, therefore, it is possible to use the degradation signals to estimate the failure time distribution, the RUL, etc. The degradation signals are obtained by a proper degradation model, which consists in developing a good probability model that is capable of describing the degradation process.

More specifically, reliability is the probability that a system or component will operate properly for a specific period of time under design operating conditions (such as temperature, volts, etc.) without failure. In other words, reliability can be used as a measure of the success of the system to provide its function adequately.

Mathematically, reliability $R(t)$ is the probability that a system will be successful in the interval from time 0 to time t:

$$R(t) = \Pr(T > t) \quad t \geq 0, \tag{3.1}$$

where T is a random variable denoting the time-to-failure or failure time. Which is the time until the system first enter the down (failure) state:

$$T = \inf\{t : \text{system state} = \text{down}\}, \tag{3.2}$$

And the unreliability $F(t)$, which is a measure of failure, is defined as the probability that a system will fail by time t:

$$F(t) = \Pr(T \leq t) \quad \forall t \geq 0, \tag{3.3}$$

in other words, $F(t)$ is the cumulative distribution function (*cdf*), also called failure distribution function.

If the time-to-failure random variable T has a density function $f(t)$, then the reliability function $R(t)$ is defined as [127, p. 10]:

$$R(t) = \int_0^t f(x)dx, \tag{3.4}$$

and the function:

$$\begin{aligned} h(t) &= \frac{f(t)}{R(t)} \\ &= \frac{f(t)}{1 - F(t)}, \end{aligned} \tag{3.5}$$

is called the failure or hazard rate [47, p. 25]. The term $h(t)dt$ is the probability that a device at the age of t will fail in the time interval t to $(t + dt)$. The importance of the hazard function lies in that it indicates the change in the failure rate over the life of a population of components by plotting their hazard functions on a single axis.

In reliability theory, several types of probability distributions are used; for example, exponential, Weibull, gamma, lognormal, among others. A brief description of some of these distribution functions will be given below.

The exponential distribution is one of the most widely used in reliability engineering because it is relatively easy to handle in performing reliability analysis, and many engineering items exhibit constant hazard rate during their useful life [32]. Its probability density function (*pdf*) is defined by

$$f(t) = \lambda e^{-\lambda t} \quad t \geq 0,\ \lambda > 0, \tag{3.6}$$

where λ is the distribution parameter which is also known as the constant failure rate.

And the reliability function given by (3.4) and the exponential distribution (3.6), is defined as:

$$\begin{aligned} R(t) &= \int_t^{\infty} \lambda e^{-\lambda t} dt \\ &= e^{-\lambda t}. \end{aligned} \tag{3.7}$$

Reliability (3.7) refers to the probability that a device's lifetime is larger than t, the probability that the device will survive beyond time t, or the probability that the device fail after time t. Remark that $R(0) = 1$ and $R(\infty) = 0$ and that reliability function is a non increasing function of t.

From (3.5) and using (3.6) and (3.7) it is evident that, for the exponential distribution, the failure rate function is the failure rate:

$$h(t) = \frac{\lambda e^{-\lambda t}}{e^{-\lambda t}} = \lambda. \tag{3.8}$$

The exponential distribution has the memoryless property, which means that the current reliability status does not depend on the previous one. This situation does not represents the phenomenon of aging which is very important for reliability theory. Intuitively, aging represents an increase of failure risk as a function of time in use. To introduce this dependency, the following definition of reliability can be used [47]:

$$\Pr(T > t) = R(t) = e^{\left(-\int_0^t \lambda(v) dv\right)}. \tag{3.9}$$

In the case of the Weibull distribution which is used to represent several physical phenomena, its probability density function is defined by [179]:

$$f(t) = \frac{\beta t^{\beta-1}}{\eta^{\beta}} \exp\left(-\frac{t}{\eta}\right)^{\beta}, \tag{3.10}$$

where β and η are the shape and scale parameters, respectively.

The popularity of this distribution stands on the fact that, depending on the parameters, it may describe both increasing and decreasing failure rates.

The gamma distribution is especially useful for reliability modeling of those asset lifetimes which degradation can be explained by the shock accumulation [47].

The lognormal distribution is a continuous probability distribution of a random variable whose logarithm is normally distributed. The lognormal distribution is applied to the description of the dispersion of the component failure rate data.

Table 3.1 presents some of the most widely distribution functions used in reliability theory and summarizes their *pdf*, *cdf*, reliability functions, and hazard rates.

TABLE 3.1: Common used continuous distributions.

Distribution	Formulae	References
Exponential	$f(t) = \lambda e^{-\lambda t}, t \geq 0$ $F(t) = 1 - e^{-\lambda t}$ (3.11) $R(t) = e^{-\lambda t}, \quad t \geq 0$ $h(t) = \lambda$	Deloux, Castanier, et al. [33], Finkelstein [43], Guenab, Weber, et al. [58], Khelassi, Theilliol, et al. [73–75], Oliveira and Yoneyama [115], and Wu, Wang, et al. [182]
Weibull	$f(t) = \frac{\beta t^{\beta-1}}{\eta^{\beta}} \exp\left(-\frac{t}{\eta}\right)^{\beta}$ $F(t) = 1 - \exp\left(-\frac{t}{\eta}\right)^{\beta}$ (3.12) $R(t) = \exp\left(-\frac{t}{\eta}\right)^{\beta}$ (3.13) $h(t) = \frac{\beta}{\eta}\left(\frac{t}{\eta}\right)^{\beta-1}$ (3.14)	Bicking, Weber, et al. [9], Grosso, Ocampo, et al. [54], Jiang and Jardine [67], Khelassi, Jiang, et al. [72], and Toscano and Lyonnet [164]
Gamma	$f(t) = \frac{\lambda^{\beta}}{\Gamma(\beta)} t^{\beta-1} e^{-\lambda t}$ (3.15) $F(t) = \frac{\lambda^{\beta}}{\Gamma} \int_0^t x^{\beta-1} e^{-\lambda x} dx$ (3.16) $R(t) = \frac{\lambda^{\beta}}{\Gamma(\beta)} \int_t^{\infty} x^{\beta-1} e^{-\lambda x} dx$ (3.17) $h(t) = \frac{t^{\beta-1} e^{-\lambda t}}{\int_0^{\infty} x^{\beta-1} e^{-\lambda x} dx}$ (3.18)	Çinlar [19], Langeron, Grall, et al. [82], Lawless and Crowder [84], Lu and Meeker [95], and Noortwijk [112]
Lognormal	$f(t) = \frac{1}{\sigma t \sqrt{2\pi}} \exp\left[-\frac{(\ln t - \mu)^2}{2\sigma^2}\right]$ (3.19) $F(t) = \Phi\left(\frac{\ln t - \mu}{\sigma}\right)$ (3.20) $R(t) = 1 - \Phi(\frac{\ln t - \mu}{\sigma})$ (3.21) $h(t) = \frac{f(t)}{1 - \Phi\left[(\ln t - \mu)/\sigma\right]}$ (3.22)	Chen and Zheng [24], Langeron, Grall, et al. [82], and Meeker, Escobar, et al. [103]

From the reliability theory, another useful concepts like the Mean Time To Failure (MTTF) and Availability will be explained. The MTTF is the expected life of the device and it can be evaluated through the following standard equation [34]:

$$\begin{aligned} \text{MTTF} = E(T) &= \int_0^\infty t f(t) dt \\ &= \int_0^\infty R(t) dt \,. \end{aligned} \tag{3.23}$$

For repairable devices, the MTTF represents the mean time to the first failure. After it is repaired and put into operation again, the average time to the next failure is indicated by the mean time between failures (MTBF). Under perfect repairs, MTBF is equal to MTTF. Since there is usually an aging effect in most devices, MTBF decreases as more failures are experienced by the device. The time needed to perform a repair is called mean time to repair (MTTR). Then, it is possible to define the availability as:
Definition 3.3. *Availability*: The availability is defined as the probability that the device is available when is needed and is often used as a measure of its performance.

It is expressed as:

$$A = \frac{\text{MTTF}}{\text{MTTF} + \text{MTTR}} . \tag{3.24}$$

The failure rate of many devices exhibits the *bathtub curve* shown in Figure 3.2 which is divided into three sections [78]:

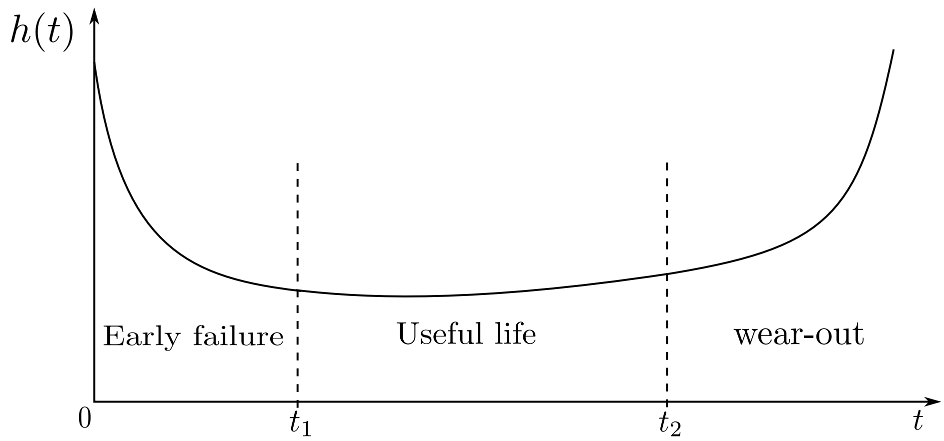

FIGURE 3.2: Bathtub curve of hazard rate.

- In the interval $(0, t_1)$, which is usually short, a decreasing-failure-rate (DFR) is observed. This is often referred to as the early failure period and the failures that occur in this interval are called early failures, burn-in failures, or infant mortality failures. They are mainly due to manufacturing defects and can be eliminated using burn-in techniques.

- In the interval (t_1, t_2), the failure rate is not completely constant, although it is often assumed to be constant. This period is often referred to as the useful life of the asset or the constant-failure-rate period. The failures that occur in this interval are called chance failures or random failures. They are usually caused by chance events like accidents, overloading, and a combination of the underlying complex physical failure mechanisms.
- In the interval (t_2, t_∞), the failure rate is increasing. This period is often called the increasing-failure-rate (IFR) period or the wear-out failure period. The failures that occur in this period are due to wear-out, aging, or serious deterioration of the device. The life of the device is close to its end once entering this period unless there is preventive maintenance or major overhauls to revitalize the device.

The bathtub curve represents the behaviors of the failure or hazard rate according time in three different intervals of the asset life. These intervals could be modeled using some of the distribution functions presented in Table 3.1.

In this thesis, the exponential function distribution will be used to model the reliability of the devices because of its constant failure rate property. It is an excellent model for the long flat "useful life" portion of the bathtub curve. In fact, most components and systems spend most of their lifetimes in this portion of the bathtub curve.

3.2 Reliability modeling

3.2.1 Reliability models with covariates

The term *covariate* comes from statistics and refers to a variable that is possible to predict as the result of a study. In reliability theory, a covariate is used to model or explain (also known as *explanatory variable*) the influence of different risk factors over the failure rate (hazard) of the assets [53].

In reliability models, the covariates are used to model the effect of internal process variables or environmental factors, such as voltage, temperature, humidity, vibration, frequency, usage, among others. The reliability models with covariates are classified into two groups, the non-parametric and the semi-parametric models [53]. A brief review on them is given below.

The non-parametric models are used to avoid unrealistic assumptions when the form of degradation path or distribution of degradation measure is unspecified, or when the failure data involves complex distributions, or when the volume of observations is small and the accurate fitting to a known distribution is difficult. There are for instance the following models:

- **Proportional Hazard Model (PrHM):** This model estimates the effects of different covariates affecting the MTTF of a system. Most of the models used to estimate the hazard of an asset are based on this model proposed by Cox [30], a review on them can be found in [77].

  The PrHM is expressed as [30]:

$$h(t, \boldsymbol{z}) = h_0(t)\psi(\gamma \boldsymbol{z}), \tag{3.25}$$

  where, $h_0(t)$ is the unspecified baseline hazard function which is dependent on time only and without influence of covariates. The positive functional term, $\psi(\gamma \boldsymbol{z})$, is dependent on the effects of different factors, which have multiplicative effect on the baseline hazard function. The covariate function, $\psi(\gamma \boldsymbol{z})$, is represented by a row vector consisting of regression coefficients γ and a column vector consisting of the covariates $\boldsymbol{z}$. In this case, unlikely to the assumption made in Figure 3.2, the hazard rate is not constant.

- **Additive Hazard Model (AHM):** Additive hazard model is expressed as:

$$h(t, \boldsymbol{z}) = h_0(t) + \psi(\gamma \boldsymbol{z}), \tag{3.26}$$

  where the positive or negative functional term, $\psi(\gamma \boldsymbol{z})$, is dependent on the effects of different factors, which have an additive effect on the baseline hazard function. This model provides the means for modeling a circumstance when the hazard is not zero at time zero.

- **Mixed Additive-Multiplicative Model:** this model contains both a multiplicative and an additive components and specifies that the hazard is associated with a multidimensional covariate process $\boldsymbol{z} = (W^T, X^T)^T$ and takes the form [93]:

$$h(t|\boldsymbol{z}) = g\{\beta_0^T W(t)\} + h_0(t) f\{\gamma_0^T X(t)\}, \tag{3.27}$$

  with $\theta_0 = [\beta_0^T, \gamma_0^T]^T$ being a vector of unknown regression coefficients, g and f are known link functions and h_0 is an unspecified baseline hazard function under $g = 0$ and 1.

- **Accelerated Failure Time Model:** this model is used to obtain reliability and failure rate estimates of devices and components in a much shorter time. It can be expressed as [151]:

$$Y = \log(t) = \mu(\boldsymbol{z}) + \sigma\epsilon, \tag{3.28}$$

where $Y = \log(t)$ is the lifetime (assumed to be log), $\boldsymbol{z}$ is the applied stress vector which distribution has a location parameter $\mu(\boldsymbol{z})$ and a constant scale parameter σ, $\sigma > 0$ and ϵ is a random variable whose distribution does not depend on $\boldsymbol{z}$.

- **Proportional Intensity Model (PIM):** this model was introduced by Cox [30] and is intended to model the failures and repairs processes of repairable systems which incorporate explanatory variables, covariates or markers [68, 97], which are influencing factors such as stress, temperature, humidity, vibration, and use rate. It is described by:
$$h(t|N(t), \boldsymbol{z}(t)) = h_{0j}(t)\exp(\boldsymbol{z}(t), \boldsymbol{\gamma}_j), \tag{3.29}$$
where $N(t)$ represents a random variable for the number of failure in $(0, t]$, and $\boldsymbol{z}(t)$ denotes the covariate process up to time t. $h(t|N(t), \boldsymbol{z}(t))$ and $h_{0j}(t)$ are the intensity function and the baseline intensity function, respectively, and $\boldsymbol{\gamma}_j$ is the regression coefficient for the jth stratum.

- **Proportional Covariates Model:** proposed by Sun, Ma, et al. [156] it overcomes some shortcomings of proportional hazard model, it assumes that the covariate of a system is proportional to the hazard of the system. The generic expression is:
$$Z_r(t) = C(t)h(t), \tag{3.30}$$
where the covariate function and the baseline covariate function, both depending on time are represented by $Z_r(t)$ and $C(t)$, respectively, and $h(t)$ represents the hazard of the system. This expression indicates that the covariates of a system changes when the hazard of this system changes.

In contrast, in semi-parametric models, the paths degradation form or degradation distribution are known or partially specified. These models can be specified as:

- **Weibull Proportional Hazard Model (WPHM):** the Weibull Proportional Hazard Model is based on PrHM when the failure is assumed to follow a Weibull distribution. This model is expressed as [63, 187]:
$$h(t; \boldsymbol{z}(t)) = \frac{\beta}{\eta}\left(\frac{t}{\eta}\right)^{\beta-1}\psi(\boldsymbol{\gamma}\boldsymbol{z}(t)), \tag{3.31}$$
where $\beta > 0$ and $\eta > 0$ are the shape and scale parameter of the Weibull distribution, respectively.

- **Logistic Regression Model (LRM):** this model is used to relate the probability of an event to a set of covariates. Given the current degradation features $\boldsymbol{z}(t)$, and assuming the odds ratio between the reliability function $R(t|\boldsymbol{z}(t))$ and the cumulative distribution function $F(t|\boldsymbol{z}(t)) = 1 - R(t|\boldsymbol{z}(t))$ [92]:

$$\frac{R(t|\boldsymbol{z}(t))}{1 - R(t|\boldsymbol{z}(t))} = \exp(\alpha + \boldsymbol{\gamma}\boldsymbol{z}(t)), \tag{3.32}$$

where $\alpha > 0$ and $\boldsymbol{\gamma}$ are the model parameters to be estimated. Then the reliability expression is given by:

$$R(t|\boldsymbol{z}(t)) = \frac{\exp(\alpha + \boldsymbol{\gamma}\boldsymbol{z}(t))}{1 + \exp(\alpha + \boldsymbol{\gamma}\boldsymbol{z}(t))}. \tag{3.33}$$

3.2.2 Models for degradation data

A degradation process, also known as deterioration, wear or aging, of physical components, is generally inevitable in engineering systems and, it can be originated due to mechanical contact, shocks, usage, and environmental agents such as temperature, humidity, vibration, etc. The degradation of a component can lead to a loss of reliability, which can be viewed as a reduction in performance or efficiency levels which can generate a system failure or shut-down. The rate at which deterioration occurs is a function of time and/or usage intensity [14, 155]. Hence, the monitoring of components degradation level in complex systems is of great importance. [53].

The degradation occurrence is a kind of stochastic process which could be modeled in several approaches. Generally, the degradation models are built from degradation data by fitting it to a model or distribution. A very comprehensive review on degradation models in reliability can be found in [52], where the authors classify them into two major groups according to how degradation data is collected, i.e., data obtained in normal operation and data obtained under accelerated conditions.

i) **Normal degradation models:** these models are built from data obtained at normal operating conditions. These models can be classified into two groups: degradation models with and without stress factors.

   - Degradation models without stress factors are for example the general degradation path model, random process model, linear/nonlinear regression models, mixture model, and time series model; in which the degradation measure is not a function of a defined stress and the related reliability is estimated at fixed level of stress [172].

     Stress-Strength Interference model (SSI): in this model, the stress has a random dispersion Y, which results from the applied loads. This dispersion is modeled by a distribution function $H_Y(z)$. Hence, asset reliability can be described as [106]:

$$\begin{aligned} R(t) = \Pr(X > Y) &= \int_{-\infty}^{+\infty} \int_{z}^{+\infty} H_Y(z) G_X(x) dx dy \\ &= \int_{-\infty}^{+\infty} \int_{-\infty}^{x} H_Y(z) G_X(x) dy dx, \end{aligned} \tag{3.34}$$

where $G_X(x)$ is a random dispersion in inherent asset strength (X).

This model implies that asset reliability corresponds to the event that strength exceeds stress. In [183] the authors classify the SSI models into three groups: deterministic degradation, random strength degradation process [59] and upper and lower bounds [158].

Cumulative damage/shock model: in this model, it is assumed that the damage threshold (strength) is constant and the stress (damage) is variable. It is based on cumulative damage theory for a degradation process exposed to discrete stress. It is assumed that an asset is subjected to shocks that occur randomly in time. Each shock imparts a quantity X_i of damage to the asset, which fails when a threshold is exceeded. The reliability $R(t)$ over time can be expressed according to a Poisson process with intensity λ [106]:

$$R(t) = \sum_{k=0}^{\infty} e^{-\lambda t} \frac{(\lambda t)^k}{k!} G_X^k(D), \tag{3.35}$$

here G is the distribution of the amount of damage per shock, k is the number of shocks that occur over the interval $[0, t]$, and D is the threshold.

- Degradation models with stress factors: in these models, the degradation measure is a function of a defined stress. Degradation models with stress factors are for example the stress-strength inference model, cumulative damage/shock model, and diffusion process model; where the degradation measure is a function of a defined stress.

General degradation path model: the general degradation path model fits the degradation observation by a regression model with random coefficients [67]. Lu and Meeker [95] develop a Monte Carlo simulation procedure to calculate an estimate of the distribution function of the time-to-failure, and they propose the following general assumptions in which the test and measurement should be conducted:

(a) Sample assets are randomly selected from a population or production process and random measurement errors are independent across time and assets.

(b) Sample assets are tested in a particular homogeneous environment (e.g., the same constant temperature).

(c) The measurement (or inspection) times are prespecified. They are the same across all the test assets, and may or may not be equally spaced in time. This assumption is used for constructing confidence intervals for the time-to-failure distribution.

For each asset in a random set of size n, it is assumed that degradation measurements are available for prespecified times $(t_1, t_2, ..., t_s)$. Generally, until the observed degradation path (z) crosses a prespecified critical level D or until time t_s, which comes first. The sample path of the ith asset at time t_j is given by:

$$z_{ij} = \eta_{ij} + \varepsilon_{ij} = \eta(t_j; \Phi, \Theta_i) + \varepsilon_{ij} \quad i = 1, 2, ..., n, \tag{3.36}$$

$$\varepsilon_{ij} \sim N(0, \sigma_\varepsilon^2), \quad j = 1, 2, ..., m_{\Theta_i} \leq m, \tag{3.37}$$

where t_j is the time of the jth measurement; η_{ij} is the actual path of the ith asset at time t_j; ε_{ij} is the measurement error with constant variance σ_ϵ^2; Φ is the vector of fixed effect parameters common for all assets; Θ_i is the ith asset random effect parameter vector that represents individual asset characteristics; m is the total number of possible measurements in the experiment; and m_{Θ_i} is the total number of measurements of the ith asset.

Assuming that Θ_i $(i = 1, 2, ..., n)$ follows a multivariate distribution function $G_\Theta(\cdot)$. The distribution function of T, the failure time, can be written as:

$$\Pr(T \leq t) = F_T(t) = F_T(t; \Phi, G_\Theta(\cdot), D, \eta). \tag{3.38}$$

Random process model: this kind of model fits the degradation measures at each observation by a specific distribution with time-dependent parameters [184]. This method collects multiple degradation data at a certain time and treats it as dispersed points. The observations at time instant t_j are assumed to follow a S-normal distribution with $\mu(t_i)$ and $\sigma(t_i)$. To find the equation for $\mu(t)$ and $\sigma(t)$ a linear regression is used. Assuming that the degradation measure at time t follows a Weibull distribution with constant shape β and time-dependent scale parameter $\eta(t) = b\ \exp(-at)$, the reliability function can be described as:

$$R(t) = \Pr(T \geq t) = \Pr(X(t) > D) = \exp\left(\frac{-D^{\beta}}{b\, e^{-at}}\right), \tag{3.39}$$

where, a and b are constants, $X(t)$ is degradation level at time t, and D is the threshold level.

Mixture model for hard and soft failures: this method consists in obtaining two observation samples: catastrophic failures (hard) and degradation (soft), and then builds a mixture model with both data [191]. This can be modeled as:

$$F(t) = p(z)F_c(t) + [1 - p(z)]F_d(t), \tag{3.40}$$

where, $F(t)$ is the cumulative density function (*cdf*) of t, $p(z)$ is the proportion of components failed catastrophically within specified observed degradation value z, $F_c(t)$ and $F_d(t)$ are respectively the catastrophic failure *cdf* of t and degradation failure *cdf* of t (lifetime).

Time series model: it is a technique used to predict individual system performance reliability in real-time considering multiple failure modes. It includes an on-line multivariate monitoring and anticipation (using a Kalman filter) of selected performance measures and conditional performance reliability estimates [96].

Other commonly used degradation models: Brownian motion (or Wiener process) and Gamma processes are continuous-time models that are appropriate for modeling continuous degradation processes. Nowadays, these models as well as Markov models are widely applied as degradation modeling techniques [14, 71, 89, 98, 112, 128, 153].

ii) **Accelerated degradation models:** accelerated degradation models provide information about reliability at normal conditions using degradation data obtained at an accelerated time with or without stress conditions. Degradation process can be very slow in an industrial application at normal stress level and have a high MTBF, which makes difficult to estimate the failure time distribution of components with high-reliability [103, 161, 185].

Therefore, to obtain data quickly from a degradation test, an accelerated life test is performed. This test consists in applying an increasing level of acceleration variables, such as vibration amplitude, temperature, corrosive media, load, voltage, pressure [150]. However, this kind of tests is a costly approach.

General assumptions of accelerated degradation models are:

(a) Degradation is not a reversible process.

(b) A model applies to a single degradation process, mechanism, or failure mode.

(c) Degradation of a test asset's performance before the test starts is negligible.

(d) The failure processes at higher stress levels are the same as at the design or use stress levels.

Accelerated degradation models can be physics-based or statistical based. In the following, a quick review on those categories is presented.

- Physics-based models: these models are used for accelerated life tests when the deterioration is caused by thermal and non-thermal parameters, speed, load, corrosive environment, vibration amplitude, etc., in order to estimate their service lives. Applications can include dielectrics, semiconductors, battery cells, lubricant, plastic, insulating fluids, capacitors, bearings, and spindles.

  Arrhenius model: this model is used when the damage is caused by temperature, especially for: dielectrics [49], semi-conductors [103, 123], battery cells, lubricant, and plastic.. In general, it is used to describe many products that fail as a result of degradation due to chemical reactions or metal diffusion. The nominal time τ to failure is [108]:

$$\tau = A\, e^{\dfrac{E}{(k\,T)}}, \tag{3.41}$$

  where E is the activation energy of the reaction in eV, k is the Boltzmann's constant, 8.3171×10^5 eV/K, T is the absolute Kelvin temperature, A is a constant that depends on product geometry, specimen size and fabrication, test method and others factors.

  Eyring model: this model is used for accelerated life test with respect to the thermal and non-thermal variable. The Eyring relationship for nominal life τ as a function of absolute temperature T is:

$$\tau = \frac{A}{T}\, e^{\dfrac{B}{(k\,T)}}, \tag{3.42}$$

  here A and B are constant parameters of the product and test method, and k is Boltzmann's constant. For the small range of absolute temperature in most applications, (A/T is essentially constant, and (3.42) is close to the Arrhenius relationship (3.41)).

Inverse power model: this model is used to analyze accelerated life test data of many electronic and mechanical components such as insulating fluids, capacitors, bearings, and spindles in order to estimate their service lives when the acceleration operating parameters are non-thermal e.g. speed, load, corrosive medium, and vibration amplitude [69, 148]. It is based on the inverse power law relationship between nominal life τ of a product and the accelerating variable V, and it is expressed as:

$$\tau(V) = \frac{A}{V^{\gamma_1}}, \tag{3.43}$$

here A and γ_1 are parameters characteristics of the product, specimen geometry and fabrication, the test method, etc.

- Statistics-based models: these models have been developed to estimate the hazard of assets with covariates in both the reliability and biomedical fields. A review on statistics-based models can be found in [53].

  In these methods, techniques as standard regressions can be applied to most aging degradation data, as such data are usually complete. However, these models are usually nonlinear in the parameters. In such cases, nonlinear regression methods must be used, which introduces considerable complexity [7].

3.3 Conclusions

In this chapter, the link between reliability and degradation has been explained, followed by a literature review on reliability modeling and degradation models for reliability estimation. The degradation modeling consists in fitting degradation data to a model or a probability distribution. The degradation data can be obtained at the normal operating condition or at accelerated ones.

The reliability modeling approaches are related to probability distributions. In this sense, the choice of the probability distribution depends on the application, asset and, system nature.

The hazard model with covariates is one of the most common statistical models in reliability and survival analysis. Some of them have been presented and grouped into non-parametric and semi-parametric models. In such a way, an explanation about covariates and how they explain the failure rate and its integration into probability distributions has been addressed.

Some models to specific physical system have been reviewed, those models can be used to fit degradation data by adjusting parameters.

In this thesis, the exponential distribution will be used to model the reliability of the assets and their aging phenomenon as described in (3.9). Moreover, the hazard models with covariates will be used to explain the aging process, particularly, the PrHM proposed by [30] because it can explain the degradation process of a large variety of physical systems in a simplified way.

Chapter 4

Reliability Assessment

This chapter addresses the reliability modeling and assessment of dynamic system using structure function, Bayesian and Dynamic Bayesian networks. This chapter also presents the complexity of reliability modeling and how the inference algorithms are able to handle it. Reliability Importance Measures as indicators of components importance into the system reliability are also presented and explained. All these concepts are then illustrated through an example consisting of a Drinking Water Network system.

4.1 System reliability

Generally, systems are composed by subsystems or components. If the state of the subsystems or components can be known, the state of the system can also be known. System structure can be explained through two fundamental relations: series and parallel [60].

Only binary components will be considered, i.e. components having only two states: operational (up) and failed (down). Let x_i denote the state of component i, where $i = 1, \ldots, n$ and,

$$x_i = \begin{cases} 1 & \text{if component } i \text{ is up} \\ 0 & \text{if component } i \text{ is down} \end{cases} . \tag{4.1}$$

Also, it will be assumed that the system can only have two states: up or down. The dependence of a system state on the states of its components will be determined by means the so-called structure function.

The structure function allows to determine the dependency of the state of the system regarding the state of its components. This function, denoted as $\Phi(\mathbf{x})$, indicates the status of the system (success or failure) given the state of each component.

Now, let $\mathbf{x} = (x_1, x_2, ..., x_n)$ denotes the state of the n components. It can have one of 2^n values which correspond to the possible combinations of the states (working or failed) for the n components. Therefore, the state of the system is characterized by $\Phi(\mathbf{x})$ which is a binary value function where

$$\Phi(\mathbf{x}) = \begin{cases} 1 & \text{if the system is in working state} \\ 0 & \text{if the system is in failed state} \end{cases}. \tag{4.2}$$

4.1.1 Reliability of series and parallel systems

A serial system is called to be up if and only if all its components are up (see Figure 4.1(a)). Formally, the reliability of a serial system is denoted as:

$$\Phi(\mathbf{x}) = x_1 \cdot x_2 \cdots x_n = \prod_{i=1}^{n} x_i. \tag{4.3}$$

A parallel system is called to be up if and only if one of its components is up (see Figure 4.1(b)). Formally, the reliability of a parallel system is denoted as:

$$\Phi(\mathbf{x}) = 1 - (1 - x_1)(1 - x_2) \cdots (1 - x_n) = 1 - \prod_{i=1}^{n}(1 - x_i). \tag{4.4}$$

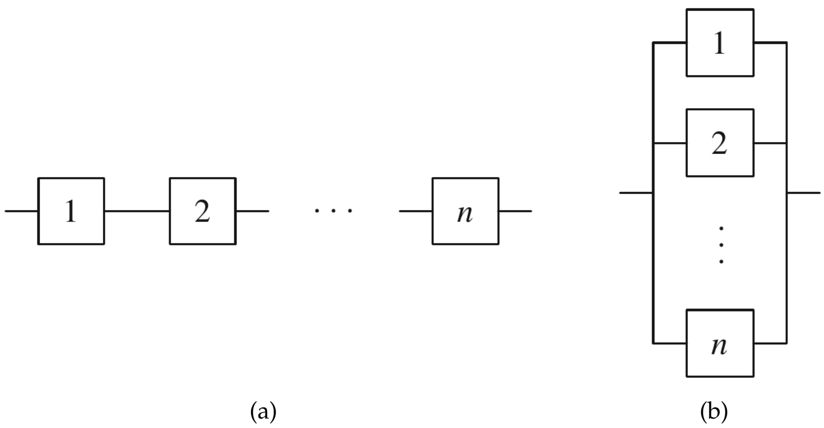

FIGURE 4.1: Representation of series (a) and parallel (b) systems.

For instance, the structure function can be computed using either the minimal path sets ($P_1, P_2, \ldots, P_s$) which are the minimal sets of elements of the system whose functioning (i.e., being up) ensures that the system is up,

$$\Phi_p(\mathbf{x}) = 1 - \prod_{j=1}^{s} \left(1 - \prod_{i \in P_j} x_i\right). \tag{4.5}$$

Or the minimal cut sets (C_1, C_2, ..., C_k) which are the minimal sets of elements of the system whose failure (i.e. being down) causes the failure of the system,

$$\Phi_c(\mathbf{x}) = \prod_{j=1}^{k} \left(1 - \prod_{i \in C_j} (1 - x_i) \right). \tag{4.6}$$

Now, let us assume that the state of the ith component is described by a binary random variable X_i, defined by

$$\Pr(X_i = 1) = p_i, \Pr(X_i = 0) = q_i = 1 - p_i. \tag{4.7}$$

where 1 corresponds to the operational (up) state and 0 corresponds to the failure (down) state.

It will be assumed that all components are mutually independent. This implies a considerable simplification, due that for independent components, the joint distribution of X_1, $X_2, \ldots, X_n$, is completely determined by components reliabilities $p_1, p_2, \ldots, p_n$.

Let $\mathbf{X} = (X_1, X_2, \ldots, X_n)$ be the system state vector, which is a random vector. Consequently, the system structure function $\Phi(\mathbf{X}) = \Phi(X_1, X_2, \ldots, X_n)$ becomes a binary random variable, i.e. $\Phi(\mathbf{X}) = 1$ corresponds to the system up state and $\Phi(\mathbf{X}) = 0$ corresponds to the system down state.

Hence, the system reliability (r_0) is the probability that the system structure function equals 1:

$$r_0 = \Pr(\Phi(\mathbf{X}) = 1). \tag{4.8}$$

Since, $\Phi(\cdot)$ is a binary random variable, it can be written as:

$$r_0 = E\left[\Phi(\mathbf{X})\right]. \tag{4.9}$$

Therefore, in a serial system, its structure function is given by $\Phi(\mathbf{X}) = \prod_{i=1}^{n} X_i$. Thus:

$$r_0 = E\left[\Phi(\mathbf{X})\right] = \prod_{i=1}^{n} p_i. \tag{4.10}$$

And a parallel system, its structure function is given by $\Phi(\mathbf{X}) = 1 - \prod_{i=1}^{n}(1 - X_i)$. Thus:

$$r_0 = E\left[\Phi(\mathbf{X})\right] = 1 - \prod_{i=1}^{n} (1 - p_i). \tag{4.11}$$

A series system does not have any redundancy because there is only one way for the system to work properly; that is, all components have to work properly. In a parallel system, there are $2^n - 1$ different ways for the system to work properly in which each component constitutes a different way [78].

4.1.2 Reliability of series-parallel systems

There are more complex structures that can be explained as combinations of series and parallel structures. Nevertheless, in the cases where such structure reduction cannot be performed, e.g. the case of bridge structure (Figure 4.2), the pivotal decomposition approach is used to compute the system reliability.

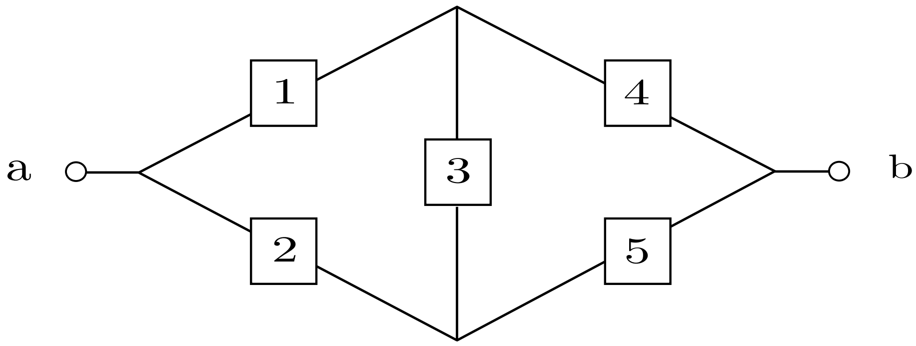

FIGURE 4.2: Bridge structure.

Let $(\alpha_i; \mathbf{p})$ denote the vector $\mathbf{p}$ with its ith component replaced by α_i. Hence, $(1_i; \mathbf{p}) = (p_1, ..., p_{i-l}, 1, p_{i+l}, \ldots, p_n)$.

The pivotal decomposition method consists in computing the reliability of the system *pivoting* around a component by taking it as fully reliable (up) or completely unreliable (down). In this way, the problem is reduced to compute the system reliability of serial and parallel systems.

Example 4.1.1. Consider the bridge structure system shown in Figure 4.2. The best choice is to pivot around element 3. Suppose that component 3 is up. Then the bridge becomes a series connection of two parallel subsystems consisting of elements 1, 2 and 4, 5, respectively. Its reliability is

$$r(1_3; \mathbf{p}) = [1 - (1 - p_1)(1 - p_2)][1 - (1 - p_4)(1 - p_5)]. \tag{4.12}$$

Now, consider that component 3 is down, then the bridge becomes a parallel connection of two series systems: one with components 1, 4 and the second with components 2, 5. Its reliability is $r(0_3; \mathbf{p}) = 1 - (1 - p_1p_4)(1 - p_2p_5)$. Therefore, the system reliability is $r_o = p_3r(1_3; \mathbf{p}) + (1 - p_3)r(0_3; \mathbf{p})$.

The final result is:

$$r_o = E[\Phi(\mathbf{X})] = p_1p_3p_5 + p_2p_3p_4 + p_2p_5 + p_1p_4 - p_1p_2p_3p_5 \quad (4.13)$$
$$- p_1p_2p_4p_5 - p_1p_3p_4p_5 - p_1p_2p_3p_4 - p_2p_3p_4p_5 + 2p_1p_2p_3p_4p_5. \quad (4.14)$$

The same results can be obtained by using minimal cuts and path sets. For example, the bridge has four minimal path sets: $\{1,3,5\}$, $\{2,3,4\}$, $\{1,4\}$, and $\{2,5\}$. Thus, the random structure function is:

$$\Phi(\mathbf{X}) = 1 - (1 - X_1X_3X_5)(1 - X_2X_3X_4)(1 - X_2X_5)(1 - X_1X_4). \quad (4.15)$$

Finally, the terms in parentheses are expanded, the expression is simplified using the fact that $X_i^k = X_i$ and replacing the reliability of each component.

4.2 Reliability assessment using BNs

4.2.1 Bayesian Networks

Basically, a Bayesian Networks (BN) computes the probability distribution in a set of variables according to the prior knowledge of some variables and the observation of others [65]. The BNs are also called as Direct Acyclic Graphs (DAGs).

Let **A** and **B** be two nodes with two possible states ($\mathbf{S}_1$ and $\mathbf{S}_2$, see Figure 4.3). A probability is associated to each state of the node. This probability is defined *a priori* for root nodes and computed by inference for the others. The *a priori* probabilities of node **A** are Pr(**A**=$\mathbf{S}_{A1}$) and Pr(**A**=$\mathbf{S}_{A2}$).

A Conditional Probability Table (CPT) is associated to node **B** and defines the conditional probability of the state of **B** given the state of **A** (Pr(**B**|**A**)). Thus, the BN inference computes the marginal distribution Pr(**B**=$\mathbf{S}_{B1}$):

$$\begin{aligned}\Pr(\mathbf{B} = \mathbf{S}_{B1}) =& \Pr(\mathbf{B} = \mathbf{S}_{B1}|\mathbf{A} = \mathbf{S}_{A1})\Pr(\mathbf{A} = \mathbf{S}_{A1}) \\ &+ \Pr(\mathbf{B} = \mathbf{S}_{B1}|\mathbf{A} = S_{A2})\Pr(\mathbf{A} = \mathbf{S}_{A2}).\end{aligned} \quad (4.16)$$

In the Bayesian network approach the probabilistic interactions of the components of a system are represented using a DAG which nodes represent the variables and the arcs between nodes represent the causal relationships between variables [35]. Basically, BNs compute the probability distribution in a set of variables according to the prior knowledge of some variables and the observation of others [66].

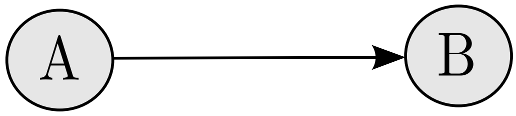

FIGURE 4.3: Basic Bayesian Network.

A Conditional Probability Table (CPT) is associated with node **B** and defines the conditional probability of the state of **B** given the state of **A** (Pr(**B**|**A**)) (Table 4.1). The conditional probability is a measure of the probability of an event given that another event has occurred.

TABLE 4.1: CPT of the BN shown in Figure 4.3

A	**B**	
	S_{B1}	S_{B2}
S_{A1}	Pr(**B** $= S_{B1}$|**A** $= S_{A1}$)	Pr(**B**=S_{B2}|**A** $= S_{B1}$)
S_{A2}	Pr(**B** $= S_{B1}$|**A** $= S_{A2}$)	Pr(**B**=S_{B2}|**A** $= S_{B2}$)

4.2.2 Inference mechanism

Bayesian networks are easy to use thanks to their graphical interpretation. But, the probabilistic inference mechanism constitutes their real strength. The inference of a BN is able to compute the marginal probability distribution of any variable according to:

- Observation or measurements of variables (evidence).
- The likelihood regarding the state of certain variables.
- The conditional probability distribution between variables.

In this thesis, the BN and DBN models have been programed using the Bayes Net toolbox [104], which supports many different inference algorithms, such as:

- Exact inference for static BNs:

  junction tree

  variable elimination

  brute force enumeration (for discrete nets) linear algebra (for Gaussian nets)

Pearl's algorithm (for polytrees)

- Approximate inference for static BNs:

  likelihood weighting

  Gibbs sampling

  loopy belief propagation

- Exact inference for DBNs:

  junction tree

  frontier algorithm

  forwards-backwards (for Hidden Markov Models (HMMs))

- Approximate inference for DBNs:

  Boyen-Koller

  factored-frontier/loopy belief propagation

The inference algorithms explanation are outside the scope of this thesis. Although, more information can be found in [65, 120].

Nevertheless, it is worth mentioning that all inference mechanisms use the Bayes theorem to propagate the probabilities on the variables and to update the probabilities of all the variables given the observations of states or likelihoods of states.

Nowadays, the current research on inference algorithms is focused on their efficiency, in reducing the computing time needed when handling complex models with a high number of variables.

4.2.3 Dynamic Bayesian Networks

A special case of Bayesian Network called Dynamic Bayesian Network (DBN) is used to model the time dependency of a process. In a DBN the random variables are time indexed, so the process state $S_A : \{s_1^A, ..., s_M^A\}$ is represented by nodes $\mathbf{A}_k$ and $\mathbf{A}_{k+\Delta t}$ at time instants k and $k + \Delta t$, respectively. The time dependence is represented by an arc and the temporal evolution of the variables is represented by successive time slices as shown in Figure 4.4 (for simplicity let Δt be equal to 1).

The transition probability between the states of the variable at time instant k to $k+1$ is defined by a CPT inter-time slices. Given the probability distribution $\Pr(\mathbf{A}_k)$ at time instant k, the network leads by inference to a unique distribution $\Pr(\mathbf{A}_{k+1})$ at time instant $k+1$. The computation over time of $\Pr(\mathbf{A}_k)$ is performed by iterative inferences starting from $k=0$ and $\Pr(\mathbf{A}_0)$ [8].

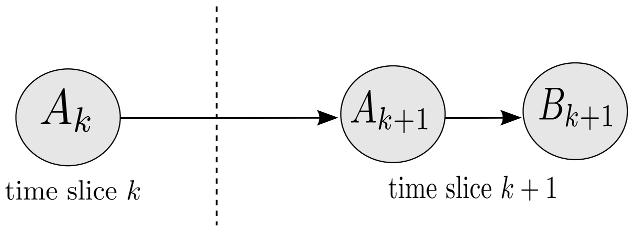

FIGURE 4.4: DBN model for the ith component.

4.2.4 Component reliability

Recall from Section 3.1 that reliability is the probability that a system will perform its functioning satisfactorily for a given period of time and under stated operating conditions.

Generally, an exponential function is used to model the reliability as expressed in (3.9) as:

$$R_i(t) = e^{-\int_0^t \lambda_i(v)dv}$$

where λ_i is the failure rate that is obtained from the ith component under different levels of load. In discrete-time, the reliability can be expressed as:

$$R_i(k+1) = e^{\left(-T_s \sum_{v=0}^{k+1} \lambda_i(v)\right)} \tag{4.17}$$

where T_s is the sampling time.

The decay of the components reliability can be modeled using a Markov chain (MC) process. This type of process is very useful in system reliability modeling due to its memoryless property, which means, that the state transitions only depend on the current and next state, and it does not depend on the previous state or the amount of time that the process has stayed in the current state, making it an effective tool for system reliability analysis [176].

Let e_i be a discrete random variable in the Markov process representing the state of the ith component with two possible mutually exclusive states, i.e. up (Up) and down (Dn).

The probabilistic state transition between the states is defined by:

$$\mathbf{P}_{\text{MC}} = \begin{bmatrix} 1 - p_{12} & p_{12} \\ 0 & 1 \end{bmatrix} \tag{4.18}$$

where $p_{12} \cong \lambda \Delta t$: λ represents a constant failure rate and Δt the time interval, and p_{12} can be interpreted as the probability that the component goes from state Up to Dn after Δt.

In the case of components whose failure rate depends on time, their reliability can be modeled by a semi- Markov chain.

The MC is homogeneous if the transition probabilities of the states are independent on time. In a semi-Markov chain, the memoryless property is relaxed, which means that the state transition depends on the current state and the transition time. Therefore, the probability matrix (4.18) becomes dependent on time:

$$\mathbf{P}_{\text{MC}}(e_i(k+1)|e_i(k)) = \begin{bmatrix} 1 - p_{12}(k) & p_{12}(k) \\ 0 & 1 \end{bmatrix}. \tag{4.19}$$

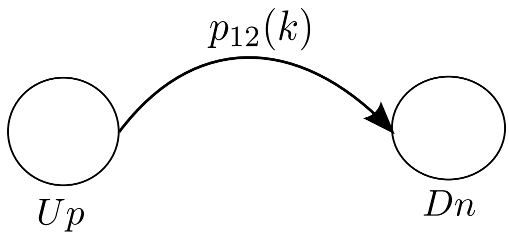

FIGURE 4.5: Semi-Markov chain for the component reliability.

From (4.19) it is clear that the failure rate is the probability of component state to be Dn at instant time $k + 1$ given that its state was Up at time k, this is:

$$\lambda_i(k) = \Pr(e_i(k+1) = Dn|e_i(k) = Up). \tag{4.20}$$

If the state at next instant time $(k + 1)$ is used then to compute the state at instant time $(k + 2)$ and so on, the MC is transformed into a semi-Markov chain (Figure 4.5).

The semi-Markov chain is modeled by a Dynamic Bayesian Network with a CPT evolving according to time. In this case the evolution is represented in two time slices (Figure 4.6) [8].

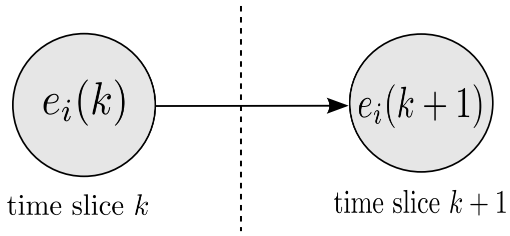

FIGURE 4.6: DBN model for the ith component.

Therefore, DBN computes the component reliability using:

$$R_i(k+1) = \Pr(e_i(k+1) = Up). \tag{4.21}$$

which follows expression (4.17).

4.2.5 System reliability modeling using BN

The use of BNs to reliability modeling allows to model several structures based on minimal path/cut sets, or logical combination of components states by using AND or OR gates [78].

Let e_i be a random variable representing the state of the ith component denoted as:

$$\Pr(X_i = 1) = \Pr(e_i = Up); \;\; \Pr(X_i = 0) = \Pr(e_i = Dn). \tag{4.22}$$

Assume that the state of the components are known, once the minimal path sets of the system are identified, its states (i.e., if the minimal path set is up or down) are represented by a random variable as a node in the DBN. The state of the components of the system are also represented as nodes in the DBN and are connected to their respective minimal path set node. Note that the probabilities of the component states are computed by inferences in the DBN modeling of the semi Markov chain described above.

Finally, the state of the system (i.e., system reliability) is represented by a random variable in the top node of the BN which is connected to the minimal path set nodes (Figure 4.8).
Example 4.2.1. For example, consider the system presented in Figure 4.7 composed by three components. It is clear that with a minimum of two components the system can performs its function (link point A to point B) satisfactorily, being {1, 3} and {2, 3} the minimal path sets of the system.

Then, it is possible to build a BN of the system reliability from its minimal path sets (see Figure 4.8), being e_i the probability of the ith component state, P_i the probability of the

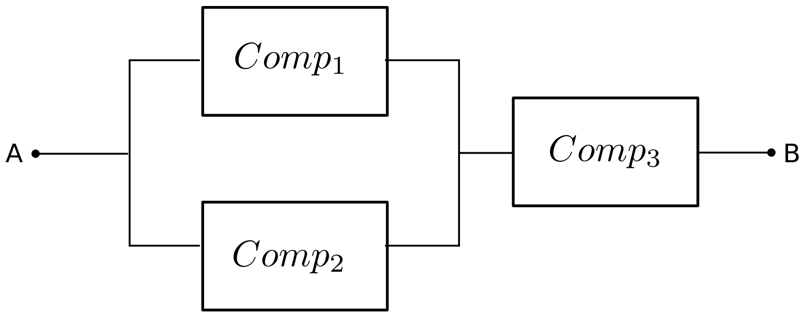

FIGURE 4.7: Three components system example.

state of the ith minimal path set and S the probability of the system state [177].

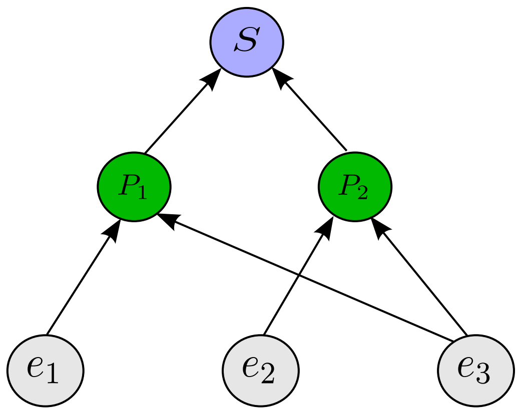

FIGURE 4.8: Bayesian Network of system reliability.

Table 4.2 presents the CPT of node P_1. P_1 depends on the states of the components e_1 and e_3 and its behavior corresponds to an AND gate, i.e., all the components in a success path should be available for the system to be available. Node P_2 has another CPT which depends on the states of components e_2 and e_3.

TABLE 4.2: CPT for node P_1.

e_1	e_3	P_1	
		Up	Dn
Up	Up	1	0
Up	Dn	0	1
Dn	Up	0	1
Dn	Dn	0	1

Table 4.3 presents the CPT of node S. It depends on the state of success path nodes P_1 and P_2 and has the behavior of an OR gate, i.e., if there is at least one success path up, then the system will be up.

TABLE 4.3: CPT for node S.

P_1	P_2	S	
		Up	Dn
Up	Up	1	0
Up	Dn	1	0
Dn	Up	1	0
Dn	Dn	0	1

It is possible then to compute the probability distribution for each variable conditioned by the values of the other variables in the graph. This feature is particularly important in case a control system must work in real-time, because in that case evidences acquired about a state variable must be propagated to update the state of the rest of the domain. Therefore, the reliability of the system (R) is computed using the BN as:

$$R = \Pr(S = Up). \tag{4.23}$$

In the case of complex structure systems with high amount of components the computing of the structure function becomes non trivial.

4.3 Drinking Water Network example

Drinking Water Networks (DWN) are usually constituted of a large number of interconnected components that may be classified as active or passive components. The active elements are those which can be commanded to control the flow and/or the pressure of water in particular sections of the system, such as pumps and valves. The passive elements are those that cannot be directly commanded, such as pipes and tanks. These elements transport water to demand nodes from the potable water sources at specific pressure levels to satisfy the consumers demand. Moreover, DWNs systems require appropriate instrumentation to perform real-time control actions over the network and manage its performance. Usually, they are managed in a hierarchical control structure which delivers the appropriate control actions to the pumping stations or valves, and local controllers ensure the correct execution and meet the specific requirements in the network.

A WDN can be represented as the one of Figure 4.9, which is composed by sources (water supplies), water demand sectors, and pipelines which interconnect them. It also contains active elements like pumps and valves. The considered DWN corresponds to a subnetwork of the Barcelona water transport network [178].

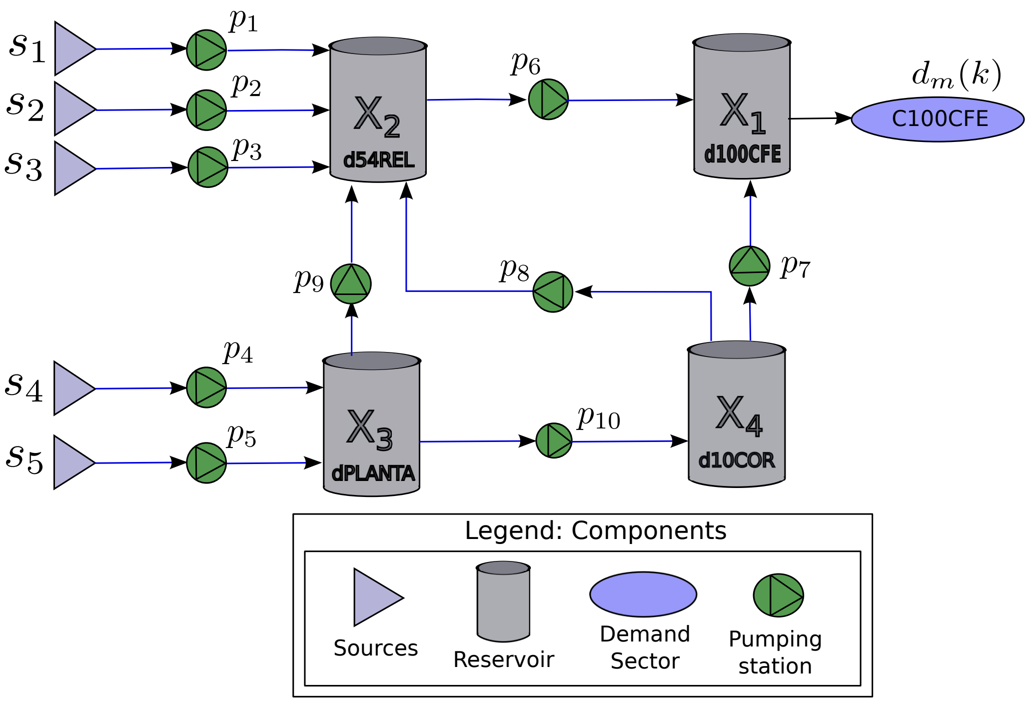

FIGURE 4.9: Drinking water network diagram.

This network consists of 5 sources and 1 sink. It is assumed that the demand forecast at the sink ($d_m(k)$) is known (Figure 4.10), and that any single source can satisfy this required water demand. It is also assumed that the volume of the tanks should be between a minimum and maximum safety levels.

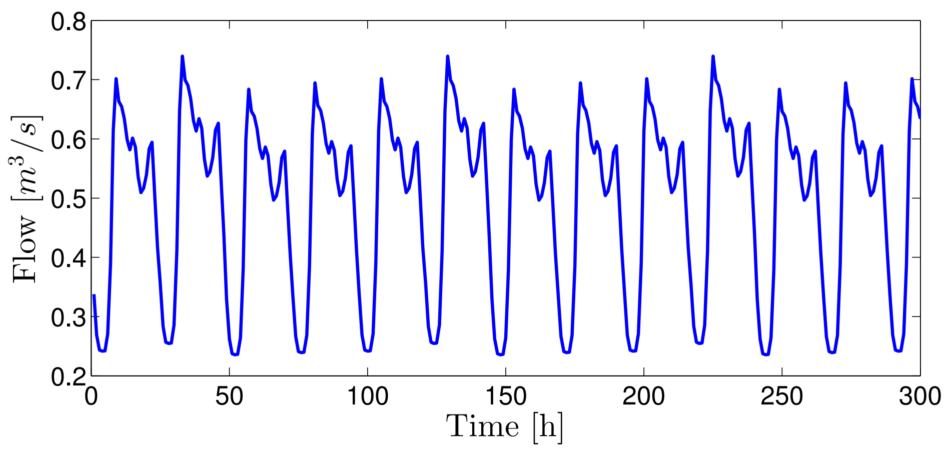

FIGURE 4.10: Drinking water demand.

Regarding the reliability of a DWN, in the literature, it is classified into two main categories. The first one, named *hydraulic reliability*, is related to the probability that a DWN can supply the consumer demands over a specified time interval under specified environmental conditions, i.e., the transport of desired *quantities and qualities* of water at required pressures to desired appropriate locations at desired appropriate times. The second one, named *topological reliability*, refers to the probability that a given network is physically connected given the mechanical reliabilities of its components [119].

This thesis and the methodology proposed here are focused only on the topological reliability. Moreover, the reliability modeling illustrated here concerns only to the active components which can be directly commanded.

The DWN reliability is modeled using a DBN as follows: first, system components must be identified. In this case there are 10 pumps, 5 sources, 4 tanks and several pipes.

Secondly, the minimal path sets should be determined. A minimal path set is composed by those components which allow a flow path between sources and sinks, such as pipes, tanks and pumps. A list of the components that correspond to each minimal path set is presented in Table 4.4. There are nine minimal path sets in the system of Figure 4.9. Each minimal path set is available depending on the reliability of its components.

TABLE 4.4: Components and minimal path sets relationship.

	A_1	A_2	A_3	A_4	A_5	e_1	e_2	e_3	e_4	e_5	e_6	e_7	e_8	e_9	e_{10}
P_1	×					×					×				
P_2		×					×				×				
P_3			×					×			×				
P_4				×					×		×			×	
P_5				×					×			×			×
P_6				×					×		×		×		×
P_7					×					×	×			×	
P_8					×					×		×			×
P_9					×					×	×		×		×

Note that pipes and tanks are considered perfectly reliable so they do not provide significant information to the network. Nevertheless, sources are included in the minimal path sets merely for illustrating the procedure.

Provided the information of Table 4.4, the DBN presented in Figure 4.11 is built as follows: nodes e_i and A_i are drawn for each component. Note that nodes e_i have two time slices in time k and $k+1$ following the approach of Section 4.2.4.

Then, these nodes are interconnected to their minimal path set nodes P_i using arcs. Finally, each minimal path set node is interconnected to the system reliability node S [178].

Initially, at instant $k = 0$, the pumps and the system are assumed to be fully reliable, i.e. their reliability is 1. Then, the probability of each node is computed using their CPT.

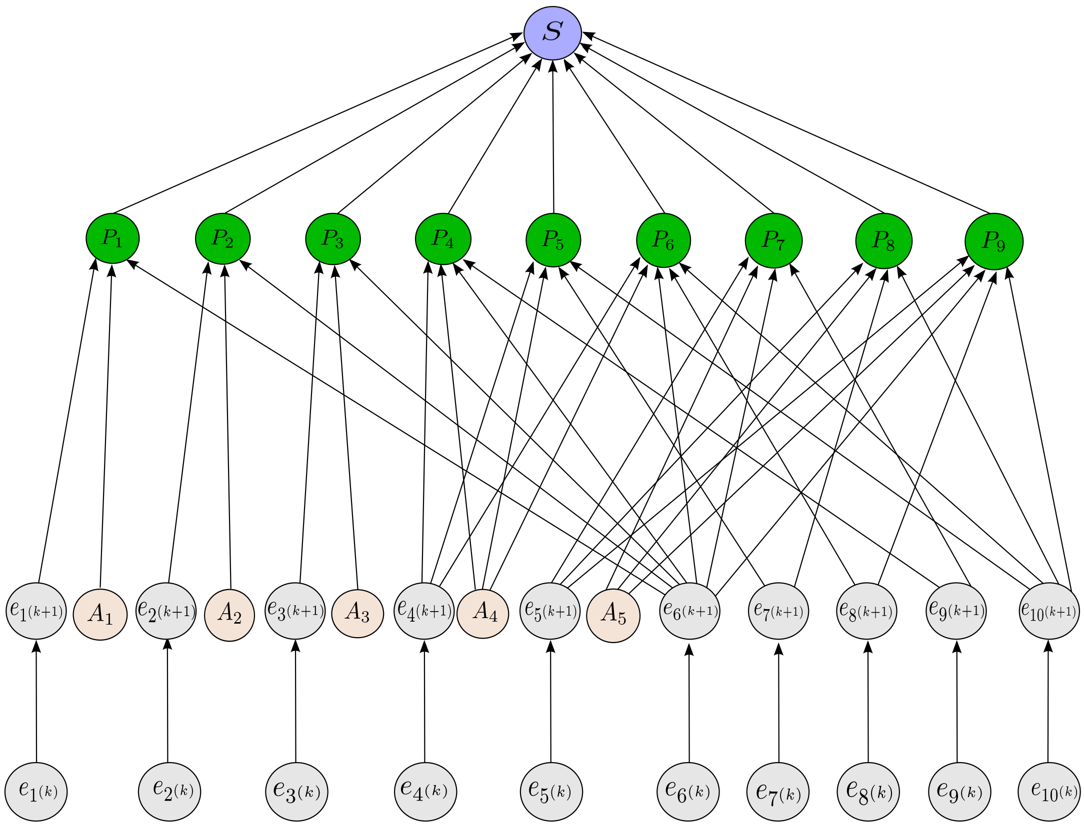

FIGURE 4.11: Dynamic Bayesian network model of the DWN.

At each sampling time, the reliability R_i of each pump is computed according to its failure rate using a MC (Figure 4.11). Its behavior follows an exponential distribution as stated in (3.9). Note that it is independent of the previous states of the component. It only depends on its present state. In the DBN, this corresponds to the CPT shown in Table 4.5.

TABLE 4.5: Inter-time slices CPT for node $e_i(k+1)$.

$e_i(k)$	$e_i(k+1)$	
	Up	Dn
Up	1-$\lambda_i^0 \cdot T_s$	$\lambda_i^0 \cdot T_s$
Dn	0	1

The CPT of node P_1 is shown in Table 4.6. This CPT depends on the states of the source 1 (A_1) and pumps 1 and 5 (e_1, e_5). Its behavior corresponds to an AND gate.

It is assumed that with one source it is possible to satisfy the water demand. Thus, the availability of the system can be assured as long as at least one of paths P_i is available, which corresponds to the CPT of node S shown in Table 4.7. It depends on the state of nodes P_1 to P_9 and has the behavior of an OR gate.

TABLE 4.6: CPTs for nodes P_1.

A_1	$e_1(k+1)$	$e_6(k+1)$	P_1	
			Up	Dn
Up	Up	Up	1	0
Up	Up	Dn	0	1
Up	Dn	Up	0	1
Up	Dn	Dn	0	1
Dn	Up	Up	0	1
Dn	Up	Dn	0	1
Dn	Dn	Up	0	1
Dn	Dn	Dn	0	1

TABLE 4.7: CPT for node S.

P_1	P_2	P_3	$\ldots$	P_9	S	
					Up	Dn
Up	Up	Up	$\ldots$	Up	1	0
Up	Up	Up	$\ldots$	Dn	1	0
-	-	-	$\ldots$	Up	1	0
$\vdots$	$\vdots$	$\vdots$	$\ddots$	$\vdots$	$\vdots$	$\vdots$
Dn	Dn	Dn	$\ldots$	Dn	0	1

4.4 Reliability Importance Measures

There are indices that can be used to take actions according to the analysis made of the system reliability and availability. These measures are frequently of significant value in performing trade-off analysis in system design or suggesting the most efficient way to operate and maintain a system or prioritizing improvement efforts.

Reliability importance measures were first introduced by [12], and they are classified into two groups: Reliability Importance Measures (RIMs) and Structural Importance Measures (SIMs). The RIMs evaluate the relative importance of a component taking into account its contribution to the overall system reliability while the SIMs provide the relative importance of a component taking into account its position into the system structure.

These metrics can be defined either according to their functional aspect, taking into account the minimal path sets, or according to their dysfunctional aspect, considering the minimal cut sets. As both are equivalent, in this thesis only the functional aspect is used.

The aim from the system reliability analysis point of view, is to use the RIMs to identify the weakness or strengths in the system and to quantify the impact of component failures over system functioning.

4.4.1 Birnbaum's Importance Measure

The Birnbaum importance measure [12] also known as Marginal Importance Factor (MIF) is related to the probability of a component to be critical for the system functioning. It is defined as:

Definition 4.1. The B-reliability importance of component i for the functioning of the system, denoted as $I_B(i;\mathbf{p})$, for a coherent system with independent components is defined as:

$$\begin{aligned} I_B(i;\mathbf{p}) =& \Pr(\Phi(\mathbf{X}) = 1|X_i = 1) - \Pr(\Phi(\mathbf{X}) = 1|X_i = 0) \\ =& \frac{\partial R(\mathbf{p})}{\partial p_i} \\ =& R(1_i;\mathbf{p}) - R(0_i;\mathbf{p}). \end{aligned} \tag{4.24}$$

The notation $R(1_i;\mathbf{p})$ denotes the reliability of the system in which the ith components is replaced by an absolutely reliable one, while $R(0_i;\mathbf{p})$ denotes the reliability of the system in which the ith component is failed.

The Birnbaum's measure is the probability that the failure or functioning of the ith component coincides with system failure or functioning. This approach is well known from classical sensitivity analysis. Moreover, it can be interpreted as the maximum lost in system reliability when the ith component changes from the condition of perfect functioning to a failed condition.

Note that Birnbaum's importance measure ($I_B(i;\mathbf{p})$) of the ith component depends only on the structure of the system and the reliabilities of the other components. $I_B(i;\mathbf{p})$ is independent of the actual reliability of the ith component (p_i). This may be regarded as a weakness of Birnbaum's measure.

4.4.2 Critical Reliability Importance Measure

The Critical Reliability Importance, also known as Critical Importance Factor (CIF), was introduced by Lambert [81] and it is defined as:

Definition 4.2. The critical reliability importance of component i for system functioning, denoted by $I_{CIF}(i;\mathbf{p})$, is defined as the probability that ith component works and is critical for the system functioning given that the system is functioning.

$$\begin{aligned} I_{CIF}(i;\mathbf{p}) =& p_i \frac{\Pr(\Phi(\mathbf{X})=1|X_i=1)-\Pr(\Phi(\mathbf{X})=1|X_i=0)}{\Pr(\Phi(\mathbf{X})=1)} \\ =& \frac{p_i}{R(\mathbf{p})} I_B(i;\mathbf{p}). \end{aligned} \tag{4.25}$$

Moreover, this can be interpreted as the probability that the ith component has caused a system failure when it is known that the system is failed.

4.4.3 Fussell-Vesely Reliability Importance Measure

The Fussell-Veselly (FV) importance measure also known as the Diagnostic Importance Factor (DIF) was proposed initially in the context of fault tree [45, 168]. It is classified in c-type and p-type. The c-type FV importance, takes into account the contribution of component to system failure, and its definition is based on minimal cuts. The p-type FV importance, takes into account the contribution of a component to system functioning, and it is derived from the minimal path sets. It represents the probability that at least one minimal path containing the ith component works, given that the system is functioning.
Definition 4.3. The Fussell-Veselly, p-FV (c-FV) reliability importance measure of component i, denoted by $I^p_{DIF}(i;\mathbf{p})$ ($I^c_{DIF}(i;\mathbf{p})$), is defined as the probability that a minimal path (cut) containing the ith component exists and causes system function (failure).

$$\begin{aligned} I^p_{DIF}(i;\mathbf{p}) =& \Pr\{\exists\, \boldsymbol{P} \in \overline{\mathscr{P}}_i\; s.t. X_j = 1\; \forall\, j \in \boldsymbol{P} | \Phi(\mathbf{X}) = 1\} \\ =& \frac{p_i \Pr\{(1_i,\mathbf{X}) : \exists \boldsymbol{P} \in \overline{\mathscr{P}}_i\; s.t.\; X_j = 1\; \forall\, j \in \boldsymbol{P}\}}{R(\mathbf{p})} \\ =& \Pr(X_i = 1 | \phi(\mathbf{X}) = 1) \end{aligned} \tag{4.26}$$

$$\begin{aligned} I^c_{DIF}(i;\mathbf{p}) =& \Pr\{\exists\, \boldsymbol{C} \in \overline{\mathscr{C}}_i\; s.t. X_j = 0\; \forall\, j \in \boldsymbol{C} | \phi(\mathbf{X}) = 0\} \\ =& \frac{q_i \Pr\{(0_i,\mathbf{X}) : \exists\, \boldsymbol{C} \in X_j = 0\; \forall\, j \in \boldsymbol{C}\}}{1 - R(\mathbf{p})} \\ =& \Pr(0_i | \phi(\mathbf{X}) = 0) = \Pr(X_i = 0 | \phi(\mathbf{X}) = 0) \end{aligned} \tag{4.27}$$

where $\boldsymbol{P} \in \overline{\mathscr{P}}_i$ ($\boldsymbol{C} \in \overline{\mathscr{C}}_i$) denotes the minimal path (cut) containing the ith component.

As both are equivalent, the notation I_{DIF} will be used.

I_{DIF} can be interpreted as the probability that the functioning of component i contributes to the functioning of the system given that the system is not failed.

4.4.4 Reliability Achievement Worth

The Reliability Achievement Worth (RAW) describes the increase of the system reliability if the ith component is replaced by a perfect reliable one. It is defined as:

Definition 4.4. The RAW, denoted by $I_{RAW}(i;\mathbf{p})$ qualifies the maximum possible percentage of system reliability increase generated by the ith component. It is expressed as:

$$\begin{aligned} I_{RAW}(i;\mathbf{p}) =& \frac{\Pr(\Phi(1_i,\mathbf{X})=1)}{\Pr(\Phi(\mathbf{X})=1)} \\ =& \frac{\Pr(\Phi(X)=1|X_i=1)}{\Pr(\Phi(\mathbf{X})=1)} \\ =& 1+\frac{q_i}{R(\mathbf{p})}I_B(i;\mathbf{p}). \end{aligned} \tag{4.28}$$

4.4.5 Reliability Reduction Worth, RRW

The Reliability Reduction Worth (RRW) measure [86] reflects the reduction of system reliability if the ith component is failed. It is defined as:

Definition 4.5. The RRW, denoted as $I_{RRW}(i;\mathbf{p})$ expresses the potential damage produced to the system by the failure of the ith component.

$$\begin{aligned} I_{RRW}(i;\mathbf{p}) =& \frac{Pr(\Phi(\mathbf{X})=1)}{\Pr(\Phi(0_i,\mathbf{X})=1)} \\ =& \frac{\Pr(\Phi(\mathbf{X})=1)}{\Pr(\Phi(\mathbf{X})=1|X_i=0)} \\ =& \frac{1}{1-\frac{p_i}{R(\mathbf{p})}I_B(i;\mathbf{p})}. \end{aligned} \tag{4.29}$$

4.5 Example

For the computation of the RIMs consider the DWN system described in Example 4.3. it is supposed that sources, tanks ans pipelines are perfectly reliable and only actuators are affected by a loss of reliability according to (3.9).

The aim of computing the RIMs in this example is to know, from different points of view, the importance of the pumps reliability to the overall system reliability. In this Section it is done in a static approach, since the failure rate is constant. Later, in Section 6.3.5, the analysis is done dynamically taking into account the evolution of the failure rate.

First of all, a static RIM analysis is performed in order to get better knowledge on them. Component reliability is assumed to follow (3.9) with λ_i (Table 4.8) and the mission time is $t = T_M$ (2000 hours). The corresponding results are presented in Table 4.9 and Table 4.10.

TABLE 4.8: Pump failure rates

$\lambda\ [h^{-1} \cdot 10^{-4}]$									
p_1	p_2	p_3	p_4	p_5	p_6	p_7	p_8	p_9	p_{10}
9.85	10.70	10.50	1.40	0.85	0.80	11.70	0.60	0.74	0.78

TABLE 4.9: Pumps Reliability Importance Measures at T_M=2000

Pump	$\lambda\ [\cdot 10^{-4}]$	R_i [%]	I_B[%]	I_{DIF}[%]	I_{CIF}[%]	I_{RAW}[%]	I_{RRW}[%]
p_1	9.85	13.94	4.54	14.61	0.77	0.10	0.10
p_2	10.70	11.76	4.43	12.32	0.63	0.10	0.10
p_3	10.50	12.24	4.45	12.83	0.66	0.10	0.10
p_4	1.40	75.57	8.78	77.54	8.05	0.10	0.11
p_5	0.85	84.37	13.72	86.56	14.04	0.10	0.11
p_6	0.80	85.21	87.48	98.58	90.39	0.11	1.04
p_7	11.70	9.63	12.89	10.99	1.50	0.11	0.10
p_8	0.60	88.69	5.81	89.40	6.25	0.10	0.11
p_9	0.74	86.24	12.66	88.06	13.24	0.10	0.11
p_{10}	0.78	85.55	8.11	86.77	8.42	0.10	0.11

In Table 4.10 pumps are sorted according to their reliability importance measures. Remark that pump 6 is the most critical according to all RIMs. It is also interesting to highlight that some RIMs give a similar pump criticality order: CIF and RRW are equivalent, and MIF provides a close result.

This *a priori* knowledge can be used to decide how to distribute the control efforts through the control algorithm. A dynamical RIM analysis will be presented in Section 6.3.5.

4.6 Conclusions

In this chapter, the system reliability computation from the reliability of its components or subsystems has been presented. Basically, this can be done by using the system configuration structure, i.e. serial and parallel systems, and its corresponding expression or in the case of complex system configurations by using the pivotal decomposition method.

TABLE 4.10: *A priori* classification of the pumps

λ_i	R_i	I_B	I_{DIF}	I_{CIF}	I_{RAW}	I_{RRW}
p_7	p_8	p_6	p_6	p_6	p_6	p_6
p_2	p_9	p_5	p_8	p_5	p_7	p_5
p_3	p_{10}	p_7	p_9	p_9	p_1	p_9
p_1	p_6	p_9	p_{10}	p_{10}	p_2	p_{10}
p_4	p_5	p_4	p_5	p_4	p_3	p_4
p_5	p_4	p_{10}	p_4	p_8	p_4	p_8
p_6	p_1	p_8	p_1	p_7	p_5	p_7
p_{10}	p_3	p_1	p_3	p_1	p_9	p_1
p_9	p_2	p_3	p_2	p_3	p_{10}	p_3
p_8	p_7	p_2	p_7	p_2	p_8	p_2

It has also addressed the concepts of MC, BN, and DBN. These concepts have been applied to model the reliability of a DWN system.

In this chapter, a review of the available RIMs has been performed. These reliability index measures have been evaluated for a DWN system as a tool to identify the importance of each pump to the system functioning.

The RIMs have shown to be an objective criterion that can be used to redistribute the control effort among the available system actuators to avoid, for instance, their degradation.

Chapter 5

Control System

This chapter addresses the concepts involved in control systems and presents the control approaches used in this thesis. Those control methodologies include the Model Predictive Control (MPC) and the Linear-Quadratic Regulator (LQR), which can be used to implement a Health-Aware Control scheme as it will be demonstrated later.

5.1 Model Predictive Control

Model Predictive Control (MPC) was developed in the 70's and has evolved considerably providing a wide range of control methods that have in common the use of an explicit model of the process to calculate the future control input by the minimization of an objective function. These controller design methods lead to schemes which basically have the following ideas [18]:

- The use of an explicit model to predict the process output at future time instants (prediction horizon).
- The computation of a control sequence that involves the minimization of an objective function.
- A receding strategy which slides the prediction horizon towards the future at each time instant, and the application at each step of the first element of the computed control sequence.

This control method has the following advantages:

- It involves very intuitive concepts which make it relatively easy to implement and tune.
- It can be used to control a wide variety of processes, from those with simple dynamics to those with long delay times or nonminimum phase or unstable.

- It can be extended to the multivariable case.
- It naturally introduces the feed forward action to compensate measurable disturbances.
- Constraints can be considered in the design process.
- It is an open methodology which allows future extensions.

As any other control approach, it also has its drawbacks. One of these is the large computation time needed for its implementation in systems with fast dynamics where real-time operation is required. Computational time increases, even more, when constraints are considered. In a system with simple dynamics or high sampling time, this is not a problem [18].

Moreover, the weakest point in this control method is the need of a suitable model of the process. In the design algorithm, a prior knowledge of the model is fundamental, and the results are affected by the discrepancies between the real process and its model.

5.1.1 MPC strategy

Model-based predictive control (MPC) is a discrete-time technique where an explicit dynamic model of the plant is considered to predict the system outputs over a finite prediction horizon (H_p), while control actions are manipulated throughout a finite control horizon (H_c) in order to minimize a given cost function, with $H_c < H_p$.

This strategy is implemented using the scheme shown in Figure 5.1, where the predicted future system outputs are computed using a model of the system and the proposed optimal future control actions. The control actions are computed by optimizing a given cost function and its constraints.

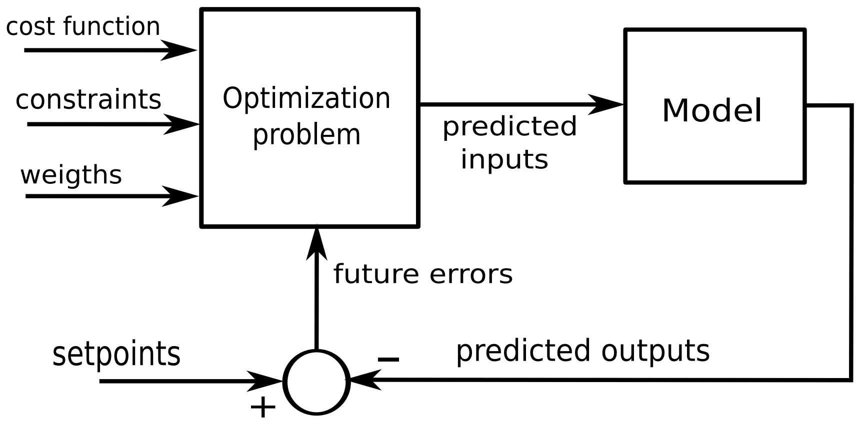

FIGURE 5.1: Basic structure of a Model Predictive Control

In order to explain the MPC technique, consider the following discrete-time linear dynamic model of a system described in the state-space form as:

$$\begin{aligned} x(k+1) &= Ax(k) + Bu(k) \\ y(k) &= Cx(k) \end{aligned} \tag{5.1}$$

where for each $k \in \mathbb{Z}^+, x(k) \in \mathbb{R}^n$ is the state, $u(k) \in \mathbb{R}^p$ is the control input, $y(k) \in \mathbb{R}^q$ is the measured output, $A \in \mathbb{R}^{n\times n}$ is the state matrix, $B \in \mathbb{R}^{q\times p}$ is the input matrix and $C \in \mathbb{R}^{q\times n}$ is the output matrix.

A prediction model is obtained by applying (5.1) recursively along the prediction horizon, obtaining (5.2), where $u(k+j|k)$ is the predicted control input and $\hat{y}(k+j|k)$ is the predicted output, corresponding to $k+j$ computed at time instant k. If control inputs $\Delta u(k+j|k)$ must be specified, equation (5.3) can be used.

$$\underbrace{\begin{bmatrix} \hat{y}(k+1|k) \\ \hat{y}(k+2|k) \\ \vdots \\ \hat{y}(k+H_p|k) \end{bmatrix}}_{\hat{Y}} = \underbrace{\begin{bmatrix} CA \\ CA^2 \\ \vdots \\ CA^{H_p} \end{bmatrix}}_{\Theta} x(k) + \underbrace{\begin{bmatrix} CB & 0_{q\times p} & \cdots & 0_{q\times p} \\ CAB & CB & \cdots & 0_{q\times p} \\ \vdots & \vdots & \ddots & 0_{q\times p} \\ CA^{H_p-1}B & CA^{H_p-2}B & \cdots & \sum\limits_{i=0}^{H_p-H_c} CA^iB \end{bmatrix}}_{\Omega} \underbrace{\begin{bmatrix} \hat{u}(k|k) \\ \hat{u}(k+1|k) \\ \vdots \\ \hat{u}(k+H_c-1|k) \end{bmatrix}}_{\hat{U}} \tag{5.2}$$

$$\underbrace{\begin{bmatrix} \hat{u}(k|k) \\ \hat{u}(k+1|k) \\ \vdots \\ \hat{u}(k+H_c-1|k) \end{bmatrix}}_{\hat{U}} = \underbrace{\begin{bmatrix} I_p & 0_{p\times p} & \cdots & 0_{p\times p} \\ I_p & I_p & \cdots & 0_{p\times p} \\ \vdots & \vdots & \ddots & \vdots \\ I_p & I_p & \cdots & I_p \end{bmatrix}}_{T_{H_c}^{I_p}} \underbrace{\begin{bmatrix} \Delta\hat{u}(k|k) \\ \Delta\hat{u}(k+1|k) \\ \vdots \\ \Delta\hat{u}(k+H_c-1|k) \end{bmatrix}}_{\Delta\hat{U}} + \underbrace{\begin{bmatrix} I_{p\times p} \\ I_{p\times p} \\ \vdots \\ I_{p\times p} \end{bmatrix}}_{[I_p]_{H_c}} \hat{u}(k-1) \, . \tag{5.3}$$

The control input values are obtained by the minimization of a cost function. The resulting first control action $\hat{u}(k|k)$ is injected to the system while $\hat{u}(k+i|k)\ \forall\ i = 1, ..., H_c - 1$ are discarded. At next time instant $k+1$, $y(k+1)$ is measured and the optimization problem is solved again. Thus, $\hat{u}(k+1|k+1)$ is calculated moving the prediction horizon forward, following the sliding window concept [18]. This methodology is represented in Figure 5.2, where the past outputs and control input sequences (shown in the left side) are used to compute the future output sequence over H_p and future control inputs sequences over H_c, such that the cost function is minimized.

The cost function generally includes a term for the tracking error and the control actions, among others. For instance, the optimization problem (5.3) aims at minimizing the square

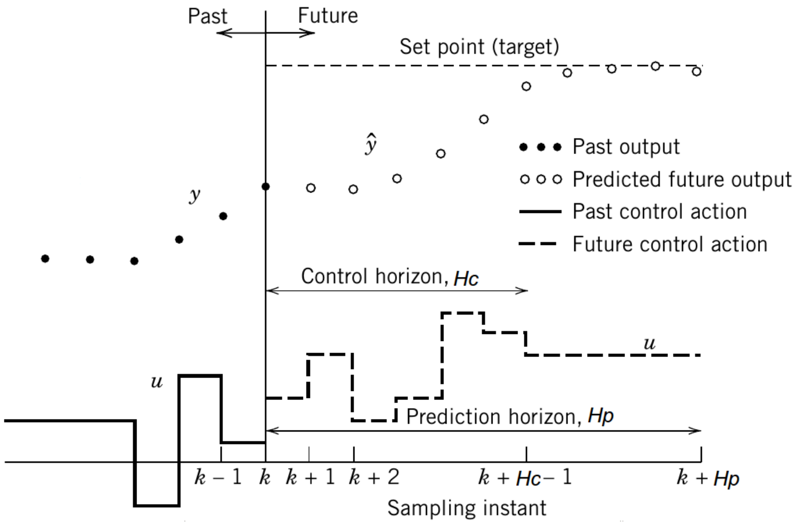

FIGURE 5.2: Model Predictive Control basic concept.

of the tracking error, and the square of the energy and its increments.

$$\begin{aligned}
\underset{\substack{(\hat{u}(k|k),...,\\ \hat{u}(k+H_c-1|k))\\ \Delta\hat{u}(k|k),...,\\ \Delta\hat{u}(k+H_c-1|k))}}{\text{minimize}} \quad & J(k) = \sum_{j=0}^{H_p-1}\sum_{i=1}^{q}\alpha_i(k)\left(\hat{y}_i(k+j|k) - y_{ref,i}(k)\right)^2 \\
& + \sum_{j=0}^{H_c-1}\sum_{i=1}^{p}\rho_i(k)\hat{u}_i(k+j|k)^2 + \sum_{j=0}^{H_c-1}\sum_{i=1}^{p}\delta_i(k)\Delta\hat{u}_i(k+j|k)^2 \\
\text{subject to} \quad & \underline{\boldsymbol{u}} \le \hat{\boldsymbol{u}}(k+j|k) \le \overline{\boldsymbol{u}} \quad j = 0,..,H_c-1 \\
& \underline{\boldsymbol{y}} \le \hat{\boldsymbol{y}}(k+i|k) \le \overline{\boldsymbol{y}} \quad i = 1,..,H_p
\end{aligned} \tag{5.4}$$

where $y_{ref,i}$ is the ith output reference, α_i is the weight for the tracking error, ρ_i is the weight for the energy, δ_i is the weight for the energy variations, and $\underline{\boldsymbol{u}}$, $\overline{\boldsymbol{u}}$, $\underline{\boldsymbol{y}}$ and $\overline{\boldsymbol{y}}$, are the lower and upper bounds of the control effort and system outputs, respectively.

Such optimization problem can be casted as the Quadratic Programing (QP) problem (5.5) by introducing (5.2) and (5.3) into (5.4).

$$\begin{aligned}
\underset{\Delta\hat{U}}{\text{minimize}} \quad & \tfrac{1}{2}\Delta\hat{U}^T H \Delta\hat{u} + b^T\Delta\hat{U} \\
\text{s.t.} \quad & Ar\Delta\hat{U} \le br \\
& Br\hat{Y} \le cr \\
& lb \le \hat{Y} \le ub,
\end{aligned} \tag{5.5}$$

where:

$$H = 2(\tilde{\boldsymbol{\delta}} + [T_{Hc}^{Ip}]^T\Omega^T\tilde{\boldsymbol{\alpha}}\Omega[T_{Hc}^{Ip}] + [T_{Hc}^{Ip}]^T\tilde{\boldsymbol{\rho}}[T_{Hc}^{Ip}]) \tag{5.6}$$

$$b = 2\Big(u(k-1)^T[I_p]_{Hc}^T\Omega^T\tilde{\boldsymbol{\alpha}}\Omega T_{Hc}^{Ip} + x(k)^T\Theta^T\tilde{\boldsymbol{\alpha}}\Omega T_{Hc}^{Ip} \\ + u(k-1)^T[I_p]_{Hc}^T\tilde{\boldsymbol{\rho}}T_{Hc}^{Ip} - Y_{ref}^T\tilde{\boldsymbol{\alpha}}\Omega T_{Hc}^{Ip}\Big) \tag{5.7}$$

$$Ar = \begin{bmatrix} T_{Hc}^{Ip} \\ -T_{Hc}^{Ip} \end{bmatrix} \tag{5.8}$$

$$br = \begin{bmatrix} [I_p]_{Hc}\overline{\boldsymbol{u}} - [I_p]_{Hc}u(k-1) \\ [I_p]_{Hc}(-\underline{\boldsymbol{u}}) + [I_p]_{Hc}u(k-1) \end{bmatrix} \tag{5.9}$$

$$Br = \begin{bmatrix} \Omega T_{Hc}^{Ip} \\ -\Omega T_{Hc}^{Ip} \end{bmatrix} \tag{5.10}$$

$$cr = \begin{bmatrix} [I_n]_{Hp}\overline{\boldsymbol{y}} - \Theta x(k) - \Omega[I_p]_{Hc}u(k-1) \\ -[I_n]_{Hp}\underline{\boldsymbol{y}} + \Theta x(k) + \Omega[I_p]_{Hc}u(k-1) \end{bmatrix}, \tag{5.11}$$

and $[I_n]_{Hp}$ is block column matrix composed by $H_p \times 1$ blocks of identity matrices of $n \times n$; and T_{Hc}^{Ip} is a block lower triangular matrix composed by $H_c \times H_c$ blocks of identity matrices of $p \times p$, and $\tilde{\boldsymbol{\alpha}}$ is a block diagonal matrix composed by H_p blocks of matrix $\boldsymbol{\alpha}$ =diag$(\alpha_1, \alpha_1, ..., \alpha_q)$, and $\tilde{\boldsymbol{\rho}}$ and $\tilde{\boldsymbol{\delta}}$ are block diagonal matrices composed by H_c blocks of matrices $\boldsymbol{\rho}$ =diag$(\rho_1, \rho_2, ..., \rho_p)$ and $\boldsymbol{\delta}$ =diag$(\delta_i, \delta_2, ..., \delta_p)$, respectively.

Alternatively, the optimization problem can be defined by using a linear cost function. For instance,

$$J(k) = \sum_{j=1}^{H_p}\sum_{i=1}^{q} \mu_i \left|\hat{y}_i(k+j|k) - y_{ref,i}(k+j)\right| + \\ + \sum_{j=1}^{H_c}\sum_{i=1}^{p} \left[\alpha_i \left|\hat{u}_i(k+j-1|k)\right| + \rho_i \left|\Delta\hat{u}_i(k+j-1|k)\right|\right], \tag{5.12}$$

where μ_i, α_i, and ρ_i are weighting factors for the tracking error, the control input and the control input increments, respectively.

Let $\lambda \in \mathbb{R}^q$, $\theta \in \mathbb{R}^p$, $\phi \in \mathbb{R}^p$ and $\eta \in \mathbb{R}$ [18] be such that

$$\begin{array}{rcccl} -\lambda_i(k+j) & \le & \hat{y}_i(k+j|k) - r_i(k+j) & \le & \lambda_i(k+j)\ \forall\, i = 1,\cdots,q \text{ and } j = 1,\cdots,H_p \\ -\theta_i(k+j) & \le & \hat{u}_i(k+j-1|k) & \le & \theta_i(k+j)\ \forall\, i = 1,\cdots,p \text{ and } j = 1,\cdots,H_c \\ -\phi_i(k+j) & \le & \Delta\hat{u}_i(k+j-1|k) & \le & \phi_i(k+j)\ \forall\, i = 1,\cdots,p \text{ and } j = 1,\cdots,H_c \end{array} \tag{5.13}$$

$$0 \le \sum_{j=1}^{H_p}\sum_{i=1}^{q}\lambda_i(k+j) + \sum_{j=1}^{H_c}\sum_{i=1}^{p}\alpha_i\theta_i(k+j) + \sum_{j=1}^{H_c}\sum_{i=1}^{p}\rho_i\phi_i(k+j) \le \eta(k). \tag{5.14}$$

So, $\eta(k)$ is an upper bound for the cost function J and the optimization problem now involves minimizing the upper bound η as follows:

$$\underset{\left(\Delta\hat{U}(k),\Lambda(k),\Theta(k),\Phi(k),\eta(k)\right)}{\text{minimize}} \quad \eta(k) \tag{5.15}$$

subject to

$$\begin{array}{rcccl} -\mathit{\Lambda}(k) & \leq & \Theta x(k)\Omega T_{H_c}^{I_p}\Delta\hat{U}(k) + \Omega[I_p]_{H_c}u(k-1) - Y_{ref} & \leq & \mathit{\Lambda}(k) \\ -\mathit{\Theta}(k) & \leq & T_{H_c}^{I_p}\Delta\hat{U}(k) + [I_p]_{H_c}u(k-1) & \leq & \mathit{\Theta}(k) \\ -\mathit{\Phi}(k) & \leq & \Delta\hat{U}(k) & \leq & \mathit{\Phi}(k) \\ 0 & \leq & [\mu]_{H_p}^T\mathit{\Lambda}(k) + [\rho]_{H_p}^T\mathit{\Theta}(k) + [\alpha]_{H_c}^T\mathit{\Phi}(k) & \leq & \eta(k) \end{array} \tag{5.16}$$

where $\mu = [\mu_1\mu_2\cdots\mu_q]^T$, $\alpha = [\alpha_1\alpha_2\cdots\alpha_q]^T$, $\rho = [\rho_1\rho_2\cdots\rho_q]^T$,

$$\mathit{\Lambda}(k) = \begin{bmatrix} \lambda(k+1) \\ \lambda(k+2) \\ \vdots \\ \lambda(k+H_p) \end{bmatrix}, \tag{5.17}$$

$$\mathit{\Theta}(k) = \begin{bmatrix} \theta(k+1) \\ \theta(k+2) \\ \vdots \\ \theta(k+H_c) \end{bmatrix}, \text{and} \tag{5.18}$$

$$\mathit{\Phi}(k) = \begin{bmatrix} \phi(k+1) \\ \phi(k+2) \\ \vdots \\ \phi(k+H_c) \end{bmatrix}. \tag{5.19}$$

The inequalities in (5.16) can be rewritten as:

$$\Omega T_{H_c}^{I_p}\Delta\hat{U}(k) - \mathit{\Lambda}(k) \leq -\Theta x(k) - \Omega[I_p]_{H_c}u(k-1) + Y_{ref} \tag{5.20}$$

$$-\Omega T_{H_c}^{I_p}\Delta\hat{U}(k) - \mathit{\Lambda}(k) \leq \Theta x(k) + \Omega[I_p]_{H_c}u(k-1) - Y_{ref} \tag{5.21}$$

$$T_{H_c}^{I_p} - \mathit{\Theta}(k) \leq -[I_p]_{H_c}u(k-1) \tag{5.22}$$

$$-T_{H_c}^{I_p} - \mathit{\Theta}(k) \leq [I_p]_{H_c}u(k-1) \tag{5.23}$$

$$\Delta\hat{U}(k) - \mathit{\Phi}(k) \leq 0_{pH_c} \tag{5.24}$$

$$-\Delta\hat{U}(k) - \mathit{\Phi}(k) \leq 0_{pH_c} \tag{5.25}$$

$$[1]_{qH_p}^T\mathit{\Lambda}(k) + [\rho]T_{H_c}^{I_p}\mathit{\Theta}(k) + [\alpha]T_{H_c}^{I_p}\mathit{\Phi}(k) - \eta(k) \leq 0 \tag{5.26}$$

$$-[1]_{qH_p}^T\mathit{\Lambda}(k) - [\rho]T_{H_c}^{I_p}\mathit{\Theta}(k) - [\alpha]T_{H_c}^{I_p}\mathit{\Phi}(k) \leq 0 \tag{5.27}$$

and the constraints in the control efforts as

$$\begin{bmatrix} T_{H_c}^{I_p} \\ -T_{H_c}^{I_p} \\ [I_p]_{H_c} \\ -[I_p]_{H_c} \end{bmatrix} \Delta\hat{U} \leq \begin{bmatrix} [I_p]_{H_c}(\overline{u} - u(k-1)) \\ [I_p]_{H_c}(u(k-1) - \underline{u}) \\ [I_p]_{H_c}\Delta\overline{u} \\ -[I_p]_{H_c\Delta\underline{u}} \end{bmatrix}. \tag{5.28}$$

Finally, optimization problem can (5.15)-(5.16) be written as the following Linear Programming (LP) problem:

$$\begin{aligned} \underset{a(k)}{\text{minimize}} \quad & c^T a(k) \\ \text{s.t.} \quad & f_1 a(k) \leq b_1(k) \end{aligned} \tag{5.29}$$

where

$$a(k) = \begin{bmatrix} \Delta\hat{U}(k) \\ \Lambda(k) \\ \Theta(k) \\ \Phi(k) \\ \eta(k) \end{bmatrix}, \tag{5.30}$$

$$c = \begin{bmatrix} [0_p]_{H_c} \\ [0_q]_{H_p} \\ [0_p]_{Hc} \\ [0_p]_{Hc} \\ 1 \end{bmatrix}, \tag{5.31}$$

$$f_1 = \begin{bmatrix} \Omega T_{H_c}^{I_p} & -I_{qH_p} & 0_{qH_p \times pH_c} & 0_{qH_p \times pH_c} & 0_{qH_c} \\ -\Omega T_{H_c}^{I_p} & -I_{qH_p} & 0_{qH_p \times pH_c} & 0_{qH_p \times pH_c} & 0_{qH_c} \\ T_{H_c}^{I_p} & 0_{pH_c \times qH_p} & -[I]_{H_c} & 0_{pH_c \times pH_c} & 0_{pH_c} \\ [I]_{H_c} & 0_{pH_c \times qH_p} & 0_{pH_c \times pH_c} & -I_{pH_c} & 0_{pH_c} \\ -[I]_{H_c} & 0_{pH_c \times qH_p} & 0_{pH_c \times pH_c} & -I_{pH_c} & 0_{pH_c} \\ 0_{pH_c}^T & [\mu]_{qH_p}^T & [\rho]_{H_c}^T & [\alpha]_{H_c}^T & -1 \\ 0_{pH_c}^T & -[\mu]_{qH_p}^T & -[\rho]_{H_c}^T & -[\alpha]_{H_c}^T & 0 \\ [I_p]_{H_c} & 0_{pH_c \times qH_p} & 0_{pH_c \times pH_c} & 0_{pH_c \times pH_c} & 0_{pH_c} \\ -[I_p]_{H_c} & 0_{pH_c \times qH_p} & 0_{pH_c \times pH_c} & 0_{pH_c \times pH_c} & 0_{pH_c} \\ [I_p]_{H_c} & 0_{pH_c \times qH_p} & 0_{pH_c \times pH_c} & 0_{pH_c} & 0_{pH_c} \\ -[I_p]_{H_c} & 0_{pH_c \times qH_p} & 0_{pH_c \times pH_c} & 0_{pH_c \times pH_c} & 0_{pH_c} \end{bmatrix}, \tag{5.32}$$

and

$$b_1(k) = \begin{bmatrix} -\Theta x(k) - \Omega I_p u(k-1) + Y_{ref} \\ \Theta x(k) + \Omega I_p u(k-1) - Y_{ref} \\ -[I_p]_{H_c} u(k-1) \\ [I_p]_{H_c} u(k-1) \\ 0_{pH_c \times 1} \\ 0_{pH_c \times 1} \\ 0 \\ 0 \\ [I_p]_{H_c}(\overline{u} - u(k-1)) \\ [I_p]_{H_c}(u(k-1) - \underline{u}) \\ [I_p]_{H_c}\Delta\overline{u} \\ -[I_p]_{H_c}\Delta\underline{u} \end{bmatrix}. \tag{5.33}$$

5.2 Linear-Quadratic Regulator

The Linear-Quadratic Regulator (LQR) is a well known control design technique that provides feedback gains in a practical manner [114].

Consider the discrete-time, linear time-invariant (LTI) system given in (5.1), and given a cost function defined in a quadratic form as:

$$J_{LQR} = \frac{1}{2}\sum_{k=0}^{\infty}\left(x^T(k)Q_{LQR}x(k) + u^T(k)R_{LQR}u(k)\right) \tag{5.34}$$

where $Q_{LRQ} \in \mathbb{R}^{n_x \times n_x}$ and $R_{LRQ} \in \mathbb{R}^{n_u \times n_u}$ are Hermitian positive-definite matrices. If the system is controllable and observable, a feedback control law can be defined as:

$$u(k) = -Kx(k) \tag{5.35}$$

where the optimal feedback gain (K) is the solution of the cost function (5.34):

$$K = \left(R_{LQR} + B^T PB\right)^{-1} B^T PA. \tag{5.36}$$

The positive-definite symmetric matrix P is the solution of the discrete-time algebraic Riccati equation:

$$P = Q_{LQR} + A^T PA - A^T PB(R_{LQR} + B^T PB)^{-1}B^T PA. \tag{5.37}$$

The aim of the cost function in this thesis is to use matrix R_{LQR} as a weighting matrix for the control effort and to redistribute the control input over the available actuators based on their reliability information, while matrix Q_{LQR} is used to weight the system states for trajectory tracking.

5.3 Conclusions

This chapter presented the control methodologies used in the development of the thesis. In the case of MPC methodology, the optimization problem has been formulated using both, a common quadratic and linear cost functions which include terms for minimize the control action and its variations, and depending the control problem it can include a term for the minimization of the tracking error.

At the first glance, both, MPC and LQR are optimal control techniques, but they differ from the fact that MPC solves the optimization problem in a finite time horizon and uses the receding horizon approach, while LQR solves an optimization problem over an infinity time horizon. An important feature of MPC is the possibility of explicitly including input and state constraints in the control law.

In the MPC technique, its weights play an important role in solving the problem. The tune of these parameters can lead to aggressive control responses when the ratio between tracking error and control effort weights is larger. Also, larger horizon prediction produces a more "optimal" controller but increases it complexity.

Nevertheless, the control effort weights of both, MPC and LQR, can be selected in order to assign more or less relative importance to each actuator producing lower or higher relative actuator use. This fact can be used to assign weights according to actuators reliabilities or RIMs and in this manner achieve better levels of system reliability.

An open issue that requires further research is the procedure to obtain a cost function that can include other terms for their minimization but maintain its simplicity. However, it can lead to a nonlinear or non-convex optimization process whose solution is computationally heavy and could lead to non-implementable control schemes.

Part II

Contributions

Chapter 6

Health-Aware Control

This chapter presents the integration of reliability (as a measure of the health of the system or its components) in the control objectives in order to avoid the occurrence of catastrophic and incipient faults. Reliability analysis and failures concern the actuators of the system. This integration is formulated using the reliability importance measures in the parameters of the optimization function. The sensitivity of the system reliability to the degradation of its actuators due to their working load produced by the control action is key to redistribute the control efforts.

MPC and LQR techniques are investigated to implement such HAC approach. MPC will be applied to a DWN, and to a multirotot UAV. Moreover, an approach to reduce the degradation of system components is applied to a Twin Rotor system using MPC.

6.1 Reliability assessment for HAC

Definition 3.1 and (3.9), the reliability of the ith component of the system will be modeled using the exponential function as:

$$R_i(t) = e^{-\int_0^t \lambda_i(v)dv} \ \ \forall\, i = 1, \ldots, p,$$

where $\lambda_i(t)$ is the failure rate depending on time.

In this thesis, the overall system reliability will be computed from the reliability of its components using the Bayesian networks (see Section 4.2). Moreover, it is assumed that the overall system reliability is computed by the reliability of its actuators since they are key in achieving the system controllability. Nevertheless, this methodology could be extended to other components of the system. For instance, in a DWN, the reliability of the pipelines could be modeled as a function of the water flow and pressure [5, 80] and include it into the overall system reliability computation, or the reliability of the reservoirs could be modeled as a function of their operational time and the volume of water they store.

In any case, to achieve the goal of boosting system reliability, reliability computation should depend on controlled variables, such as voltage, current, flow, pressure, etc.

6.1.1 Failure rate

The failure rate of the actuator varies with time and the actuator usage. The failure rate in the useful life period of the actuator is assumed to depend on the impact of the load (usage) and its age.

In this thesis, and adaptation of the PrHM, proposed by Cox [30], and defined as (3.25) is used:

$$\lambda_i(t) = \lambda_i^0 \cdot g(u) \ \ \forall\, i = 1, \ldots, p, \tag{6.1}$$

where λ_i^0 is the baseline failure rate (nominal failure rate) for the ith actuator, and $g(u)$ represents the effect of the covariates depending on the applied load u. In here, is it assumed that the parameter λ_i^0 is equivalent to a constant h_0, and $g(u)$ is equivalent to $\psi(\gamma \boldsymbol{z})$, given in (3.25).

Different definitions of function $g(u)$ exists in the literature. However, the exponential form is the most commonly used. In [74, 75] the authors propose a load function based on the root-mean-square of the applied control input (u_i) up to the end of the mission (T_M), and an actuator parameter defined from the upper and lower bounds of control input.

In Guenab [57] a load function is proposed as:

$$g_i(u) = e^{\alpha\, u_i^{prom}} \quad \forall\, i = 1, ..., p, \tag{6.2}$$

where u_i^{prom} is the average level of the applied control.

In [55], the covariate function is defined as:

$$g_i(u) = e^{\beta_i ||u_{i,o:k}||_2^2} \quad \forall\, i = 1, ..., p, \tag{6.3}$$

where $\beta_i = (t_M(u_{i,max} - u_{i,min}))^{-1}$ is a shape parameter of the actuator failure for an expected life t_M.

In [74], the authors propose:

$$g_i(u) = e^{\beta_i \int_0^{t_M} u_i^2(t)dt} \quad \forall\, i = 1, ..., p, \tag{6.4}$$

where the load function is defined according to the root-mean-square of the applied control input until the end of the mission (t_M), and β_i is an actuator parameter defined as: $\beta_i = (t_M(\bar{u}_i - \underline{u}_i))^{-1}$, and $\bar{u}_i$ and $\underline{u}_i$ are the upper and lower saturation bound of u_i, respectively.

Another expression proposed in [75] is defined as:

$$g_i(u) = e^{\alpha\, u^i_{nom}} \quad \forall\, i = 1, ..., p, \tag{6.5}$$

where α is a fixed factor depending on the actuator property, u^i_{nom} is the nominal control law delivered by the ith actuator to achieve the control objective.

In this thesis, different definitions of the covariate function have been studied. Initially, in [143, 144, 146], the covariate function used represents the amount of load on the actuator corresponding to the normalized instantaneous actuator usage at each sampling time:

$$g_i(u) = \frac{u_i(k) - \underline{u}_i}{\overline{u}_i - \underline{u}_i} \quad \forall\, i = 1, ..., p, \tag{6.6}$$

where $u_i(k)$ is the control effort at time k, $\underline{u}_i$ and $\overline{u}_i$ are the minimum and maximum control efforts allowed for the ith actuator. In this case, the highest actuator load corresponds to $u_i(k) = \overline{u}_i$, which leads to the highest failure rate $\lambda_i = \lambda_i^0$.

Expression (6.6) takes into account the impact of the load at each time instant but not the previous time. In order to include the historical use, equivalent to the age of the actuator, the following covariate function was proposed in [139, 141]:

$$g_i(u(t)) = 1 + \beta_i \int_0^t |u_i(v)|dv \;\; \forall\, i = 1, \dots, p, \tag{6.7}$$

where $g_i(u_i(t))$ is defined as the cumulative applied control effort of the ith actuator from the beginning of the mission up to time instant t_f and β_i is a constant parameter.

Using (6.1) in (6.7) it yields,

$$\lambda_i(t) = \lambda_i^0 \left(1 + \beta_i \int_0^t |u_i(v)|dv\right) \;\; \forall\, i = 1, \dots, p \tag{6.8}$$

this definition implies that actuators are under a constant reliability decay due to the baseline failure rate which is increased when the actuators are used.

Expressions (6.6) to (6.3) only take into account the asset load as a factor in the covariate, whereas the definition (6.8) represents a more realistic situation because it takes into account not only the load of the asset but also the aging produced by the pass of the time.

6.2 Health-Aware Control approaches

In the proposed HAC approach, the controller is enriched with system health information provided by a monitoring module and, an accommodation process is performed to tackled the actuators degradation by adjusting the controller parameters. Figure 6.1 presents a generic block diagram of the proposed approach, where the cost function of an optimal control strategy is tuned up on the basis of health information provided by the monitoring module.

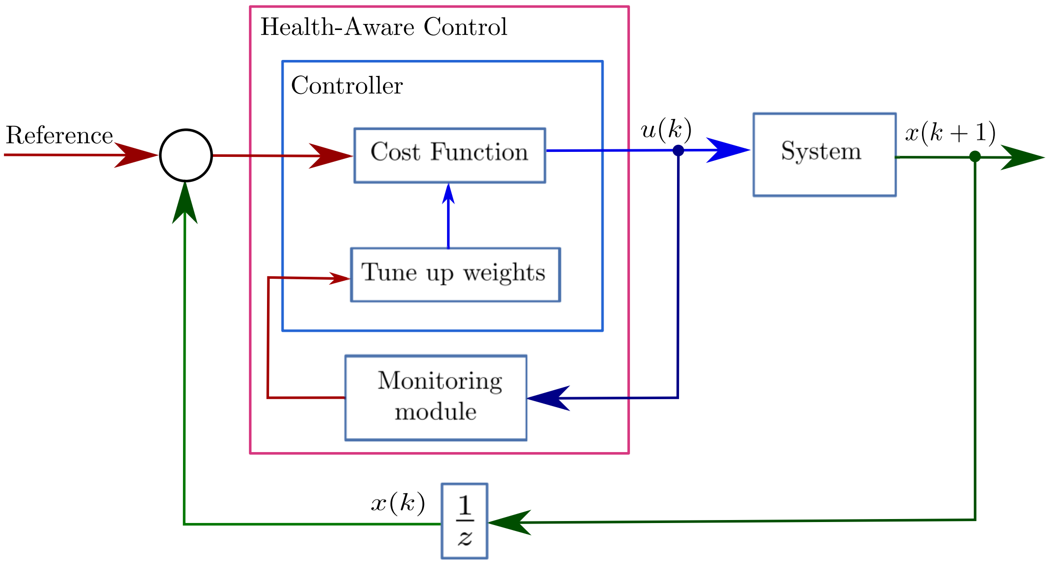

FIGURE 6.1: Generic block diagram of the proposed HAC

In the following sections, three approaches to implement the proposed HAC methodology will be presented:

1. The first is based on a MPC control and includes information about the components and system reliabilities. An MPC controller is set up based on system and component reliability.
2. An LQR controller is set up based on system and component reliability.
3. An MPC scheme is set up based on actuator usage information.

To evaluate the benefit of these approaches, some performance indicators will next proposed.

6.2.1 Performance evaluation

Different indexes are proposed to evaluate the performance, in control and reliability aspects, of the proposed HAC methodologies.

Definition 6.1. The Cumulative Control Effort (U_{cum}) index indicates the amount of energy spent controlling the system, and is given by:

$$U_{\text{cum}} = T_s \sum_{k=0}^{T_M/T_s} u(k)^T u(k) \tag{6.9}$$

where T_s and T_M are the sampling time and the mission time, respectively.

Definition 6.2. The Joint Actuator Reliability (JAR) index measures the remaining overall actuator reliability and is defined as:

$$\text{JAR} = \prod_{i=1}^{p} R_i(T_M). \tag{6.10}$$

And, the Integral Square Error defined as:

Definition 6.3. The ISE measures how well the controller follows the tracking reference.

$$\text{ISE} = \sum_{k=0}^{T_M/T_s} \sum_{i=1}^{q} \left(\hat{y}_i(k) - y_{ref,i}(k)\right)^2. \tag{6.11}$$

Additionally, the system reliability at the end of the mission time (Rs(TM)) will also be used as a performance measure.

6.3 MPC framework for system reliability optimization

6.3.1 MPC cost function

As presented in Section 5.1, the MPC algorithm allows including as many objectives as needed in the cost function. The importance of these objectives in the optimization problem is handled by the weighting parameters, such as $\alpha_i(k)$, $\rho_i(k)$, and $\delta_i(k)$ (5.4).

In this scenario, the control objectives study is done by selecting and $\delta_i(k) = 1$. This means that the MPC performs a smooth control but this effect is not part of the study, and that the reference tracking is study by directly assigning the weight ε.

In this section, the optimization problem in (5.4) is reformulated as follows:

Consequently, the cost function used is:

$$\begin{array}{ll}
\underset{\substack{(\hat{u}(k|k),...,\\ \hat{u}(k+H_c-1|k))\\ \Delta\hat{u}(k|k),...,\\ \Delta\hat{u}(k+H_c-1|k))}}{\text{minimize}} & J(k) = \varepsilon\left(\sum_{j=0}^{H_p-1}\sum_{i=1}^{q}(\hat{y}_i(k+j|k) - y_{ref,i}(k))^2\right) \\
 & +(1-\varepsilon)\left(\sum_{j=0}^{H_c-1}\sum_{i=1}^{p}\rho_i(k)\hat{u}_i(k+j|k)^2 + \sum_{j=0}^{H_c-1}\sum_{i=1}^{p}\Delta\hat{u}_i(k+j|k)^2\right) \\
\text{subject to} & \underline{\boldsymbol{u}} \leq \hat{\boldsymbol{u}}(k+j|k) \leq \overline{\boldsymbol{u}} \quad j = 0,..,H_c-1 \\
 & \underline{\boldsymbol{x}} \leq \hat{\boldsymbol{x}}(k+i|k) \leq \overline{\boldsymbol{x}} \quad i = 1,..,H_p
\end{array} \tag{6.12}$$

where $\alpha_i = 1$ and $\delta_i = 1$ for all i.

Note that a trade-off between reference tracking and energy consumption (control effort) arise. To manage this trade-off, a new weight is added to the formulation problem. Therefore, parameter ε can be used to find the appropriate equilibrium between both optimization objectives following the methodology presented later in Section 6.3.2.

6.3.2 MPC tuning methodology

The MPC tuning consists in finding the appropriate values for the weighting parameters in the cost function.

The values of ρ_i and ε in (6.12) should be selected as follows:

Step 1:

Set $\varepsilon = 0$ and tune ρ_i such that the reliability of the system at the end of the mission time is the highest.

The comparison and selection of the best approach will be performed based on the JAR criteria (6.10), and the U_{Cum} index (6.9).

Step 2:

Tune ε such that the highest system reliability is achieved at mission time $R_s(T_M)$ while ISE index (6.11) is the lowest.

The goal is to study the effect produced by the variation of parameter ε in the system reliability or in other words, the impact of the tracking error in the reliability.

Thus, the optimal value for ε which corresponds to the highest system reliability and the lowest ISE, balancing at the same time both objectives will be found.

6.3.3 Control effort redistribution

In this thesis, two approaches to improve the system reliability are studied. On one hand, a local approach which focuses on the actuators reliability, and on the other hand, the global approach which focuses on the overall system reliability.

To implement such approaches, the weight $\rho_i(k)$ in the cost function (6.12) is used as a way to redistribute the control efforts among the actuators [144]. The greater the value given to component ρ_i is, the higher importance the ith actuator will have and the more penalization it will have in the optimization problem.

The local approach attempts to preserve the component reliability:

$$\rho_i(k) = 1 - R_i(k) \; \forall \; i = 1, 2, \ldots, p. \tag{6.13}$$

This criteria aims at finding the optimal control actions and distributing them among the available actuators in such a way that actuators with lower reliability level are relieved. Hence, the use of highly reliable components is prioritized.

The local approach assumes an equivalent contribution of component reliability to system reliability. However, this is hardly ever true because their contribution depends on the system structure and the interconnection of the actuators within such structure.

The aim of the global approach is to determine the relative importance of the actuators with the objective of improving the overall system reliability. This study is based on the study of the RIMs (see Section 4.4), which provide different measures of actuator importance. For instance, by using the Birnbaum's measure as follows:

$$\rho_i(k) = I_{B,i}(k) \; \forall \; i = 1, 2, \ldots, p, \tag{6.14}$$

where $I_{B,i}(k)$ denotes the Birnbaum's measure of the ith actuator at instant time k. In this case, it is expected that components with a greater contribution to the system reliability are used less than the others.

The control strategy scheme is presented in Figure 6.2. The MPC computes the control inputs according to: the cost function, a set of bounds, the current system state and the weights ρ_i. Then, the control input is injected to the system and used to compute the component failure rates.

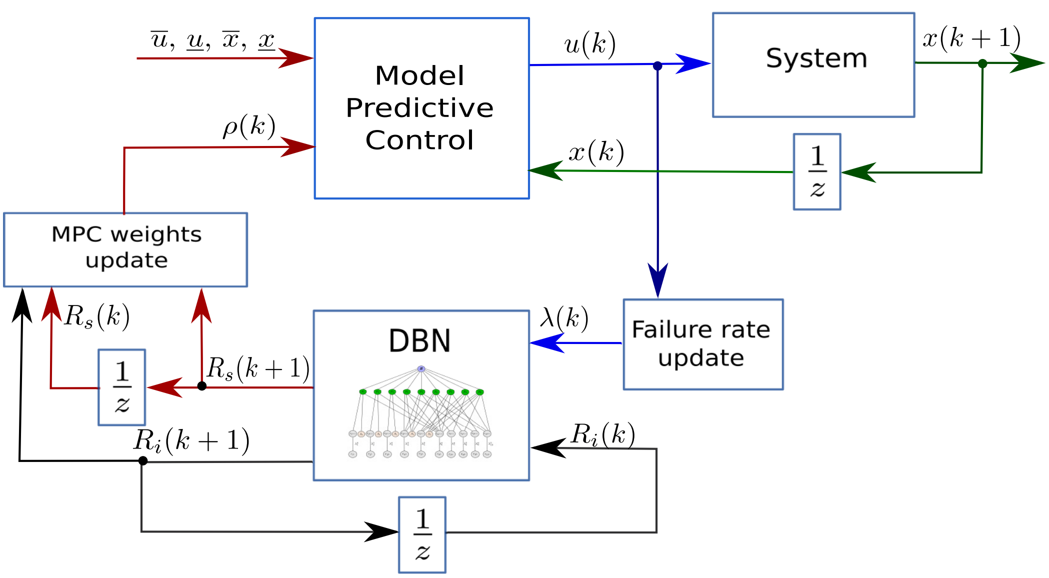

FIGURE 6.2: Block diagram of the approach

Those failure rates are used in the DBN to compute: the components reliability, the overall system reliability and the RIMs. This data is used then to update the weights ρ_i, which is used in the MPC algorithm.

6.3.4 DWN example

Consider the DWN example 4.3 (see Figure 4.9). The control objective is to supply the water demand of Figure 4.10 while keeping the volume of the tanks within a minimum and maximum security levels.

The control of the DWN system is performed applying the MPC formulation according to Section 6.3 and the cost function given by (6.12). A hierarchical control structure is assumed, where the MPC layer produces a set of set-points for the lower level flow controllers. It is also assumed the expression (6.6) as the covariates function.

Since the water demand exhibits a daily profile, a 24 hours prediction horizon has been chosen. The control horizon is set to 8 hours in order to maintain a lower quantity of variables to be computed in the optimization problem. The initial tank volumes have been set to X_0, and a sampling time of 1 hour is assumed for the upper level MPC. Table 6.1 provides the simulation parameters used. The "$\star$" sign in Table 6.8 refers to the different configuration according to the RIM values.

Assume the volume references for the tanks presented in Figure 6.3. The correct tracking of these references guarantees the secure operation of the system, for example avoiding

TABLE 6.1: Simulation parameters

Parameter	Symbol	Value				
Prediction and control horizon	H_p $[h]$ | H_c $[h]$	24 | 8				
Sampling and mission time	T_s $[h]$ | T_M $[h]$	1 | 2000				
Cost function weights	ρ_i | ε	$\{1, 1 - R_i, \star\}$ | $\{10^{-18}, ..., 1\}$				
Upper control effort bound	$\overline{U}$ $[m^3/s]$	0.75	0.75	0.75	1.20	0.85
		1.60	1.70	0.85	1.70	1.60
Lower control effort bound	$\underline{U}$ $[m^3/s]$	0	0	0	0	0
		0	0	0	0	0
Baseline failure rate	λ^0 $[h^{-1} \cdot 10^{-4}]$	9.85	10.70	10.50	1.40	0.85
		0.80	11.70	0.60	0.74	0.78
Upper state bound	$\overline{X}$ $[m^3]$	65200	3100	14450	11745	
Lower state bound	$\underline{X}$ $[m^3]$	25000	2200	5200	3500	
Initial states	X_0 $[m^3]$	45100	2650	9825	7622	

water shortages in droughts, or in rainstorms avoiding tank overflowing and the subsequent floods in rainstorms. Also, it could help when performing maintenance task in the reservoirs.

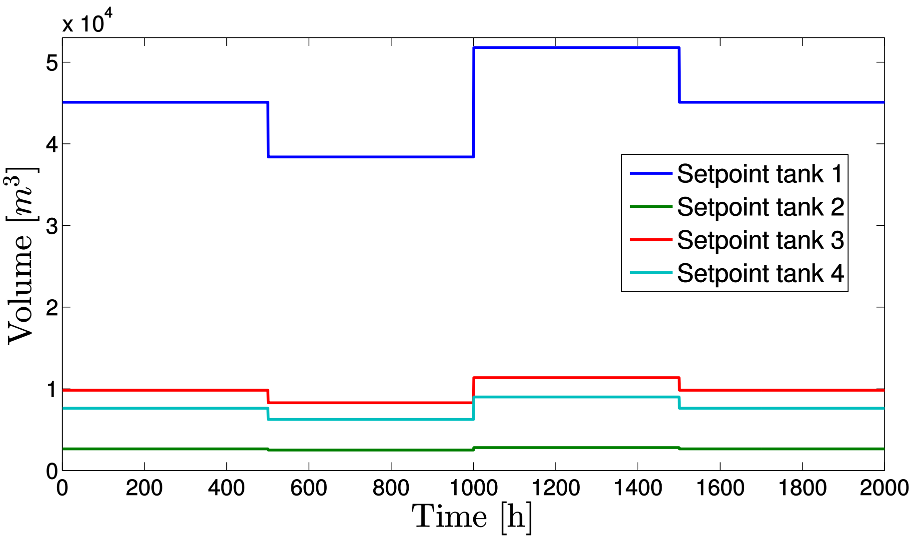

FIGURE 6.3: Volume reference for the 4 reservoirs

6.3.5 MPC tuning

The MPC tuning will follows the procedure proposed in Section 6.3.2. Therefore, the first step involves setting ε to 0. Then, the cost function will optimize two objectives, the control effort and its variations.

Previously, in Section 4.5, a RIM static analysis for the DWN system was presented. Now, a dynamic analysis which involves the computation of the overall system reliability, as well as the pump RIMs through the DBN in Figure 4.11 will be presented.

Table 6.2 presents the performance indices corresponding to several simple $\rho_i(k)$ assignments. A nominal case corresponding to the situation where no reliability information is taken into account in the control loop (i.e., $\rho_i(k) = 1$) is also considered.

TABLE 6.2: Simple $\rho_i(k)$ assignment performance

$\rho_i(k)$	$R_s(T_M)$ [%]	$U_{\text{cum}}[\cdot 10^6]$	JAR
1	97.50	1.537	0.093
$1 - R_i$	97.88	2.025	0.214
$I_{B,i}$	99.34	3.850	0.170
$I_{DIF,i}$	97.49	1.538	0.089
$I_{CIF,i}$	99.39	3.904	0.171
$I_{RAW,i}$	97.50	1.537	0.093
$I_{RRW,i}$	97.44	1.556	0.094

In both cases (local and global), improving system reliability leads to an increase in the cumulative actuator usage which indicates that the improvement of system reliability can lead to an increase of energy consumption.

According to the system reliability indexes, the best results are obtained with $\rho_i(k) = I_{CIF,i}(k)$ and $\rho_i(k) = I_{B,i}(k)$. These two RIMs provided a close pump criticality ordering in Table 4.10. $\rho_i(k) = I_{RRW,i}(k)$ does not provide a good performance, although CIF and RRW measures were expected to be equivalent according to Table 4.10.

Moreover, the local approach corresponding to $\rho_i(k) = 1 - R_i(k)$ produces the best remaining overall pump reliability but does not provide the best overall system reliability. Figure 6.4 shows the difference between the overall system reliability obtained with $\rho_i(k) = 1$ and that obtained with several simple ρ_i assignments.

Provided the results obtained in the static and dynamic RIM analysis, some combined $\rho_i(k)$ assignments will be investigated. In particular, results corresponding to combinations of MIF, CIF and RRW are provided in Table 6.3. The best results correspond to

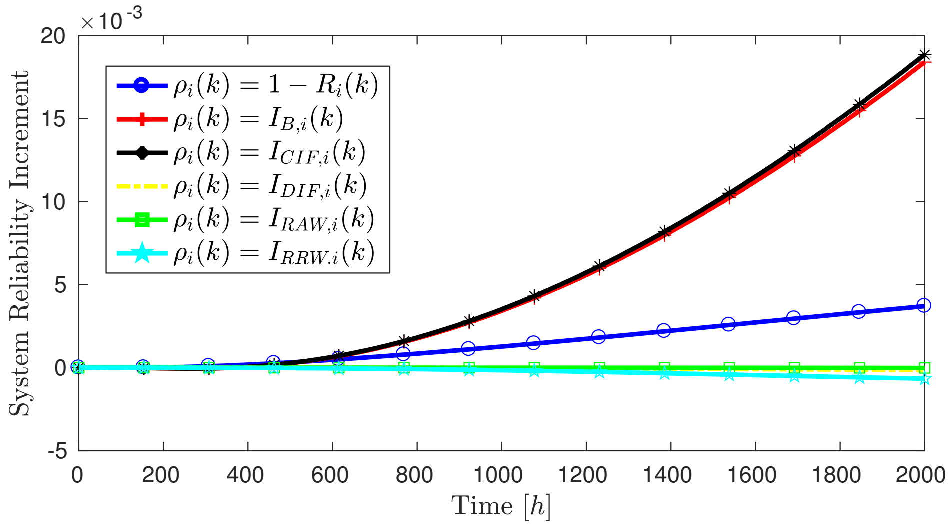

FIGURE 6.4: System reliability increment.

$\rho_i(k) = I_{CIF,i}(k) \cdot I_{RRW,i}(k)$ and $\rho_i(k) = I_{B,i}(k) \cdot I_{RRW,i}(k)$, improving the results obtained in the assignment of $\rho_i(k)$ to a single RIM.

TABLE 6.3: Combined ρ_i assignment performance

$\rho_i(k)$	$R_s(T_M)$ [%]	$U_{\text{cum}}[\cdot 10^6]$	JAR
$I_{CIF,i}(k) \cdot I_{RRW,i}(k)$	99.44	3.971	0.172
$I_{B,i}(k) \cdot I_{RRW,i}(k)$	99.42	3.946	0.172
$I_{B,i}(k) \cdot I_{CIF,i}(k) \cdot I_{RRW,i}(k)$	98.78	3.518	0.153
$I_{B,i}(k) \cdot I_{CIF,i}(k)$	98.73	3.463	0.152

Figure 6.5 shows the gain/loss of system reliability in comparison to the nominal scenario, i.e. the difference between the overall system reliability obtained in the nominal case ($\rho_i(k) = 1$) and that obtained with several combined ρ_i assignments.

Although the reliability is improved, the consumption of energy increases. This could be due to the fact that the controller tends to use more those pumps whose impact on the overall system reliability is lower.

According to their definitions, when the combination of CIF and RRW is used, the objective is to preserve those components whose reliabilities are critical for the system functioning and those that can produce the largest system reliability reduction. In the case of $\rho_i(k) = I_{CIF_i}(k) \cdot I_{RRW_i}(k)$, the objective is to preserve those components whose reliability changes would produce the highest variation and the highest reduction in the system reliability.

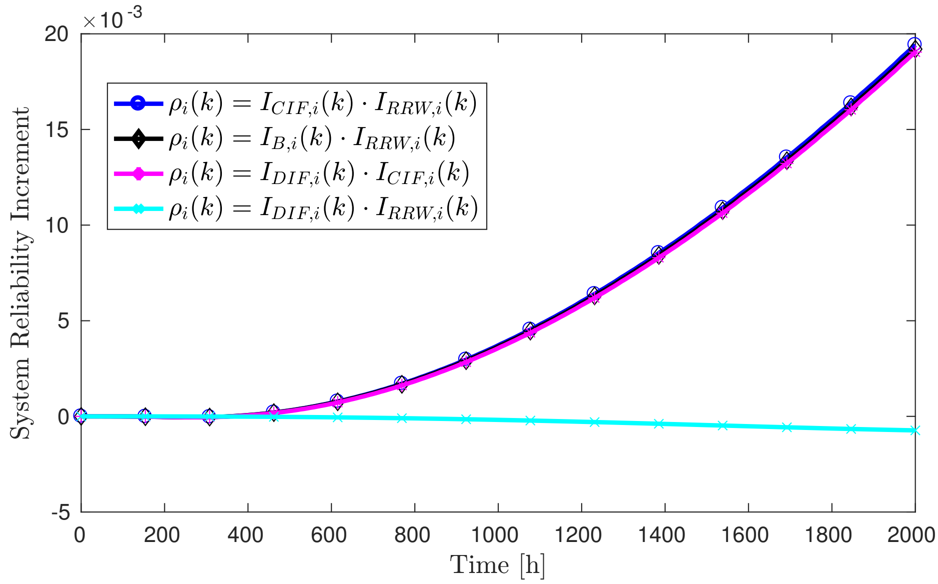

FIGURE 6.5: System reliability increment.

Figure 6.6 illustrates the improvement of system reliability with respect to the nominal scenario.

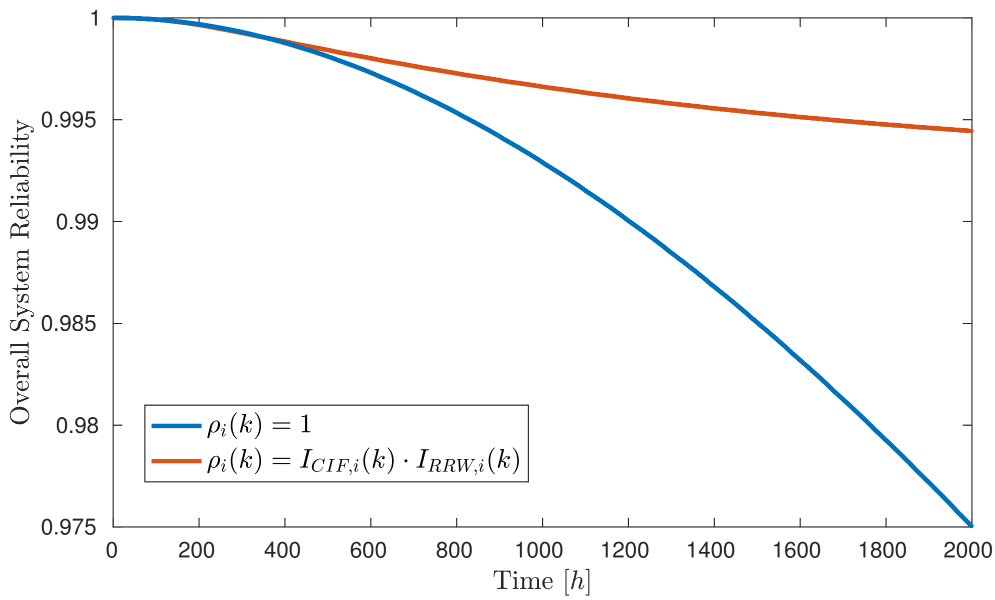

FIGURE 6.6: System reliability comparison.

Figure 6.7 shows the tanks volume corresponding to scenario where $\rho_i(k) = 1$ and $\rho_i(k) = I_{CIF,i}(k) \cdot I_{RRW,i}(k)$. Moreover, note that as the tracking error objective is not taken into account, the volume references are not achieved, but the tanks volume is between the minimum and maximum levels.

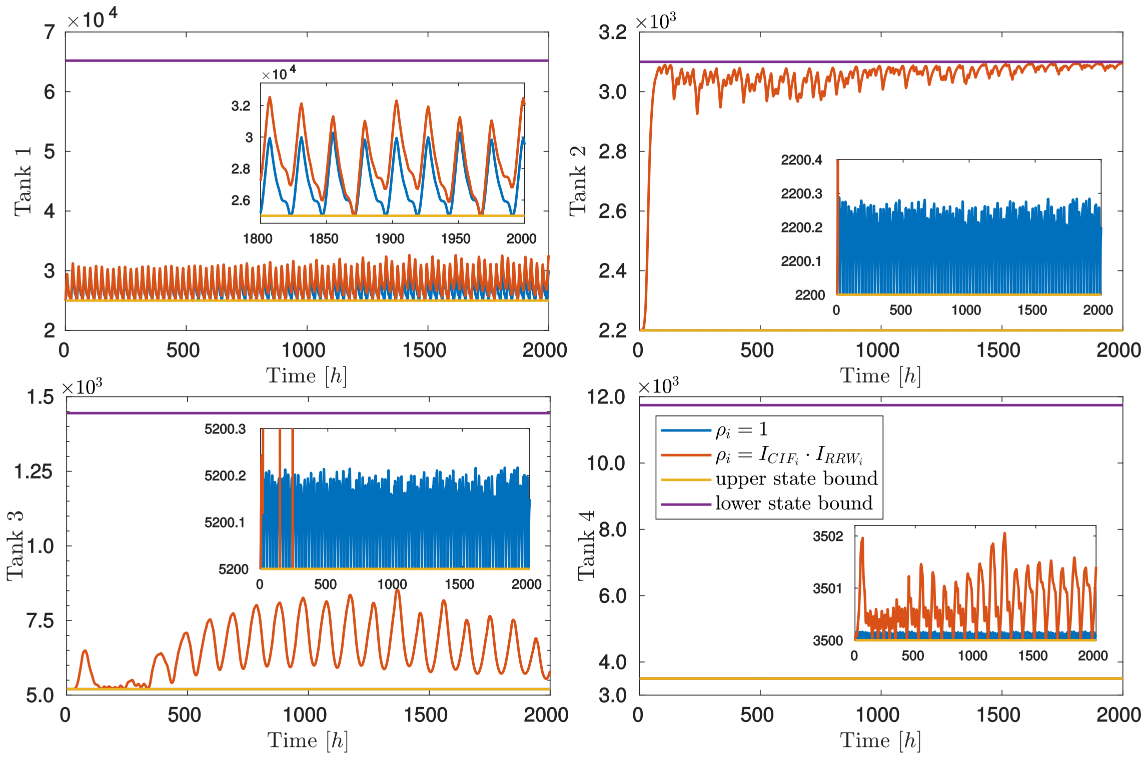

FIGURE 6.7: Tanks volume $[m^3]$: blue line corresponds to $\rho_i(k) = 1$ and red line corresponds to $\rho_i(k) = I_{CIF,i}(k) \cdot I_{RRW,i}(k)$.

Figure 6.8 shows the pump inputs corresponding to the scenario where $\rho_i(k) = 1$ and $\rho_i(k) = I_{CIF,i}(k) \cdot I_{RRW,i}(k)$. It can be seen that different pump commands are produced in each approach.

Now, consider the second step of the tuning methodology. This step aims at finding the appropriate value for parameter ε in the cost function (6.12). Parameter $\rho_i(k)$ has been chosen in order to obtain the best system reliability improvement. The selection of ε follows step 2 of the procedure presented in Section 6.3.2.

Several simulations have been done for some values of ε in the range 0 to 1. Figure 6.9 shows the system reliability obtained at the end of the mission time (T_M), where the overall system reliability behavior is, as expected, decreasing as ε approaches to 1. Nevertheless, for a value of epsilon near 1, the system reliability exhibits an increasing trend. This could be due to numerical issues in the optimization solver. Nevertheless, the trade-off between both objectives is clearly evident.

Figure 6.10 shows the ISE index obtained at the end of the mission. These results show that as ε approaches to 1, a lower ISE is obtained, as it can be expected from (6.12), since the tracking error is less penalized.

Therefore according to these results, the optimal tuning for the MPC parameters would

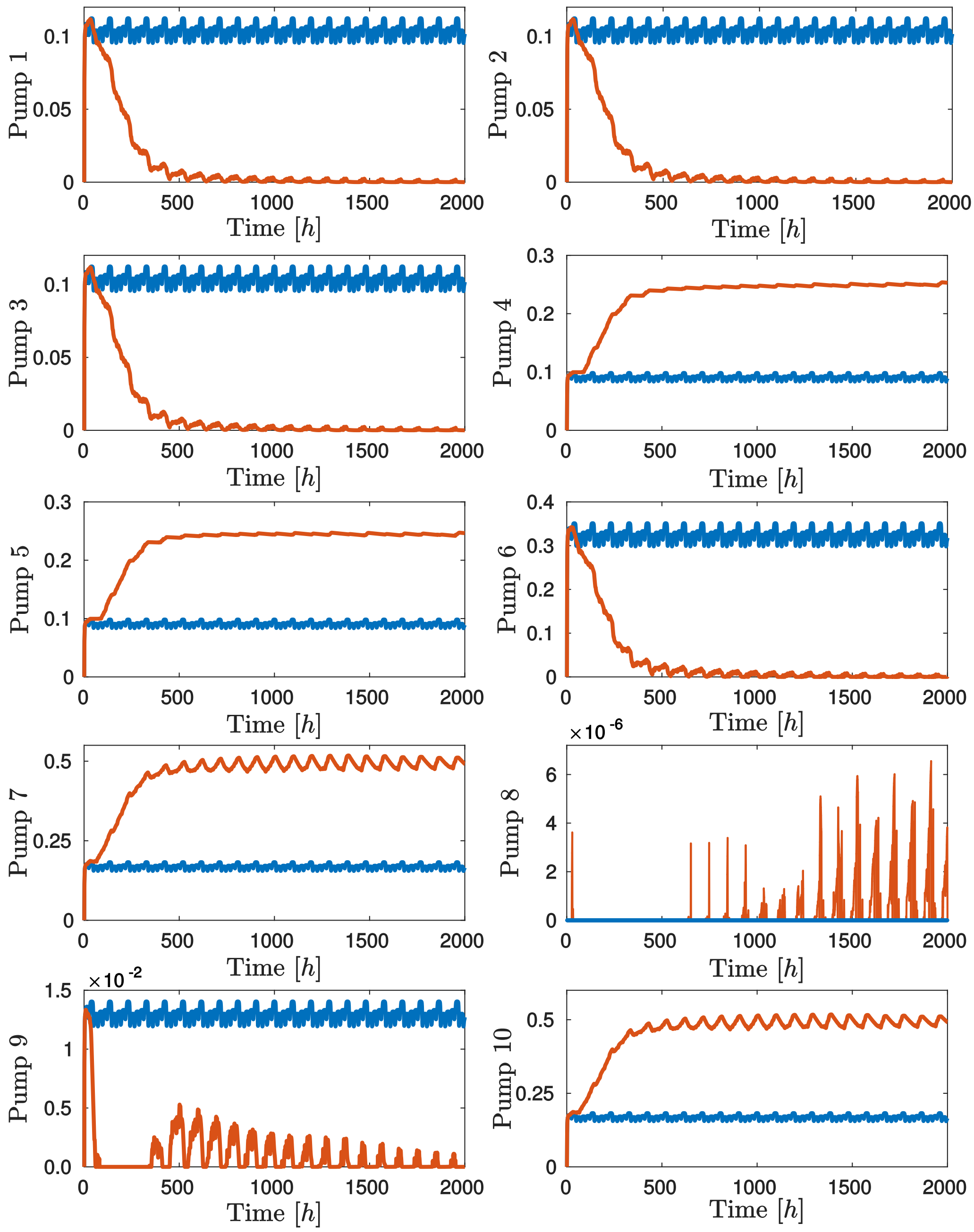

FIGURE 6.8: Pumping inputs $[m^3/h]$: blue line corresponds to $\rho_i = 1$ and red line corresponds to $\rho_i = I_{CIF,i} \cdot I_{RRW,i}$.

be: $\rho_i(k) = I_{CIF,i}(k) \cdot I_{RRW,i}(k)$, and $\varepsilon = 3.162 \times 10^{-11}$ which result in a higher system reliability and lower ISE. Figure 6.11 presents the reference tracking response of the control algorithm. Although the system follows the given references for the four tanks, there is some ripples especially for volume of tank 1. This could be due to the less weight assigned to this objective and to the fact that the water demand sector disturbs the volume of tank 1 to a greater extent than the others.

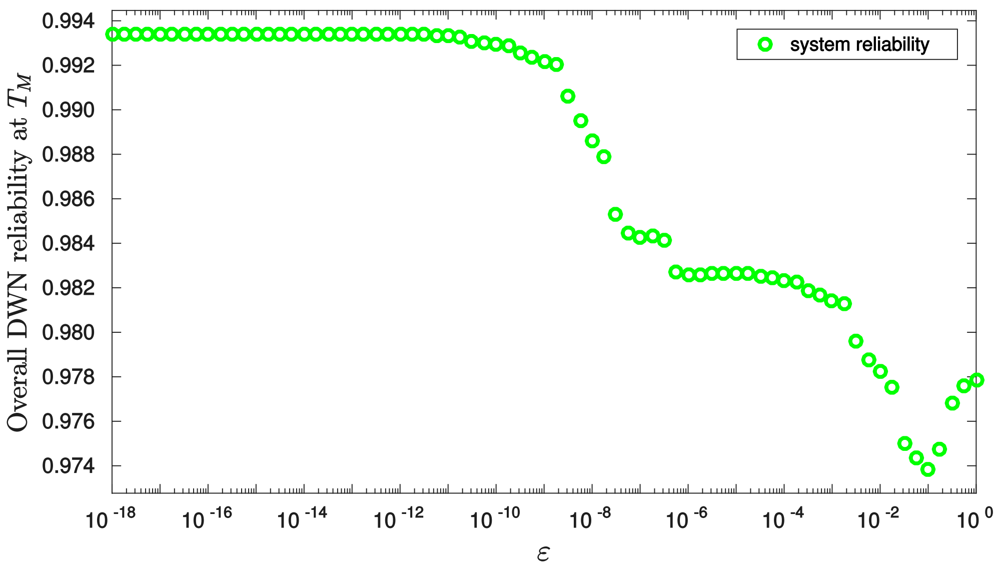

FIGURE 6.9: Overall system reliability evolution for the 4 reservoirs in semi-log scale

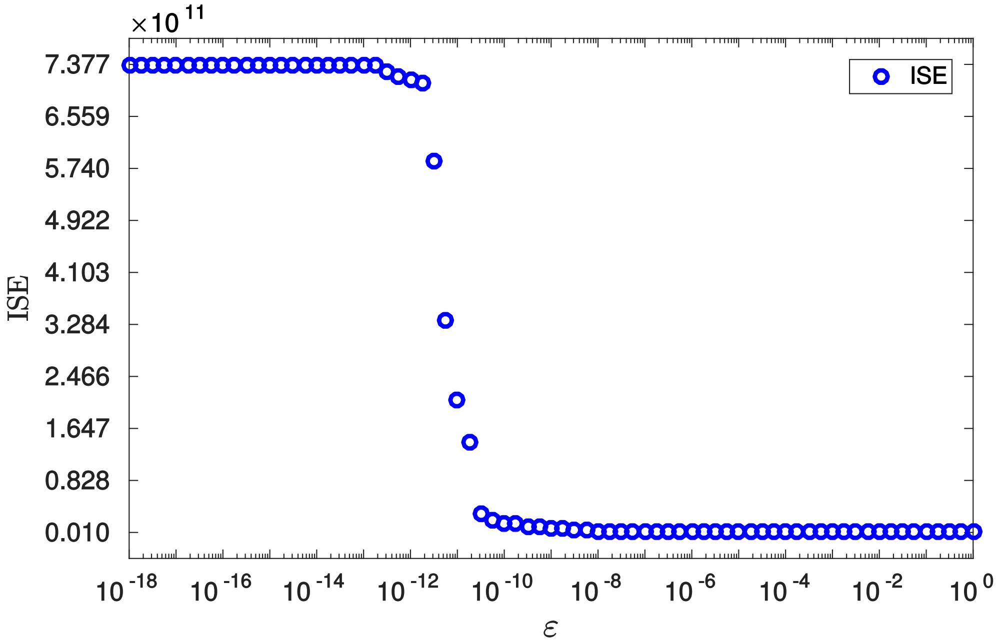

FIGURE 6.10: Tracking error for the 4 reservoirs in semi-log scale

6.3.6 Application to a DWN with multiple demands

Now, consider the DWN system presented in Figure 6.12 composed by multiple sources and demand sectors to illustrate the methodology to compute the overall system reliability of a more complex example.

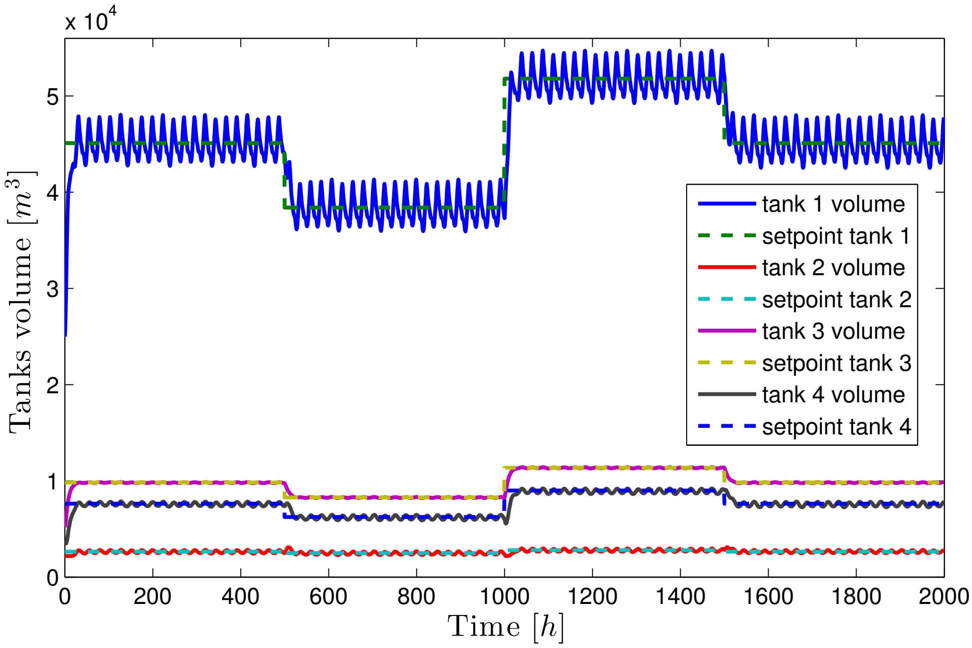

FIGURE 6.11: Tracking references of tanks

As stated in Section 4.3, this thesis and the methodology proposed here are focused only on the topological reliability.

From the system structure, it is possible to obtain a description of the system which only takes into account those components which have a reliability degradation process, in this thesis they are the actuators of the system.

Although, it is possible to make some reductions on the structure of complex systems by doing series and parallels equivalences, there are some structures that cannot be reduced and, in such cases other methods to obtain the overall system reliability expression should be used, e.g. the pivotal decomposition or the structure function computation from the minimal path/cut sets methods discussed in Section 4.1.

Moreover, this system has more than one source where water can be taken and more than one demand sector where water must be supplied. Therefore, the computation of its overall reliability is different to the system with one water demand sector. In the following, a methodology to compute it is presented:

Step 1: Assume a network with l demands. Find the h_j minimal path sets of each demand i (mps_k^j, corresponding to the kth minimal path sets of the jth demand). This involves all pumps which connect a demand with the sources.

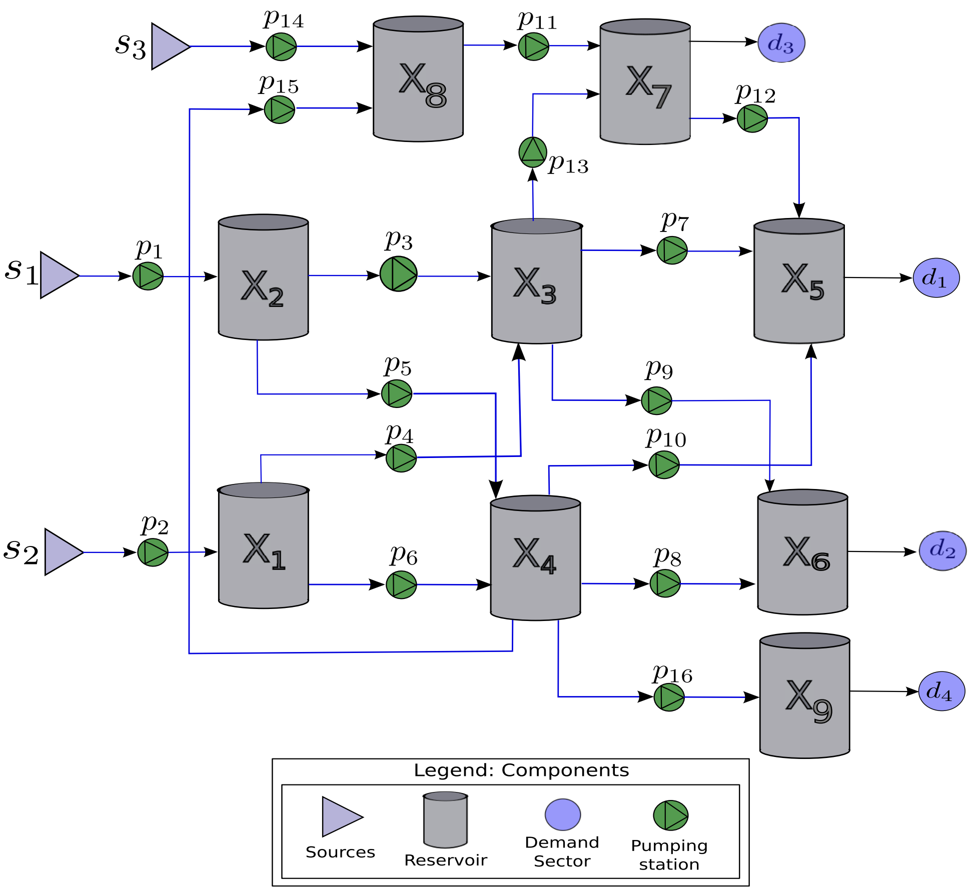

FIGURE 6.12: DWN with 3 sources and 4 demands sectors.

For instance, the system of Figure 6.12 has 20 minimal path sets distributed as follows: 9 for demand 1, 4 for demand 2, 5 for demand 3, and 2 for demand 4:

$$mps_1^1 = \{p_1, p_3, p_7\} \tag{6.15}$$

$$mps_2^1 = \{p_1, p_5, p_{10}\} \tag{6.16}$$

$$mps_3^1 = \{p_2, p_4, p_7\} \tag{6.17}$$

$$mps_4^1 = \{p_2, p_6, p_{10}\} \tag{6.18}$$

$$mps_5^1 = \{p_{14}, p_{11}, p_{12}\} \tag{6.19}$$

$$mps_6^1 = \{p_1, p_3, p_{12}, p_{13}\} \tag{6.20}$$

$$mps_7^1 = \{p_2, p_4, p_{12}, p_{13}\} \tag{6.21}$$

$$mps_8^1 = \{p_1, p_5, p_{15}, p_{11}, p_{12}\} \tag{6.22}$$

$$mps_9^1 = \{p_2, p_6, p_{15}, p_{11}, p_{12}\} \tag{6.23}$$

$$mps_1^2 = \{p_1, p_3, p_9\} \tag{6.24}$$

$$mps_2^2 = \{p_1, p_5, p_8\} \tag{6.25}$$

$$mps_3^2 = \{p_2, p_6, p_8\} \tag{6.26}$$

$$mps_4^2 = \{p_2, p_4, p_9\} \tag{6.27}$$

$$mps_1^3 = \{p_{14}, p_{11}\} \tag{6.28}$$

$$mps_2^3 = \{p_1, p_3, p_{13}\} \tag{6.29}$$

$$mps_3^3 = \{p_2, p_4, p_{13}\} \tag{6.30}$$

$$mps_4^3 = \{p_1, p_5, p_{15}, p_{13}, p_{11}\} \tag{6.31}$$

$$mps_5^3 = \{p_2, p_6, p_{15}, p_{13}\} \tag{6.32}$$

$$mps_1^4 = \{p_1, p_5, p_{16}\} \tag{6.33}$$

$$mps_2^4 = \{p_2, p_6, p_{16}\} \tag{6.34}$$

Step 2: Next, obtain the structure function of the system as:

$$\Phi(\mathbf{X}) = \prod_{j=1}^{l} \left(1 - \prod_{k=1}^{h_j} \left(1 - \prod_{p_i \in mps_k^j} X_i \right) \right) \tag{6.35}$$

where X_i is a binary random variable representing the state of the ith component (as defined in (4.7)).

Step 3: Now, the overall system reliability should be obtained by expanding the structure function expression (6.35) and then simplify it using the fact that X_i^{α}=X_i and taking the expectation (and replacing $\mathrm{P}(X_i = 1)$ by R_i).

$$R_s = E[\Phi(\mathbf{X})] \tag{6.36}$$

For the system of this example, the time spent to compute the overall system reliability was 321.5709 seconds and the reliability expression has 610 terms, which could increase exponentially as the number of minimal path increases.

Regarding the RIMs needed to apply the methodology proposed in Section 6.2, it is possible to compute them from the structure function as presented in Section 4.4.

6.4 Health-Aware LQR framework

6.4.1 LQR framework for HAC implementation

As presented in Section 5.2, the LQR algorithm minimizes the cost function (5.34), that includes two weighting matrices, R_{LQR} and Q_{LQR}. The R_{LQR} matrix weights the control effort magnitude and the Q_{LQR} one weights the system states.

Thus, matrix R_{LQR} can be used to redistribute the control effort between the actuators based on reliability information. The matrix could be assigned to a combination of RIM indexes, following a similar study to that in the previous section. However, just the following assignment will be analyzed:

$$R_{LQR}(k) = \text{diag}(I_B(k)), \tag{6.37}$$

with $I_B = [I_{B,1}, I_{B,2}, \ldots, I_{B,p}]$.

This methodology is illustrated through an example over an octorotor system. For comparison purposes, an additional scenario will be considered, where no actuator reliability is taken into account in the LQR cost function. In this second scenario R_{LQR} will be set as $R_{LQR}(k) = I$ (I is the identity matrix of proper dimensions).

6.4.2 Octorotor UAV model

To describe the dynamics of a multirotor, it is necessary to define the two frames in which it will operate: Inertial frame and Body frame, which are related by the rotation matrix. The inertial frame $\{\mathbf{I}\}$ is static and represents the reference of the multirotor while the body frame $\{\mathbf{B}\}$ is defined by the orientation of the multirotor and is situated in its center of mass (see Figure 6.13).

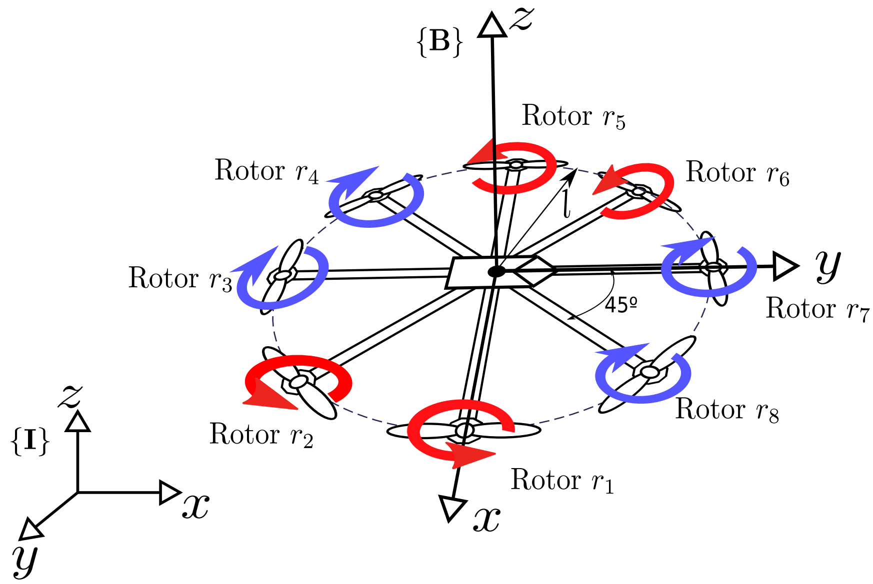

FIGURE 6.13: Octorotor PPNNPPNN structure.

The dynamics of a multirotor is given by the following equations [99]:

$$\dot{x}_I = v_x \tag{6.38}$$

$$\dot{y}_I = v_y \tag{6.39}$$

$$\dot{z}_I = v_z \tag{6.40}$$

$$\dot{v}_x = \frac{1}{m}[\cos(\phi_I)\sin(\theta_I)\cos(\psi_I) + \sin(\phi_I)\sin(\psi_I)]T \tag{6.41}$$

$$\dot{v}_y = \frac{1}{m}[\cos(\phi_I)\sin(\theta_I)\sin(\psi_I) - \sin(\phi_I)\cos(\psi_I)]T \tag{6.42}$$

$$\dot{v}_z = \frac{1}{m}[\cos(\phi_I)\cos(\theta_I)]T - g \tag{6.43}$$

$$\dot{\phi}_I = p + \sin(\phi)\tan(\theta)q + \cos(\phi)\tan(\theta)r \tag{6.44}$$

$$\dot{\theta}_I = \cos(\phi)q - \sin(\phi)r \tag{6.45}$$

$$\dot{\psi}_I = \frac{\sin(\phi)}{\cos(\theta)}q + \frac{\cos(\phi)}{\cos(\theta)}r \tag{6.46}$$

$$\dot{p} = \frac{1}{J_{xx}}\left[-(J_{zz} - J_{yy})qr - J_p q \Omega_p + \tau_x\right] \tag{6.47}$$

$$\dot{q} = \frac{1}{J_{yy}}\left[(J_{zz} - J_{xx})pr + J_p p \Omega_p + \tau_y\right] \tag{6.48}$$

$$\dot{r} = \frac{1}{J_{zz}}\left[-(J_{yy} - J_{xx})pq + \tau_z\right] \tag{6.49}$$

where J_p is the inertia moment of the motor (rotating parts) and the propeller around z axis, T is the lift force, and $\mathbf{J} = \text{diag}(J_{xx}, J_{yy}, J_{zz})$ is the inertia tensor of the octorotor body.

Then, for the octorotor with the structure PPNNPPNN as the one presented in Figure 6.13, where P and N define a positive and negative reactive motor torque respectively (represented as arrows), Ω_p is:

$$\Omega_p = -|\Omega_1| - |\Omega_2| + |\Omega_3| + |\Omega_4| - |\Omega_5| - |\Omega_6| + |\Omega_7| + |\Omega_8| \tag{6.50}$$

where Ω_i is the angular velocity of the ith motor.

Four propellers can rotate in a clockwise direction, while the remaining can rotate anticlockwise. The octorotor is moved by changing the rotor speeds. For example, increasing or decreasing together the eight propellers speeds, vertical motion is achieved. Changing only the speeds of the propellers situated oppositely produces either roll or pitch rotation, coupled with the corresponding lateral motion. Finally, yaw rotation results from the difference in the counter-torque between each pair of propellers. Moreover, the octorotor has actuator redundancy and can function with at least four propellers forming a quadrotor structure.

Notice that the arrows in Figure 6.13 represent the reactive torque of the motors. Furthermore, the system inputs Ω_i produce a lift force T and torques $\boldsymbol{\tau}$ in x, y, and z axis given by:

$$\boldsymbol{u}_v = \boldsymbol{B}_{str}\boldsymbol{u}_\Omega \tag{6.51}$$

which in its complete form is:

$$\begin{bmatrix} T \\ \tau_x \\ \tau_y \\ \tau_z \end{bmatrix} = \begin{bmatrix} k_b & k_b & k_b & k_b & k_b & k_b & k_b & k_b \\ 0 & -k_b l s(45) & -k_b l & -k_b l s(45) & 0 & k_b l s(45) & k_b l & k_b l s(45) \\ -k_b l & -k_b l c(45) & 0 & +k_b l c(45) & k_b l & k_b l c(45) & 0 & -k_b l c(45) \\ +k_d & +k_d & -k_d & -k_d & +k_d & +k_d & -k_d & -k_d \end{bmatrix} \begin{bmatrix} \Omega_1^2 \\ \Omega_2^2 \\ \Omega_3^2 \\ \Omega_4^2 \\ \Omega_5^2 \\ \Omega_6^2 \\ \Omega_7^2 \\ \Omega_8^2 \end{bmatrix}, \tag{6.52}$$

where k_b and k_d are coefficients of the motor and l is the distance between the center of mass and the center of the rotor. The parameters value which define the octorotor model are presented in Table 6.4.

TABLE 6.4: Parameters value

Parameter	Symbol	Value
Body inertia	$J_{xx} = J_{yy}$	$25 \cdot 10^{-3}$ $[kgm^2]$
Body inertia	J_{zz}	$42 \cdot 10^{-3}$ $[kgm^2]$
Propeller inertia	J_p	$104 \cdot 10^{-6}$ $[kgm^2]$
Mass	m	1.86 $[kg]$
Arm length	l	0.4 $[m]$
Thrust factor	k_b	$54.2 \cdot 10^{-6}$ $[Ns^2]$
Drag factor	k_d	$1.1 \cdot 10^{-6}$ $[Nms^2]$

Equations (6.38)-(6.49) define the nonlinear state space model of an octorotor that should be linearized to apply a health aware linear-quadratic controller (LQR) for the UAV system.

The state and inputs vectors considered are $\mathbf{x} = [x\ y\ z\ \phi\ \theta\ \psi\ v_x\ v_y\ v_z\ p\ q\ r]^T$ and $\mathbf{u} = [\Omega_1^2\ \Omega_2^2\ \Omega_3^2\ \Omega_4^2\ \Omega_5^2\ \Omega_6^2\ \Omega_7^2\ \Omega_8^2\ ]^T$, respectively, the Taylor series approximation at the hover position is applied.

The hover position corresponds to the situation where the planes xy of both frames ($\{\mathbf{I}\}$ and $\{\mathbf{B}\}$) are in parallel and the motors are generating a lifting force equal to the weight of the octorotor.

6.4.3 Octorotor LQR controller

In this example, the control of the UAV consists in a cascade structure (see Figure 6.14), where the outer loop controls the pose of the UAV in axis x and y and the inner loop controls the pose in axis z and the orientation in axis x, y and z. Note that the inner loop frequency is faster than the outer loop one.

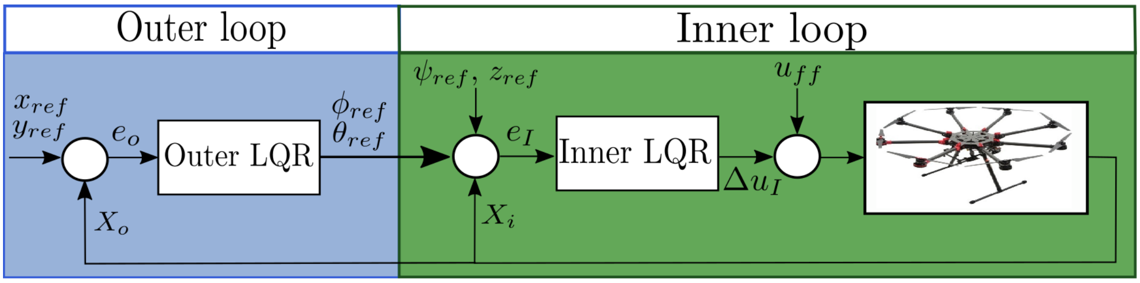

FIGURE 6.14: Control scheme.

Therefore, the linear model will be divided into two subsystems. On one hand, the inner control loop, where $\mathbf{e}_I$ is the inner state vector denoted as:

$$\begin{aligned} \mathbf{e}_I &= \boldsymbol{x}_{ref_i} - \boldsymbol{x}_i \\ &= \left[e_z \; e_\phi \; e_\theta \; e_\psi \; e_{v_z} \; e_p \; e_q \; e_r\right]^T , \end{aligned} \tag{6.53}$$

and $\Delta \boldsymbol{u}_I$ is the inner input vector denoted as:

$$\Delta \boldsymbol{u}_I = \left[\Delta\Omega_1^2 \; \Delta\Omega_2^2 \; \Delta\Omega_3^2 \; \Delta\Omega_4^2 \; \Delta\Omega_5^2 \; \Delta\Omega_6^2 \; \Delta\Omega_7^2 \; \Delta\Omega_8^2\right]^T , \tag{6.54}$$

with $\Delta\Omega_i^2 = \Omega_i^2 - u_{ff} = \Omega_i^2 - mg/(8k_b)$, where u_{ff} stands for the input providing the equilibrium point.

Therefore, the inner loop model is given by:

$$\dot{\mathbf{e}}_I(t) = \boldsymbol{A}_I \mathbf{e}_I(t) + \boldsymbol{B}_I \boldsymbol{B}_{str} \Delta \boldsymbol{u}_I(t) \tag{6.55}$$

where

$$\boldsymbol{A}_I = \begin{bmatrix} \mathbf{0}_{4\times4} & \boldsymbol{I}_{4\times4} \\ \mathbf{0}_{4\times4} & \mathbf{0}_{4\times4} \end{bmatrix} ,$$

and

$$\boldsymbol{B}_I = \begin{bmatrix} \mathbf{0}_{4\times4} \\ \boldsymbol{\beta}_I \end{bmatrix} ,$$

with $\boldsymbol{\beta}_I = \mathrm{diag}(1/m, 1/J_{xx}, 1/J_{yy}, 1/J_{zz})$ is a diagonal matrix, $\boldsymbol{I}_{4\times4}$ is the identity matrix and $\boldsymbol{B}_{str}$ is the structural matrix (6.52).

On the other hand, the outer control loop, where $\mathbf{e}_o$ is the outer state vector denoted as:

$$\begin{aligned} \mathbf{e}_o &= \boldsymbol{x}_{ref_o} - \boldsymbol{x}_o \\ &= \left[e_x \; e_y \; e_{v_x} \; e_{v_y}\right]^T, \end{aligned} \tag{6.56}$$

and $\Delta \boldsymbol{u}_o$ is the outer input vector denoted as:

$$\begin{aligned} \Delta \boldsymbol{u}_o &= [\Delta\phi \; \Delta\theta]^T \\ &= [\phi_{ref} \; \theta_{ref}]^T. \end{aligned} \tag{6.57}$$

Therefore, the outer loop model is:

$$\dot{\mathbf{e}}_o(t) = \boldsymbol{A}_o e_o(t) + \boldsymbol{B}_o \Delta \boldsymbol{u}_o(t), \tag{6.58}$$

where

$$\boldsymbol{A}_o = \begin{bmatrix} \mathbf{0}_{2\times2} & \boldsymbol{I}_{2\times2} \\ \mathbf{0}_{2\times2} & \mathbf{0}_{2\times2} \end{bmatrix},$$

and

$$\boldsymbol{B}_o = \begin{bmatrix} 0 & 0 \\ 0 & 0 \\ 0 & g \\ -g & 0 \end{bmatrix},$$

with g is the gravitational acceleration equal to 9.81 [m/s^2].

Regarding the HAC LQR-based, Figure 6.15 presents its scheme, where a module to compute the actuators and system reliabilities is attached to the inner control loop and is used to adapt the parameters of the controller, i.e. the R_{LQR} matrix of the inner loop.

6.4.4 Octorotor reliability model

In this application, the covariate is expressed as a function of the load and the age of the actuator. Therefore, the covariate function and the failure rate used are (6.7) and (6.8), respectively.

Regarding the overall system reliability, it is computed using the system structure function as presented in Section 4.1. It is assumed that the overall system reliability is determined by the reliability of its actuators and the system controllability.

Although the octorotor system has 8 actuators ($r_i \; \forall \; i \in [1, 8]$) in terms of controllability, it can flight without any problem with at least 4 of them. In such scenario the system

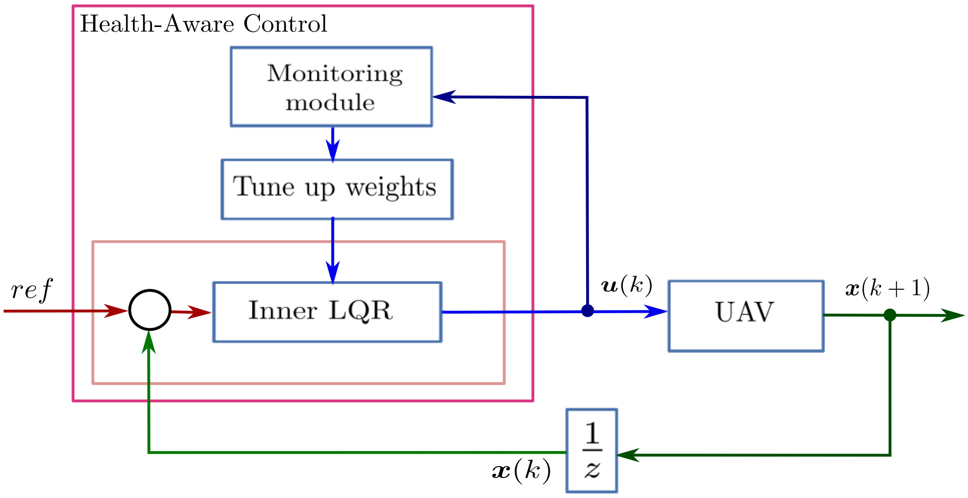

FIGURE 6.15: HAC LQR-based.

becomes a quadrotor. Among all 4-rotor configurations, the following minimal path sets which guarantee controllability can be found:

$$\zeta_1 : \{r_1, r_3, r_5, r_7\} \tag{6.59}$$

$$\zeta_2 : \{r_2, r_4, r_6, r_8\} \tag{6.60}$$

$$\zeta_3 : \{r_2, r_3, r_6, r_7\} \tag{6.61}$$

$$\zeta_4 : \{r_1, r_4, r_5, r_8\}. \tag{6.62}$$

A graphic representation of these minimal path sets is shown in Figure 6.16.

Figure 6.17 presents the reliability block diagram based on the minimal path sets (ζ_i) where R_i is the ith rotor reliability.

Then the system reliability can be computed using the pivotal decomposition method (Section 4.1). Therefore, the overall system reliability is given by:

$$\begin{aligned} R_s(t) =& R_1(t)R_3(t)R_5(t)R_7(t) + R_1(t)R_4(t)R_5(t)R_8(t) + R_2(t)R_3(t)R_6(t)R_7(t) \\ &+ R_2(t)R_4(t)R_6(t)R_8(t) - R_1(t)R_2(t)R_3(t)R_5(t)R_6(t)R_7(t) \\ &- R_1(t)R_2(t)R_4(t)R_5(t)R_6(t)R_8(t) - R_1(t)R_3(t)R_4(t)R_5(t)R_7(t)R_8(t) \\ &- R_2(t)R_3(t)R_4(t)R_6(t)R_7(t)R_8(t) \\ &+ R_1(t)R_2(t)R_3(t)R_4(t)R_5(t)R_6(t)R_7(t)R_8(t). \end{aligned} \tag{6.63}$$

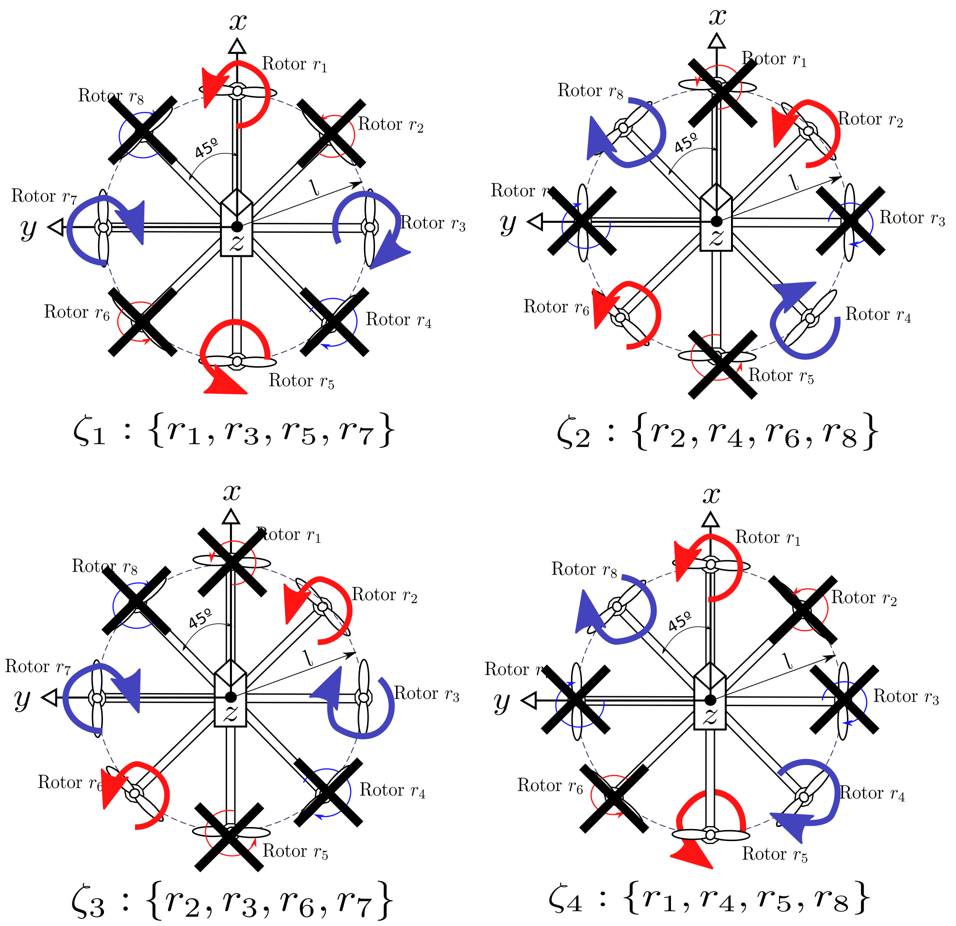

FIGURE 6.16: Minimal path sets of the octorotor system.

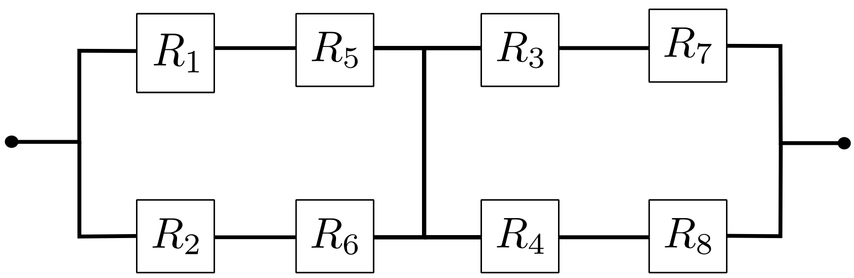

FIGURE 6.17: Reliability block diagram.

6.4.5 Simulation Results

A simulated corn field aerial supervision application has been considered. The UAV mission involves flying over a corn field of $5000m^2$ at an altitude of $5m$ departing from the ground and following a grid path trajectory, as presented in Figure 6.18. A nonlinear model of the UAV has been used as simulator, contrary to the linear one used to design the controller.

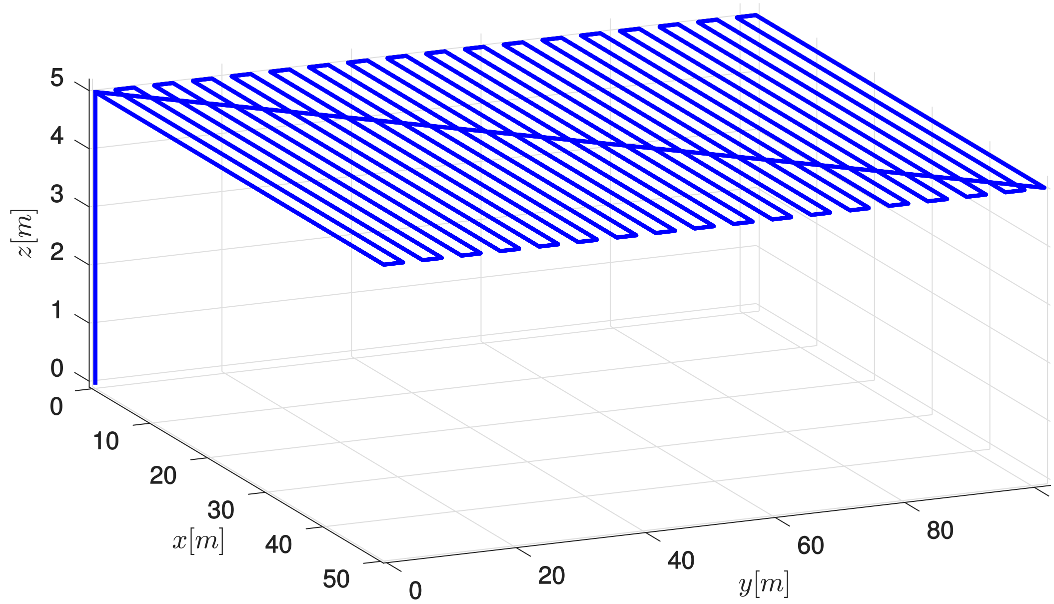

FIGURE 6.18: UAV reference trajectory.

The obtained linear model is as follows:

$$A = \begin{bmatrix} 0 & 0 & 0 & 0 & 0 & 0 & 1 & 0 & 0 & 0 & 0 & 0 \\ 0 & 0 & 0 & 0 & 0 & 0 & 0 & 1 & 0 & 0 & 0 & 0 \\ 0 & 0 & 0 & 0 & 0 & 0 & 0 & 0 & 1 & 0 & 0 & 0 \\ 0 & 0 & 0 & 0 & 0 & 0 & 0 & 0 & 0 & 1 & 0 & 0 \\ 0 & 0 & 0 & 0 & 0 & 0 & 0 & 0 & 0 & 0 & 1 & 0 \\ 0 & 0 & 0 & 0 & 0 & 0 & 0 & 0 & 0 & 0 & 0 & 1 \\ 0 & 0 & 0 & 0 & 9.81 & 0 & 0 & 0 & 0 & 0 & 0 & 0 \\ 0 & 0 & 0 & -9.81 & 0 & 0 & 0 & 0 & 0 & 0 & 0 & 0 \\ 0 & 0 & 0 & 0 & 0 & 0 & 0 & 0 & 0 & 0 & 0 & 0 \\ 0 & 0 & 0 & 0 & 0 & 0 & 0 & 0 & 0 & 0 & 0 & 0 \\ 0 & 0 & 0 & 0 & 0 & 0 & 0 & 0 & 0 & 0 & 0 & 0 \\ 0 & 0 & 0 & 0 & 0 & 0 & 0 & 0 & 0 & 0 & 0 & 0 \end{bmatrix} \quad (6.64), \quad B = \begin{bmatrix} 0 & 0 & 0 & 0 \\ 0 & 0 & 0 & 0 \\ 0 & 0 & 0 & 0 \\ 0 & 0 & 0 & 0 \\ 0 & 0 & 0 & 0 \\ 0 & 0 & 0 & 0 \\ 0 & 0 & 0 & 0 \\ 0 & 0 & 0 & 0 \\ 0.5376 & 0 & 0 & 0 \\ 0 & 39.3701 & 0 & 0 \\ 0 & 0 & 39.3701 & 0 \\ 0 & 0 & 0 & 23.9234 \end{bmatrix}, \quad (6.65)$$

and

$$C = I_{[12\times12]}. \quad (6.66)$$

The simulation parameters are presented in Table 6.5.

The tracking results of the LQR controller for the first 200 seconds in the scenario are presented in Figure 6.19, where $R_{LQR}(k) = \text{diag}(I_B(k))$, that aims at preserving the critical rotors which cause a larger impact on the system reliability. The tracking performance

TABLE 6.5: Simulation parameters

Parameter	Symbol	Value
Outer sampling time	t_{si}	0.05 $[s]$
Inner sampling time	t_{so}	0.25 $[s]$
Mission time	T_M	2000 $[s]$
Rotor parameter	β_i	$10^{-2}\ \forall\, i \in [1,8]$
Rotors baseline failure rate	λ_i^0	{21, 25, 2, 5, 16, 29, 9, 8} $\cdot 10^{-6}\ [s^{-1}]$
Rotor upper bounds	$\overline{u}_i$	$7\ \forall\, i \in [1,8]\ [N]$
Rotor lower bounds	$\underline{u}_i$	$0\ \forall\, i \in [1,8]\ [N]$
Initial states	$\boldsymbol{x}(0)$	$\mathbf{0}_{[12\times1]}\ [m]$
Feed-Forward input	$\boldsymbol{u}_{ff}$	$mg/\mathbf{8}_{[8\times1]}\ [rad/s]$
Weighting matrix Q outer loop	Q_{out}	$\mathbf{I}_{[6\times6]} \times 10^{-4}$
Weighting matrix R outer loop	R_{oit}	$\mathbf{I}_{[2\times2]}$
Weighting matrix Q inner loop	Q_{LQR}	diag([0.01, 10, 10, 0.1, 0.0001, 0.01, 0.01, 0.010, 0.01, 0.010])
Weighting matrix R inner loop	$R_{LQR}(k)$	I and $I_B(k)$

corresponding to $R_{LQR} = I$ is not explicitly shown, since it nearly corresponds to Figure 6.19.

Figure 6.20 presents the control efforts (angular velocities) in the scenarios where the Birnbaum's measure is used ($R_{LQR}(k) = \text{diag}(I_B(k))$) and $R_{LQR}(k) = I$ (i.e. $\Omega_i^{I_B}$, and Ω_i^{I}).

The overall system reliability enhancement is achieved by relieving the control efforts of those rotors which are mostly critical to the system. According to Figure 6.20, this corresponds to rotors r_1, r_2, r_5 and r_6, which have a higher failure rate according to Table 6.5, and are present in all the minimal path sets (see Figure 6.17).

Figure 6.21 provides a comparison between the system reliability obtained with assignment $R_{LQR}(k) = I$ denoted as $R_S^I(k)$ and the one obtained with assignment $R_{LQR}(k) = \text{diag}(I_B)$ denoted as $R_S^{I_B}(k)$, after having performed several missions. Under $R_{LQR}(k) = \text{diag}(I_B(k))$, the safety of the system is increased by allowing its operation until the end of the mission with a higher reliability level.

Results of the indexes for scenarios $R_{LQR}(k) = I$ and $R_{LQR}(k) = \text{diag}(I_B)$, U_{cum}, JAR, and ISE, introduced in Section 6.2.1, are summarized in Table 6.6. Similar results are achieved in both cases. Remark however, that in this scenario the cumulative actuator usage and the tracking error are both smaller when using the Birnbaum's measure.

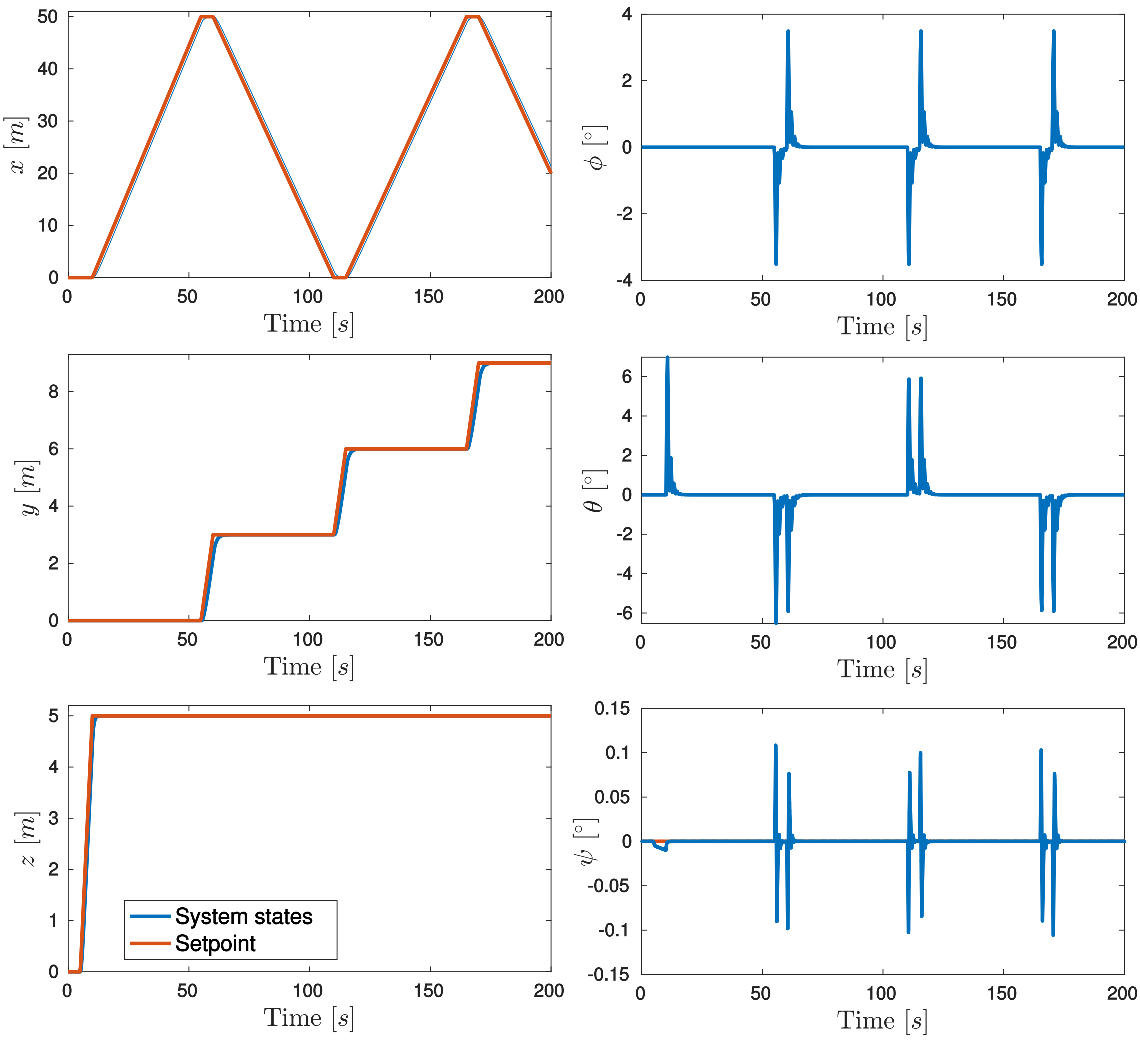

FIGURE 6.19: System states response with $R(k)$ =diag($I_B(k)$).

TABLE 6.6: Performance indexes.

$R_{LQR}(k)$	$R_s(T_M)$ $[\cdot 10^{-3}]$	$U_{\text{cum}}[\cdot 10^6]$	JAR	ISE $[\cdot 10^3]$
I	235.9971	673.3721	3.0706	70.1401
$I_B(k)$	235.9985	673.3712	3.0706	70.1229

6.5 Actuators usage management in the control loop

6.5.1 Actuator usage

On Section 6.2 and Section 6.3 the actuators usage was managed based on its impact on the overall system reliability.

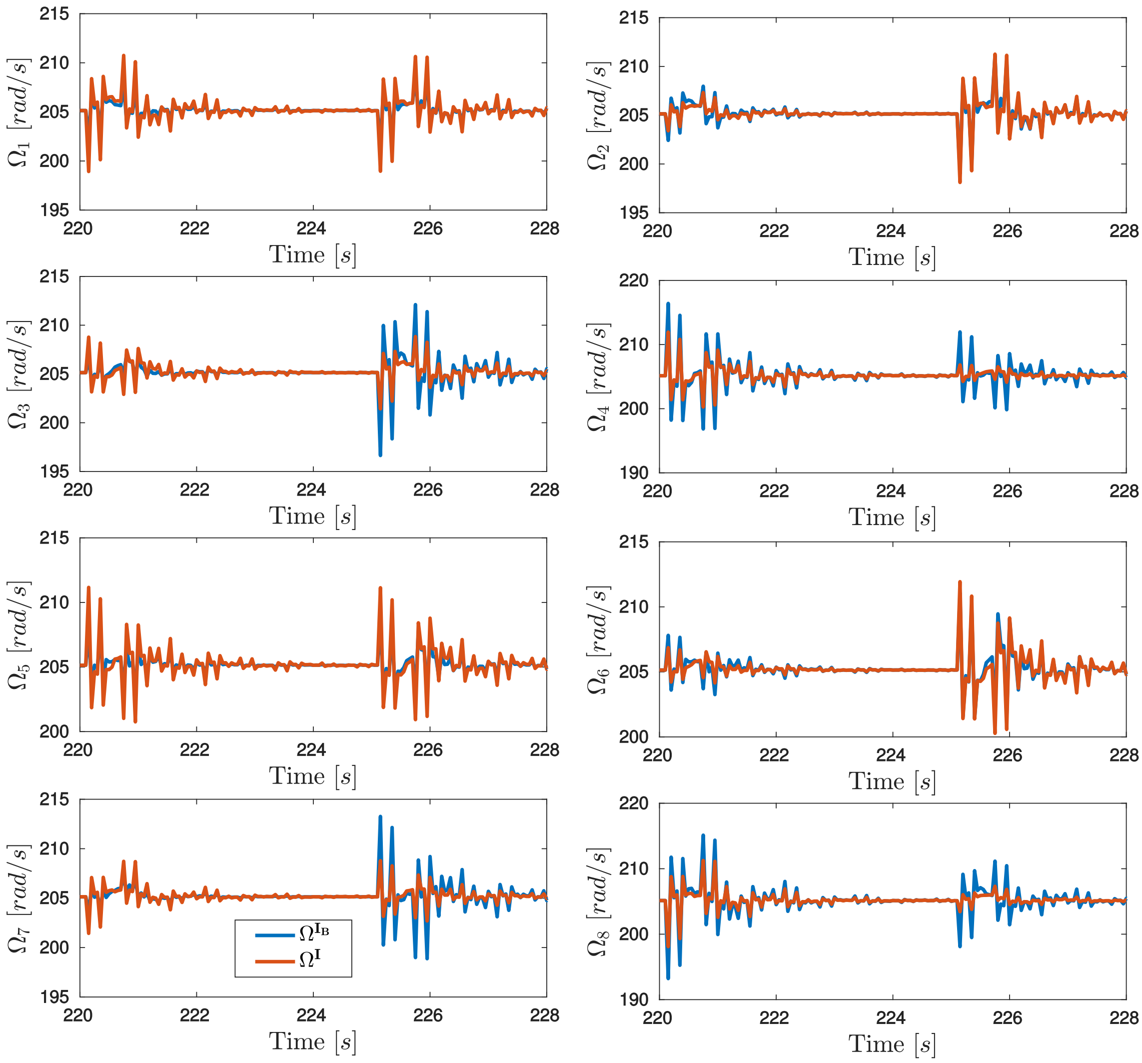

FIGURE 6.20: Angular velocities $\Omega_i^{I_B}$ and Ω_i^{I}.

Now, a model of the degradation of the actuators is used to determine the control efforts. This will be achieved in by formulating an MPC algorithm under actuator usage constraints [124].

Anticipating component faults is crucial to guarantee the process safe operation. Among all components, actuators are the most critical, since they are responsible of governing the process performance through control loops. However, due to their continuing use they are subject to stress and wear. Actually the control law could mitigate actuator degradation by deciding the proper control effort to be delivered. Thus, accounting for these degradation processes in the control law would be desirable, such that actuator faults could be prevented before next maintenance service was scheduled.

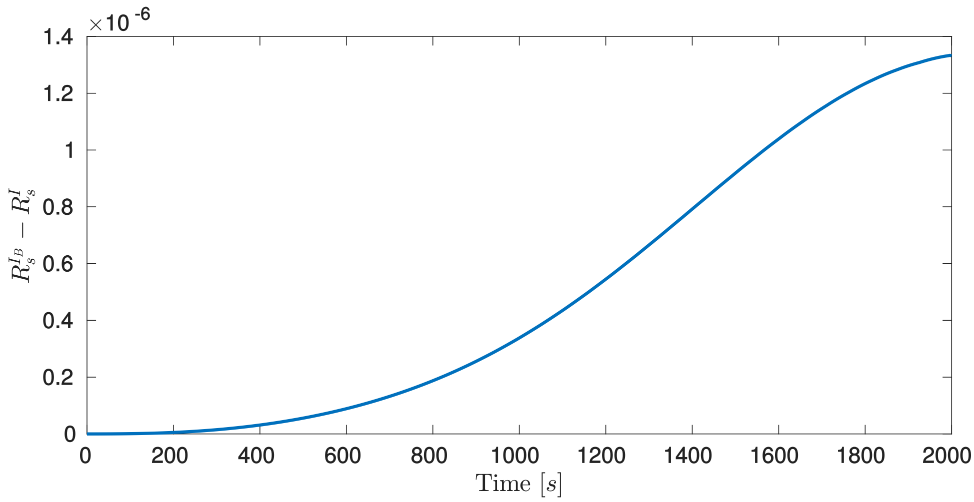

FIGURE 6.21: Difference between system reliabilities $R_S^{I_B}$ and $R_S^{\mathbf{I}}$.

Assuming that the actuator wear is proportional to the exerted control effort u, a model for the cumulative degradation $z(k) \in \mathbb{R}^p$ can be written as:

$$\boldsymbol{z}(k+1) = \boldsymbol{z}(k) + \boldsymbol{\Gamma}|\boldsymbol{u}(k)|, \tag{6.67}$$

where $\boldsymbol{\Gamma} = \text{diag}(\gamma_1, \gamma_2, \ldots, \gamma_p)$ is a diagonal matrix of degradation coefficients associated with the p elements of $\boldsymbol{z}(k)$. These coefficients are assumed to be constant and calibrated through experimental data and they may be related to measurable variables such as vibration, internal electrical resistance, or temperature, which are assumed to be known.

Assume that a maintenance service is scheduled at sample $k = k_M$. The goal consists in guaranteeing that the cumulative degradation remains below a safe threshold z_{th} during the maintenance horizon,

$$\boldsymbol{z}(k) \leq z_{th}, \ \forall \, k \in [0, k_M]. \tag{6.68}$$

6.5.2 MPC formulation under actuator usage constraints

A cumulative degradation model which assumes that the degradation of the actuators is proportional to the exerted control effort u and its variations Δu is proposed in [124, 125]. In such an approach, Pereira, Galvao, et al. [124] propose to manage the actuators degradation through the control action, imposing a threshold in the cumulative degradation of the actuators, and adapting the used actuator to this threshold, by introducing the degradation as a constraint in the cost function. In this case, the system performance is not affected because of the redundancy of the actuators in the system. If an actuator reaches its maxim degradation, its usage is reduced and compensated by the redundant actuator.

The actuators degradation model will be integrated in the cost function (5.12) which minimizes the tracking error, the control increments, and the magnitude of the control input.

Constraint (6.68) should be included in the optimization problem. However, this would require extending the prediction horizon over the maintenance horizon, becoming an intractable problem. Instead the following constraint will be considered:

$$\boldsymbol{z}(k+H_p) \leq \boldsymbol{z}_{max}(k) \tag{6.69}$$

To determine $\boldsymbol{z}_{max}$ the uniform "rationing" heuristic proposed in [124] will be followed. This heuristic states that the degradation over a prediction horizon of length $H_p < k_M$ is allowed to increase by

$$H_p \frac{\boldsymbol{z}_{th} - \boldsymbol{z}(k)}{k_M + H_p - k} \tag{6.70}$$

Therefore, the maximum degradation at the end of prediction horizon must not exceed:

$$\boldsymbol{z}_{max}(k) = \boldsymbol{z}(k) + H_p \frac{\boldsymbol{z}_{th} - \boldsymbol{z}(k)}{k_M + H_p - k} \tag{6.71}$$

From (6.67), a prediction equation for the degradation index can be written as

$$\hat{\boldsymbol{z}}(k+H_p|k) = \boldsymbol{z}(k) + \boldsymbol{\Xi}|\hat{\boldsymbol{u}}(k)| \tag{6.72}$$

where

$$\boldsymbol{\Xi} = \begin{bmatrix} \boldsymbol{\Gamma} & \mathbf{0}_{p\times p} & \cdots & \mathbf{0}_{p\times p} \\ \mathbf{0}_{p\times p} & \boldsymbol{\Gamma} & \cdots & \mathbf{0}_{p\times p} \\ \vdots & \vdots & \ddots & \vdots \\ \mathbf{0}_{p\times p} & \mathbf{0}_{p\times p} & \cdots & \boldsymbol{\Gamma} \\ \vdots & \vdots & \ddots & \vdots \\ \mathbf{0}_{p\times p} & \mathbf{0}_{p\times p} & \cdots & (H_p - H_c + 1)\boldsymbol{\Gamma} \end{bmatrix} \tag{6.73}$$

Thus, using equations (6.72) and (5.18), the constraint (6.69) can be replaced with

$$\boldsymbol{z}(k) + \boldsymbol{\Xi}\Theta \leq \boldsymbol{z}_{max} \tag{6.74}$$

Finally, (6.74) constraint should be added to the LP problem as follows:

$$\begin{aligned} \underset{a(k)}{\text{minimize}} \quad & \boldsymbol{c}^T \boldsymbol{a}(k) \\ \text{s.t.} \quad & \begin{bmatrix} \boldsymbol{f}_1 \\ \boldsymbol{f}_2 \end{bmatrix} \boldsymbol{a}(k) \leq \begin{bmatrix} \boldsymbol{b}_1(k) \\ \boldsymbol{b}_2(k) \end{bmatrix} \end{aligned} \tag{6.75}$$

where

$$\boldsymbol{f}_2 = \begin{bmatrix} \mathbf{0}_{p\times pH_c} & \mathbf{0}_{p\times qH_p} & \boldsymbol{\Xi} & \mathbf{0}_{p\times pH_c} & \mathbf{0}_p \end{bmatrix} \tag{6.76}$$

and

$$\boldsymbol{b}_2(k) = \begin{bmatrix} \boldsymbol{z}_{max}(k) - \boldsymbol{z}(k) \end{bmatrix} \tag{6.77}$$

The idea to include actuators usage constraints in the optimization problem was already presented in [124]. The contribution in this thesis consists in analyzing the role of the cost function weights in improving the system safety. Next, this methodology will be applied to a Twin Rotor MIMO system.

6.5.3 Twin Rotor MIMO system

The Twin-Rotor MIMO System (TRMS) is a laboratory setup (Figure 6.22) developed by Feedback Instruments Limited for control experiments. The system is perceived as a challenging engineering problem due to its high non-linearity, cross-coupling between its two axes, and inaccessibility of some of its states measures.

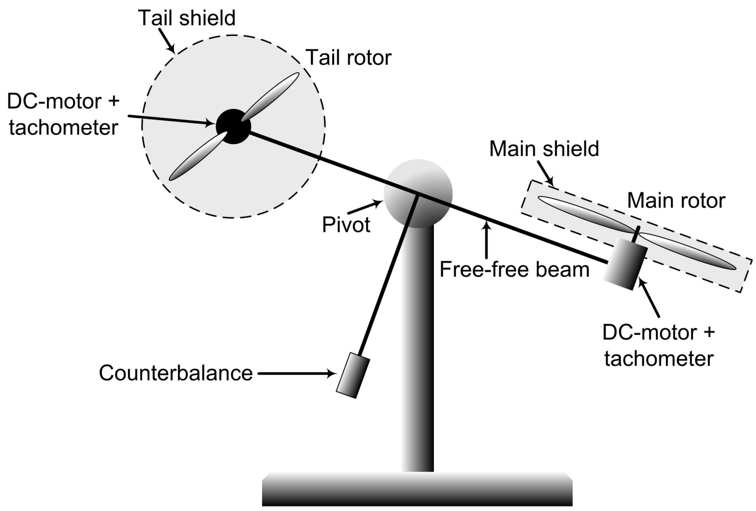

FIGURE 6.22: Components of the Twin Rotor MIMO System

The TRMS mechanical unit has two rotors (the main and the tail, both driven by DC motors) placed on a beam together with a counterbalance whose arm with a weight at its end is fixed to the beam at the pivot and it determines a stable equilibrium position. The beam can rotate freely both in the horizontal and vertical planes.

This application aims at showing the effect of the degradation on the system performance through the controller. This is part of the first results obtained in the research on this thesis.

Accurate models for TRMS are proposed by [27, 46, 130] and [135]. Each of these models lead to a set of nonlinear differential equations where the TRMS is split into simpler subsystems: the DC-Motors, the propellers and the beam. The first two have independent dynamics, that is, the main motor does not affect the behavior of the tail motor, and vice versa. The same is true for the propellers. On the other hand, the dynamics of the beam are strongly nonlinear with the presence of interaction phenomenon among the horizontal and the vertical dynamics. The state of the beam is described by four process variables: horizontal and vertical angles measured by position sensors fitted at the pivot, and their two corresponding angular velocities. The tacho-generators are used to measure the angular velocities of the rotors.

The constants of the nonlinear model are presented in Table 6.7.

Parameter	Symbol	Value
Aerodynamic force coeff. of the tail rotor for positive ω_h	k_{fhp}	$1.84 \cdot 10^{-6}[N/rpm^2]$
Aerodynamic force coeff. of the tail rotor for negative ω_h	k_{fhn}	$2.2 \cdot 10^{-6}[N/rpm^2]$
Aerodynamic force coeff. of the main rotor for positive ω_v	k_{fvp}	$1.62 \cdot 10^{-5}[N/rpm^2]$
Aerodynamic force coeff. of the main rotor for negative ω_v	k_{fvn}	$1.08 \cdot 10^{-5}[N/rpm^2]$
Angular velocity of the TRMS around the vertical axis	Ω_h	$[rpm]$
Angular velocity of the TRMS around the horizontal axis	Ω_v	$[rpm]$
Armature inductance of tail / main motor	$L_{ah/av}$	$0.86 \times 10^{-3}[H]$
Armature resistance of tail / main motor	$R_{ah/av}$	$8[\Omega]$
Cable force coefficient for negative θ_h	k_{chn}	$k_{chp} * 0.9$
Cable force coefficient for positive θ_v	k_{chp}	$8.54 \cdot 10^{-3}$
Horizontal friction coefficient of the beam subsystem	k_{oh}	$4.7 \cdot 10^{-3}$
Vertical friction coefficient of the beam subsystem	k_{ov}	$1.31 \cdot 10^{-3}$
Distance between the counterweight and the joint	l_{cb}	$0.276[m]$
Drag friction coefficient of the tail propeller	k_{th}	$5 \cdot 10^{-8}$
Drag friction coefficient	k_{tv}	$5.6 \cdot 10^{-7}$

Equilibrium pitch angle ($u_v = 0.2753V$)	θ_v^0	$0[°]$
Gyroscopic constant	k_g	0.2
Input constant of the main motor	k_2	8.5
Input voltage of the tail motor	u_h	$[V]$
Input voltage of the main motor	u_v	$[V]$
Input constant of the tail motor	k_1	6.5
Length of tail part of the beam	l_t	$0.282[m]$
Length of main part of the beam	l_m	$0.246[m]$
Length of counter-weight beam	l_b	$0.290[m]$
Mass of the counter-weight	m_{cb}	$0.068[kg]$
Mass of the counter-weight beam	m_b	$0.022[kg]$
Mass of main part of the beam	m_m	$0.014[kg]$
Mass of the tail shield	m_{ts}	$0.119[kg]$
Mass of the main DC motor	m_{mr}	$0.236[kg]$
Mass of the tail DC motor	m_{tr}	$0.221[kg]$
Moment of inertia main DC motor	J_{mr}	$2.16 \cdot 10^{-4}[kgm^2]$
Moment of inertia in tail motor	J_{tr}	$3.14 \cdot 10^{-5}[kgm^2]$
Positive constant	k_t	$2.6 \cdot 10^{-5}$
Mass of the main shield	m_{ms}	$0.219[kg]$
Mass of the tail part of the beam	m_t	$0.015[kg]$
Pitch angle of the beam	θ_v	$[°]$
Physical constant	$k_{ah/v}\varphi_{h/v}$	$0.0202[Nm/A]$
Positive constant	k_m	$2 \cdot 10^{-4}$
Radius of the tail shield	r_{ts}	$0.1[m]$
Radius of the main shield	r_{ms}	$0.155[m]$
Rotational velocity of the tail rotor	ω_h	$[rpm]$
Rotational velocity of the main rotor	ω_v	$[rpm]$
Viscous friction coefficient of the tail propeller	B_{tr}	$2.3 \cdot 10^{-5}[kg.m^2/s]$
Viscous friction coefficient of the main propeller	B_{mr}	$4.5 \cdot 10^{-5}[kg.m^2/s]$
Yaw angle of the beam	θ_h	$[°]$

The mathematical model of the TRMS is represented by the following set of nonlinear differential equations [107]:

$$\frac{di_{ah/v}}{dt} = -\frac{R_{ah/v}}{L_{ah/v}} i_{ah/v} - \frac{k_{ah/v}\varphi_{h/v}}{L_{ah/v}} \omega_{h/v} + \frac{k_{1/2}}{L_{ah/v}} u_{h/v} \tag{6.78}$$

$$\frac{d\omega_{h/v}}{dt} = \frac{k_{ah/v}\varphi_{h/v}}{J_{tr/mr}} i_{ah/v} - \frac{B_{tr/mr}}{J_{tr/mr}} \omega_{h/v} - \frac{f_{1/4}(\omega_{h/v})}{J_{tr/mr}} \tag{6.79}$$

$$\begin{aligned}\frac{d\Omega_h}{dt} =& \frac{l_t f_2(\omega_h)\cos\theta_v - k_{oh}\Omega_h - f_3(\theta_h)}{D\cos^2\theta_v + E\sin^2\theta_v + F} \\ &+ \frac{k_m \omega_v \sin\theta_v \Omega_v \left(D\cos^2\theta_v - E\sin^2\theta_v - F - 2E\cos^2\theta_v\right)}{\left(D\cos^2\theta_v + E\sin^2\theta_v + F\right)^2}\end{aligned}$$

$$+\frac{k_m \cos\theta_v \left(k_{av}\varphi_v i_{av} - B_{mr}\omega_v - f_4(\omega_v)\right)}{\left(D\cos^2\theta_v + E\sin^2\theta_v + F\right) J_{mr}} \tag{6.80}$$

$$\frac{d\theta_h}{dt} = \Omega_h \tag{6.81}$$

$$\frac{d\Omega_v}{dt} = \frac{l_m f_5(\omega_v) + k_g \Omega_h f_5(\omega_v)\cos\theta_v - k_{ov}\Omega_v}{J_v} + \frac{g\left((A-B)\cos\theta_v - C\sin\theta_v\right) - 0.5{\Omega_h}^2 H \sin 2\theta_v}{J_v} + \frac{k_t\left(k_{ah}\varphi_h i_{ah} - B_{tr}\omega_h - f_1(\omega_h)\right)}{J_v J_{tr}} \tag{6.82}$$

$$\frac{d\theta_v}{dt} = \Omega_v \tag{6.83}$$

where $u_{h/v}$ is the input voltage of the tail/main motor, $\Omega_{h/v}$ is the angular velocity around the vertical/horizontal axis, $\theta_{h/v}$ is the azimuth/pitch beam angle (horizontal/vertical plane), $\omega_{h/v}$ is the rotational velocity of the tail/main rotor, $J_{tr/mr}$ is the moment of inertia in DC-motor tail/main propeller subsystem, $k_{ah/v}\varphi_{h/v}$ is the torque constant of the tail/main motor, and J_v is the moment of inertia about the horizontal axis. Functions f_i are defined as:

$$f_1(\omega_h) = sign(\omega_h) k_{th}\omega_h^2 \tag{6.84}$$

$$f_2(\omega_h) = \begin{cases} k_{fhp}\omega_h^2 & \text{if } \omega_h \geq 0 \\ -k_{fhn}\omega_h^2 & \text{if } \omega_h < 0 \end{cases} \tag{6.85}$$

$$f_3(\theta_h) = \begin{cases} k_{chp}\theta_h & \text{if } \theta_h \geq 0 \\ k_{chn}\theta_h & \text{if } \theta_h < 0 \end{cases} \tag{6.86}$$

$$f_4(\omega_v) = sign(\omega_v) k_{tv}\omega_v^2 \tag{6.87}$$

$$f_5(\omega_v) = \begin{cases} k_{fvp}\omega_v^2 & \text{if } \omega_v \geq 0 \\ -k_{fvn}\omega_v^2 & \text{if } \omega_v < 0 \end{cases} \tag{6.88}$$

Finally, the constants of the nonlinear model (6.78)-(6.83) are defined as:

$$A = \left(\frac{m_t}{2} + m_{tr} + m_{ts}\right) l_t \qquad B = \left(\frac{m_m}{2} + m_{mr} + m_{ms}\right) l_m$$
$$C = \frac{m_b}{2} l_b + m_{cb} l_{cb} \qquad H = A l_t + B l_m + \frac{m_b}{2} l_b^2 + m_{cb} l_{cb}^2$$
$$D = \frac{m_b}{3} l_b^2 + m_{cb} l_{cb}^2 \qquad F = m_{ms} r_{ms}^2 + \frac{m_{ts}}{2} r_{ts}^2$$
$$E = \left(\frac{m_m}{3} + m_{mr} + m_{ms}\right) l_m^2 + \left(\frac{m_t}{3} + m_{tr} + m_{ts}\right) l_t^2$$

where m_{ms} and m_{ts} are the masses of the main and tail shields, m_m and m_t are the masses of the main and the tail parts of the beam, m_{mr} and m_{tr} are the masses of the main and the tail DC-motor with main and tail rotor, m_b and l_b are the mass and the length of the counter-weight beam, m_{cb} and l_{cb} represent the mass of the counter-weight and the distance between the counter-weight and the joint, and r_{ms} and r_{ts} are the radius of the main and tail shield.

6.5.4 MPC of TRMS system

Using the nonlinear model of the TRMS (6.78)-(6.83) a linear model has been obtained by linearizing around an equilibrium point ($\bar{u}_h = 0.9865$, $\bar{u}_v = 0.2753$, $\bar{\theta}_h = 1.5700$, $\bar{\theta}_v = 0$) and discretizing with a sample time $T_s = 0.015\ s$:

$$A = \begin{bmatrix} 1.0 & 0.015 & 4.1e-7 & 2.8e-8 & 2.3e-5 & -6.5e-6 & -1.9e-7 & 9.1e-9 \\ -2.8e-3 & 1.0 & 5.4e-5 & 3.7e-6 & 3.1e-3 & -8.5e-4 & -2.5e-5 & 4.9e-7 \\ 0 & 0 & 0.96 & 0.066 & 0 & 0 & 0 & 0 \\ 0 & 0 & -2.4e-3 & -1.7e-4 & 0 & 0 & 0 & 0 \\ -1.2e-8 & 1.3e-5 & -7.6e-8 & 5.1e-9 & 1.0 & 0.015 & 8.2e-7 & 8.1e-9 \\ -2.5e-6 & 1.8e-3 & -1.0e-5 & 5.4e-9 & -0.075 & 1.0 & 1.1e-4 & 1.1e-6 \\ 0 & 0 & 0 & 0 & 0 & 0 & 0.99 & 0.01 \\ 0 & 0 & 0 & 0 & 0 & 0 & -2.5e-3 & -2.5e-5 \end{bmatrix}, \tag{6.89}$$

$$B = \begin{bmatrix} 1.0e-6 & 7.2e-7 \\ 2.1e-4 & 9.0e-5 \\ 7.6 & 0 \\ 0.79 & 0 \\ 3.9e-7 & 4.0e-7 \\ 3.9e-5 & 8.0e-5 \\ 0 & 1.5 \\ 0 & 1.1 \end{bmatrix}, \tag{6.90}$$

$$\text{and} \quad C = \begin{bmatrix} 1 & 0 & 0 & 0 & 0 & 0 & 0 & 0 \\ 0 & 0 & 0 & 0 & 1 & 0 & 0 & 0 \end{bmatrix} \tag{6.91}$$

The system input vector is $u = [u_h\ u_v]^T$ and the system states are $x = [\theta_h\ \Omega_h\ \omega_h\ i_{ah}\ \theta_v\ \Omega_v\ \omega_v\ i_{av}]^T$. The control objective consists in maintaining the pitch angle θ_v and the azimuth angle θ_h in the desired angular positions under decoupling and actuator degradation effects. For the azimuth angle, a square reference signal has been defined, whereas the pitch angle reference signal has been set to 0°. As not all state variables are measured, a reduced-order state observer is used to estimate nonmeasured variables, which are the angular momentums of the beams and the armature currents of the rotors (Ω_h, Ω_v, i_{av}, i_{ah}).

Regarding the HAC for the TRMS, Figure 6.23 presents the control scheme of the approach. Here, an MPC cost function is tuned based on the degradation coefficient of the actuators. Additionally, the data provided by a monitoring module is used to changes the constrains in the optimization problem. This module monitors system control inputs and compute the degradation of the actuators according to their use.

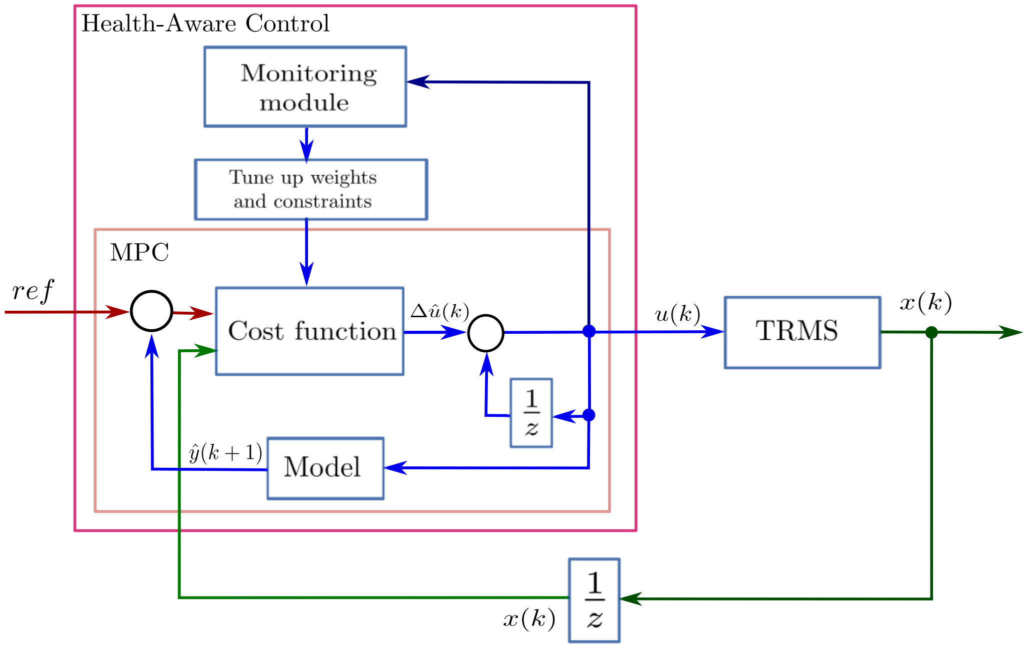

FIGURE 6.23: HAC MPC-based for TRMS.

Since actuator degradation depends on the time evolution of u, the design of a health-aware MPC law can be taken into account through two approaches: the inclusion of the degradation constraint (6.69) and the proper tuning of the weighting factors ρ and α. To study this dependency, 4 case studies are simulated using the nonlinear model of the TRMS. The general MPC parameters are summarized in Table 6.8, and the specific parameters corresponding to each case are shown in Table 6.9. In both tables, subindex 1 (2) corresponds to input u_h (u_v), except for parameter μ which is related to θ_h (θ_v). H_M is the maintenance interval, and is related to the maintenance horizon as follows: $H_M = k_M T_s$.

Simulation results are shown in Figures 6.24-6.27, for azimuth angle θ_h and pitch angle θ_v. Cumulative degradation z is shown in Figure 6.28(a) for tail and Figure 6.28(b) for main motor.

In Table 6.10 some performance indexes have been evaluated for a simulation interval of 1 hour (T_{sim}). Rows 2 and 3 indicate the integral of the square of the tracking error (ISE) corresponding to both output angles. The smaller the ISE indexes are, the better the control performance is. Rows 4 and 5 correspond to the cumulative degradation for both actuators (tail/main) at the end of simulation.

TABLE 6.8: List of MPC parameters

Parameter	Symbol	Value
Prediction horizon	H_p	80 [s]
Control horizon	H_c	4 [s]
Maintenance horizon	H_M	2 [$years$]
Sampling time	T_s	0.015 [s]
Simulation time	T_{sim}	1 [h]
Tracking weights	$\mu_1/\ \mu_2$	1
Control effort weights	$\alpha_1/\ \alpha_2$	
Control effort variation weights	$\rho_1/\ \rho_2$	
Upper control efforts	u_{1max}/u_{2max}	12 [V]
Lower control efforts	u_{1mim}/u_{2mim}	-12 [V]
Degradation threshold	z_{th1}	1
Degradation threshold	z_{th2}	1
Degradation rate	γ_1	$1.1 \cdot 10^{-11}$
Degradation rate	γ_2	$2.7 \cdot 10^{-10}$

TABLE 6.9: Case study parameters

Case	ρ_1	ρ_2	α_1	α_2	Deg. constraint
1	0	0	0	0	No
2	0	0	0	0	Yes
3	1/120	1/120	1/120	1/120	Yes
4	1/1000	1/120	1/1000	1/120	Yes

TABLE 6.10: Performance evaluation

Case	1	2	3	4
ISE Θ_h	20.2395	20.2317	21.9480	21.5749
ISE Θ_v	1.4016	1.4246	1.1740	1.1289
Z_h cum. $(\cdot 10^{-4})$	0.0305	0.0307	0.0261	0.0266
Z_v cum. $(\cdot 10^{-4})$	0.4434	0.4390	0.3109	0.3114

Case 1 corresponds to a neutral MPC control, because it does not take into account the degradation constraint, and only tracking errors are penalized in the cost function. As a result, control performance is good, but the main motor degradation at T_{sim} is higher in comparison to the other cases.

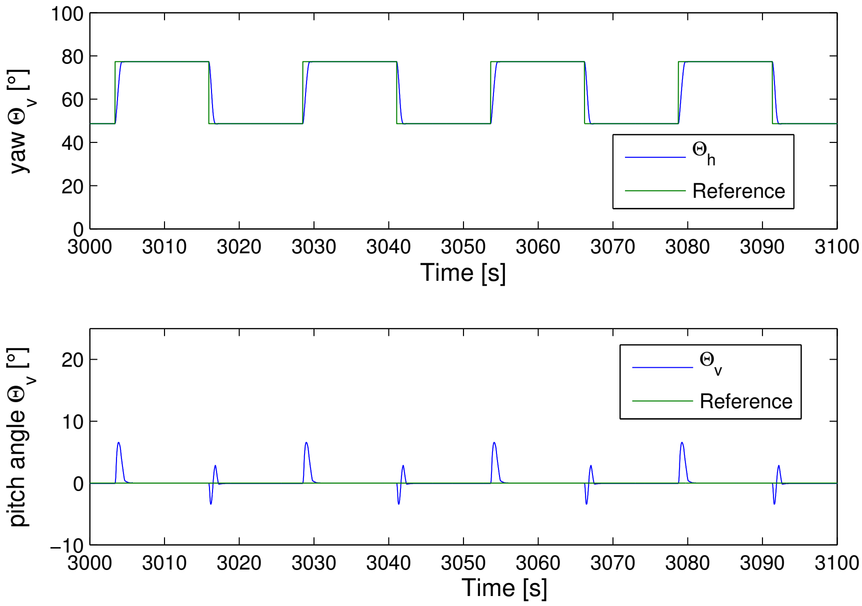

FIGURE 6.24: Response of azimuth and pitch angles for Case 1.

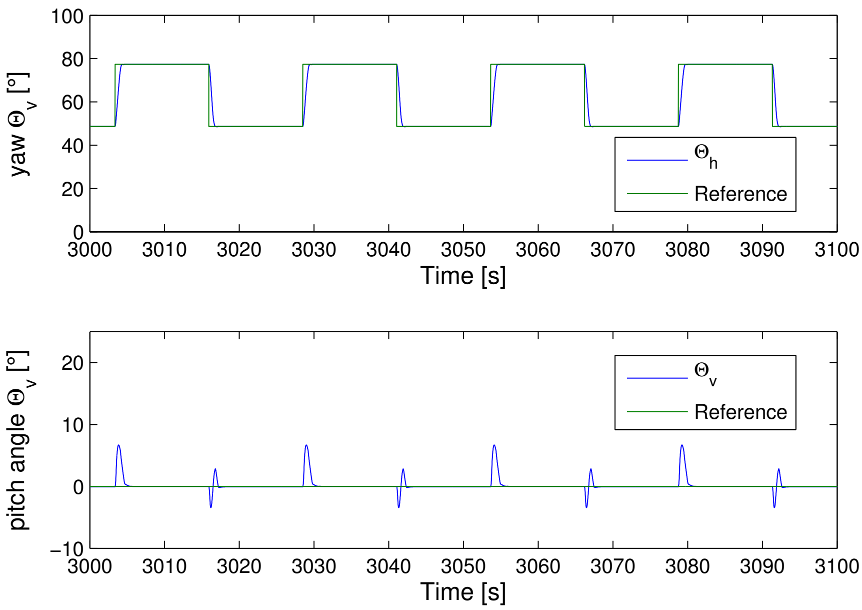

FIGURE 6.25: Response of azimuth and pitch angles for Case 2.

In Case 2, the degradation constraint is taken into account and the main motor degradation is not allowed to exceed the maximum threshold before the maintenance horizon. As a consequence the pitch control performance is degraded (i.e., ISE increases), but degradation is reduced (i.e., cumulative z decreases).

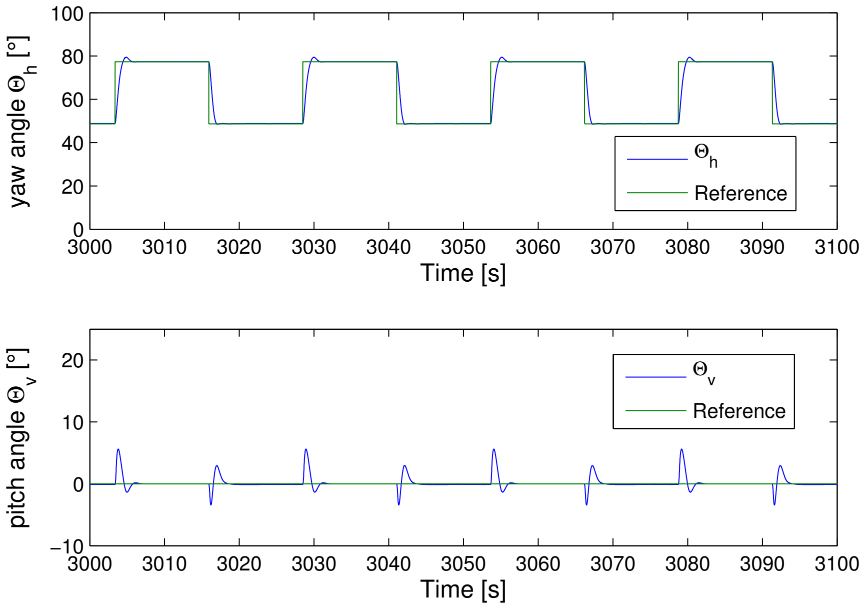

FIGURE 6.26: Response of azimuth and pitch angles for Case 3.

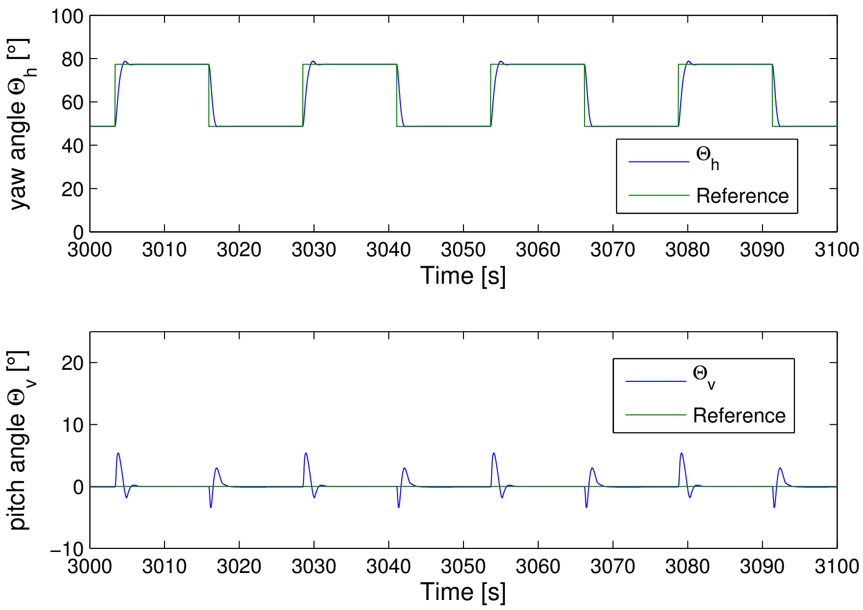

FIGURE 6.27: Response of azimuth and pitch angles for Case 4.

In Cases 3 and 4, the degradation process is also taken into account in the cost function. In Case 3 both control inputs are equally weighted in the cost function, whereas in Case 4 the weighting factors corresponding to the tail motor are smaller. The idea is to penalize the actuator that exhibits a bigger degradation coefficient, which in this case corresponds

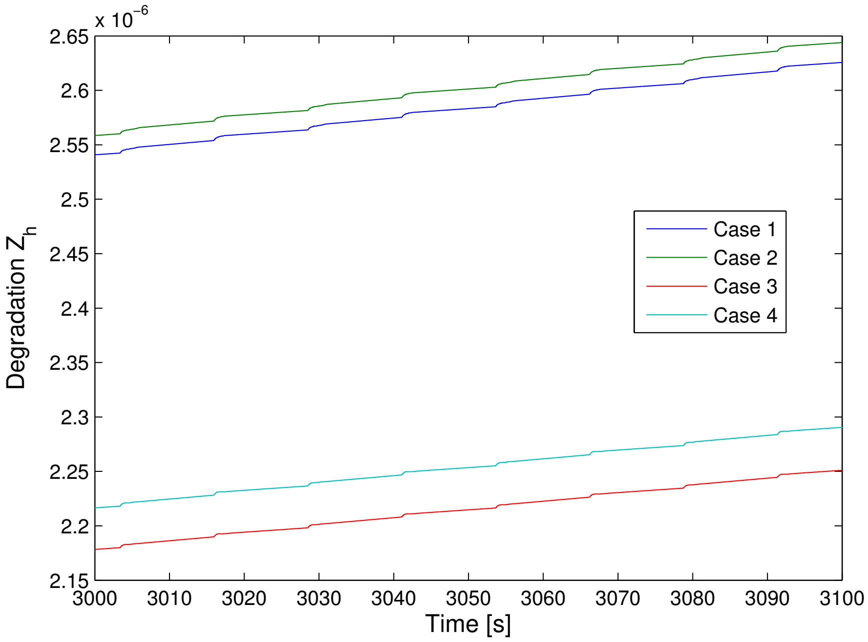

(a)

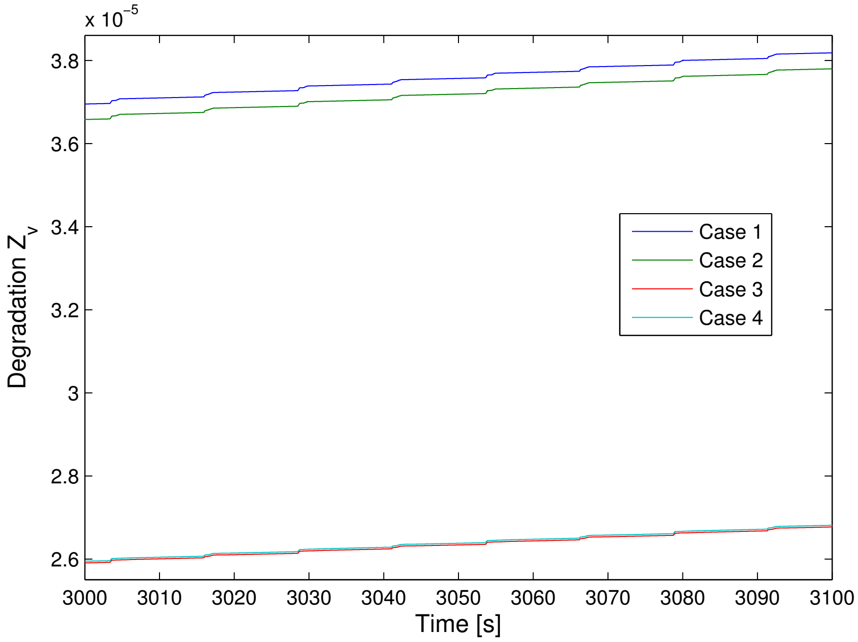

(b)

FIGURE 6.28: Degradation process, a) Horizontal plane, b) Vertical plane.

to the main motor. As a result, the main motor degradation is delayed even further away from the maintenance horizon (i.e., its cumulative degradation is reduced). However, some care must be taken when choosing the weighting factors since control performance could be deteriorated.

6.6 Conclusions

This chapter has presented Health-Aware control methodologies based on MPC and LQR algorithms. The first methodology aims to finding the most important components (the actuators in this case) based on the study of the RIMs. To achieve that, and as contribution of this, a methodology to tune the MPC cost function weights that provide best system reliability and control performance has been proposed. To handle the reliability in the optimization problem of the MPC controller, an study on different RIMs and their combinations has been carried out as part of a global approach. Moreover, a local approach that considers an equivalent contribution of component reliability to system reliability, has been studied.

The overall system reliability assessment was done using the methodology presented in Section 4.2.5, based in determining the minimal path sets, which is known to be an NP-hard problem when applied to complex system with high amount of components. Nevertheless, the DBN model may be build from other methods based on a top down analysis avoiding the specification of all path sets.

This approach was illustrated through an application on a DWN. The use of reliability measures is useful in identifying the relative importance of each actuator (pump) into the DWN with respect to the overall reliability of the system. The objective was to extend the uptime of the system by delaying, as much as possible the system reliability decrease. Another contribution is that the reliability assessment and RIMs computation were performed on-line using a DBN.

The results have demonstrated the effectiveness of the methodology. Those results show that the reliability importance measures provide better system reliability. It is worth to mention that there is a trade-off between control and reliability objectives. Such trade-off has been studied and a methodology to handle it has been proposed.

The second approach consist in a LQR tuning methodology based on the Birnbaum's reliability importance measure. The aim is to perform the control of the system and preserve its reliability by distributing the control efforts among the actuators based on their importance to the system reliability. The tuning method uses the information about system and actuators reliabilities and their importance as a policy to adjust the gain matrix $\boldsymbol{R}_{LQR}$ accordingly.

As a key contribution, in this methodology the system reliability block diagram has been obtained from the system controllability analysis. At least 4 rotors are required to assure system controllability. Therefore, the minimal path sets have been determined based on those 4-rotor configurations that guarantee system controllability.

Simulation results demonstrates the validity of this approach in terms of reliability and controllability of the octorotor through an effective health management of the UAV actuators.

Also, a third approach was presented. A degradation model has been taken into account into the design of a HAC. Results have shown that actuator degradation can be delayed not only by including a degradation constraint but also by properly tuning the control input weighting factors in the MPC cost function. This strategy has been applied to a Twin Rotor MIMO system showing that despite the presence of some system couplings, the control performance of this multivariate system is clearly affected by the health-aware control strategy. Hence, the challenge was to design a HAC scheme that delayed actuator degradation but guaranteed control performance. It has been shown that satisfying these objectives was possible.

Regarding the failure rate modeling, a review of different models used in the literature has been presented. Although a model of failure rate which considers the cumulative usage of the actuators over time has been chosen, other models could be applied, e.g. based on control effort variations. In that case, appropriate weights in the cost function could be set to improve the system reliability by making those variations softer.

Chapter 7

Reliability Interpretations

This chapter presents a comparison between two different reliability interpretations within a Health-Aware Control framework: instantaneous and expected reliability. These reliability interpretations concern the way how reliability is evaluated and how it is considered to evolve along time. The system reliability performance under both approaches is compared in a control strategy applied to a DWN.

7.1 Reliability interpretations

In this Chapter, a discussion of the work presented in [141], where two reliability interpretations were studied will be addressed. The first one corresponds to the concept of reliability which has been applied until now in this thesis. It considers that the reliability of an asset or system can be computed by (3.9):

$$R_i(t) = e^{\left(-\int_0^t \lambda_i(v)dv\right)}$$

which is a function of time and its failure rate, that is assumed to follow a defined function based on the Proportional Hazard Models (Section 3.2.1).

This reliability is a monotonically decreasing function of time and it is computed at each sampling time. Remark that the $R_i(0) = 1$ and that at each time instant $t > 0$ the reliability decreases according to its failure rate (6.1) (see Figure 7.1(a)). Let this reliability interpretation be refereed as the *instantaneous reliability*.

Generally, the objective in reliability optimization is to achieve higher levels of reliability at the end of the mission time $R_i(T_M)$ (Figure 7.1(b)), which is the probability that component i is able to satisfy its function at the end of the mission T_M, denoted as:

$$R_i(T_M) = e^{-\int_0^{T_M} \lambda_i(v)dv} \quad \forall\, i = 1, \ldots, p. \tag{7.1}$$

The other reliability interpretation considers that the reliability of an asset or a system is computed at a given time $\tau \in [0, T_M]$ [20]. Then, (3.9) becomes:

$$R_i^\tau(t) = e^{-\int_\tau^t \lambda_i(v)dv} \ \forall\, i = 1, \ldots, p. \tag{7.2}$$

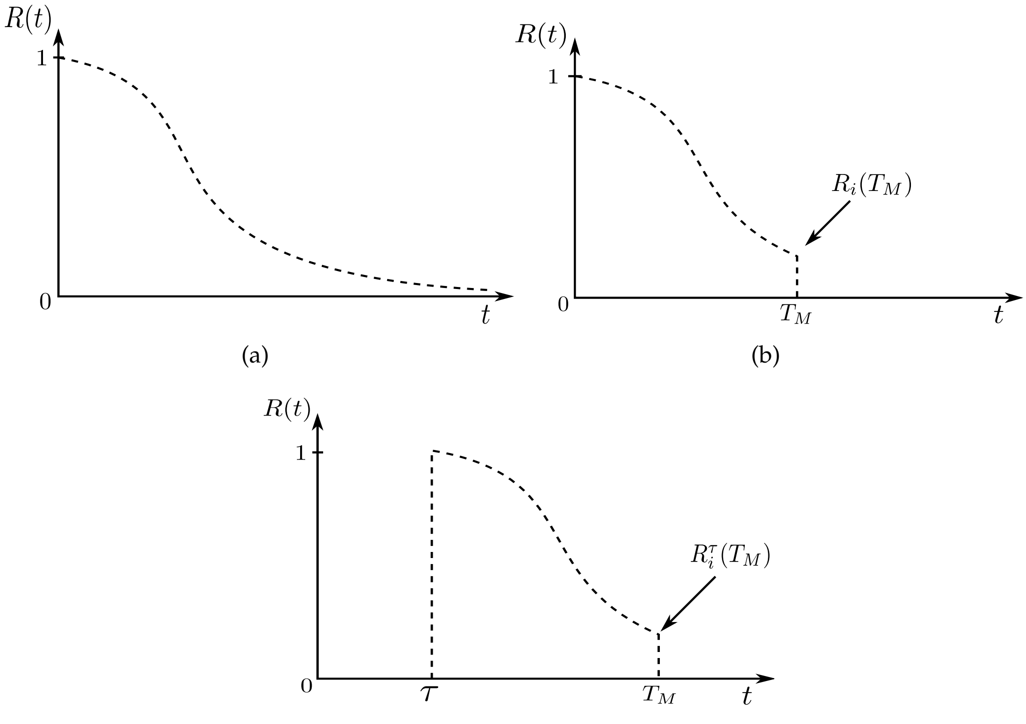

FIGURE 7.1: Reliability representation: (a) reliability evolution over time $R_i(t)$, (b) reliability at time T_M $R_i(T_M)$, (c) reliability evolution from time τ until time T_M $R_i^\tau(T_M)$.

This implies that $R_i^\tau(\tau) = 1$ at current time (Figure 7.1(c)) and it means that an asset or system remains fully reliable as long as it is not affected by a fault. Moreover, its reliability at mission time T_M evaluated at current time τ is denoted as:

$$R_i^\tau(T_M) = e^{-\int_\tau^{T_M} \lambda_i^\tau(v)dv} \ \forall\, i = 1, \ldots, p \tag{7.3}$$

where $\lambda_i^\tau(t)$ is the failure profile of the ith asset determined at time τ using (6.1) and $R_i^\tau(T_M)$ denotes the reliability at the end of the mission time T_M computed at time instant τ (see Figure 7.2).

Let the second reliability interpretation be refereed as the *expected reliability*. Assume that the component can be characterized at instant time τ by a constant failure rate in the time

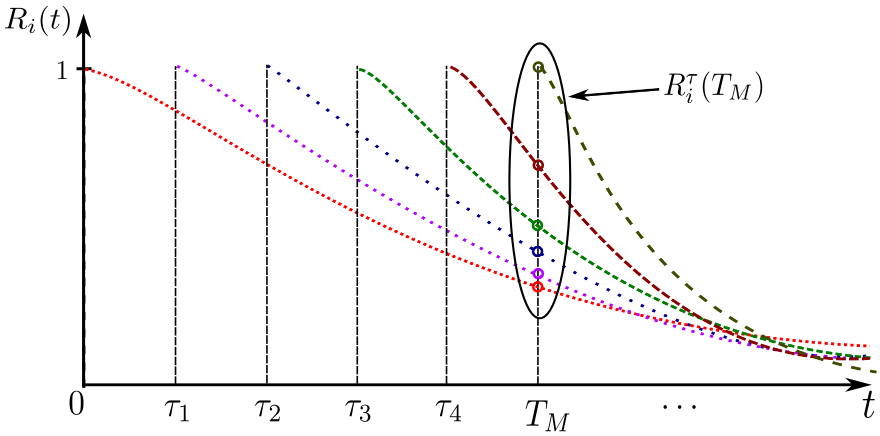

FIGURE 7.2: Expected reliability of the asset $R_i^\tau(T_M)$.

interval $[\tau, T_M]$. Hence, the corresponding reliability of the asset becomes:

$$R_i^\tau(T_M) = e^{-\lambda_i^\tau \times (T_M - \tau)} \;\; \forall\, i = 1, \ldots, p \tag{7.4}$$

where $\lambda_i(\tau)$ is the ith asset failure rate computed at time τ.

Regarding system reliability, under the first interpretation it will be called the *instantaneous system reliability*, denoted as $R_S(t)$. Under the second interpretation it will be called the *expected system reliability*, denoted as $R_S^\tau(T_M)$.

The Reliability Importance Measure (RIM) should be expressed accordingly with the expected reliability interpretation as it is presented below.

7.1.1 Importance reliability measures

As presented in Section 4.4, to measure and quantify the impact of asset failures over the functioning of the system, several indicators concerning reliability importance have been proposed, each of them with a particular purpose [79].

For instance, the Birnbaum's importance measure $\mathrm{I}_{\mathrm{B}i}$ defined in (4.24) quantifies the maximum decrease of system reliability due to reliability changes of the ith actuator.

According to both reliability interpretations, two Birnbaum's measures are proposed. On the one hand, under the instantaneous reliability interpretation, the asset Birnbaum's importance measure will be computed as in (4.24), whereas under the expected reliability interpretation the Birnbaum's importance measure will be determined as follows:

$$\mathrm{I}_{\mathrm{B}i}^\tau(T_M) = \frac{\partial R_S^\tau(T_M)}{\partial R_i^\tau(T_M)} = R_S^\tau(1_i, T_M) - R_S^\tau(0_i, T_M) \tag{7.5}$$

which denotes the asset Birnbaum's importance measure at mission time instant T_M computed at current time τ.

7.1.2 Redistribution policy

The redistribution policy discussed in Section 6.3.3 which is based on the actuators RIMs is now used to compare both reliability interpretations (i.e., instantaneous and expected). The MPC technique facilitates the implementation of a Health-Aware Control and the exploration of different redistribution policies without significant changes in the control algorithm.

Five scenarios are proposed setting a different weight (ρ_i) under the two reliability interpretations.

In the first scenario actuator reliability is targeted. Accordingly, ρ_i is set under the instantaneous reliability interpretation as follows:

$$\rho_i(k) = 1 - R_i(k). \tag{7.6}$$

In the first scenario, the instantaneous reliability interpretation is assumed.

In the second scenario the overall system reliability is targeted using the Birnbaum's importance measure. Accordingly, ρ_i is set under the instantaneous reliability interpretation as follows:

$$\rho_i(k) = I_{Bi}(k). \tag{7.7}$$

Similarly, under the expected reliability interpretation, the third scenario corresponds to:

$$\rho_i(k) = 1 - R_i^k(k_f) \tag{7.8}$$

and the fourth scenario to:

$$\rho_i(k) = I_{Bi}^k(k_f) \tag{7.9}$$

where k_f is the end of mission sample, corresponding to T_M.

In the fifth weight assignment, which is common for both reliability interpretations, no reliability feedback is taken into account, i.e., $\rho_i(k) = 1$.

7.1.3 Performance evaluation

In addition to the cumulative control effort index (U_{cum}) new indices are defined next, which will be used in assessing the health-aware control performance under both reliability interpretations.

Definition 7.1. The Cumulative System Reliability indices indicate the aggregated system reliability over the mission time.

Under the instantaneous reliability interpretation, it is denoted in discrete time as:

$$R_{S\text{cum}} = T_s \sum_{k=0}^{T_M/Ts} R_s(k). \tag{7.10}$$

And under the expected reliability interpretation it is denoted as:

$$R_{S\text{cum}}^{k_f} = T_s \sum_{k=0}^{T_M/Ts} R_s^k(k_f). \tag{7.11}$$

A higher value indicates a better management of the assets reliabilities with the objective of improving the overall system reliability.

7.2 Drinking Water Network example

Both reliability interpretations will be compared on an application to the DWN presented in Section 6.3.4. The objective is to apply the MPC HAC methodology to maintain the pumps and tanks within their bounds and extend the reliability of the system. The cost function used in this example is (6.12) with $\varepsilon = 0$, and the failure rate of the pumps is computed using (6.8) in accordance with the reliability interpretation.

The parameters of the simulation are presented in Table 7.1.

Figure 7.3 shows the instantaneous system reliability in the scenario where no reliability feedback method is applied ($\rho_i = 1$) where the overall system reliability presents a gradual decreasing behavior, which is characteristic of the instantaneous reliability interpretation. This is the nominal scenario and will be compared with the results of the other ρ_i settings.

To illustrate how reliability behaves under the expected reliability interpretation, the reliability computed at each sampling time were projected $\tau + T_M$ hours into the future.

TABLE 7.1: Simulation parameters

Parameter	Symbol	Value					
Prediction horizon	H_p	24 $[h]$					
Control horizon	H_c	8 $[h]$					
Sampling time	T_s	1 $[h]$					
Component parameter	β_i	$10^{-2}\ \forall\, i \in [1, 10]$					
Upper control bound	$\overline{u}_i$	0.75	0.75	0.75	1.20	0.85	$[m^3/s]$
		1.60	1.70	0.85	1.70	1.60	
Lower control bound	$\underline{u}_i$	$0\ \forall\, i \in [1, 10]\ [m^3/s]$					
Baseline failure rate	λ_i^0	9.85	10.70	10.50	1.40	0.85	$[h^{-1} \cdot 10^{-4}]$
		0.80	11.70	0.60	0.74	0.78	
Upper state bound	$\overline{x}_i$	65200	3100	14450	11745	$[m^3]$	
Lower state bound	$\underline{x}_i$	25000	2200	5200	3500	$[m^3]$	
Initial states	$x_i(0)$	45100	2650	9825	7622	$[m^3]$	

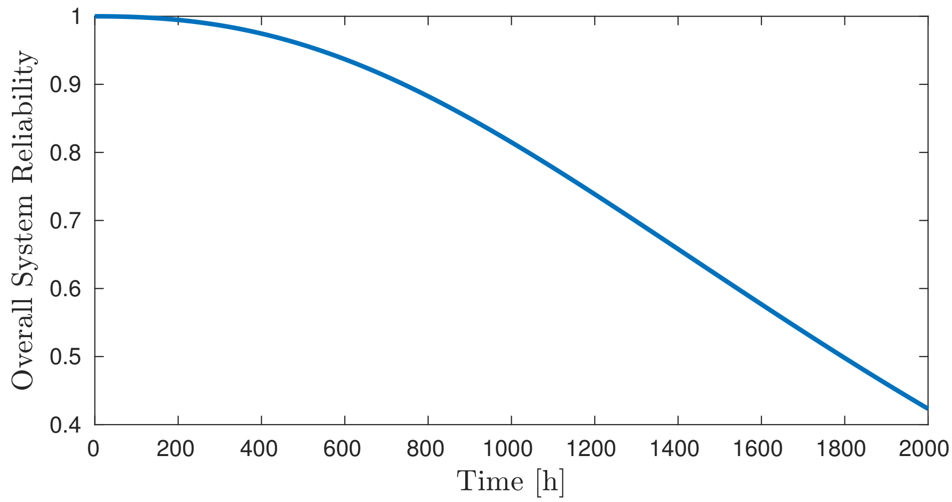

FIGURE 7.3: Instantaneous overall system reliability profile evolution with $\rho_i = 1$.

Some of those values are presented in Figure 7.4, where the overall system reliability computed at $\tau = 1$, 500, 1000, 1500, and 2000 hours is projected into the future.

Next, Figure 7.5 presents the expected overall system reliability evolution at time instant T_M, which consists of the values of each system reliability projection at T_M computed at each sampling time. In this case, the reliability starts from a value between 0 and less than 1 and moves towards 1.

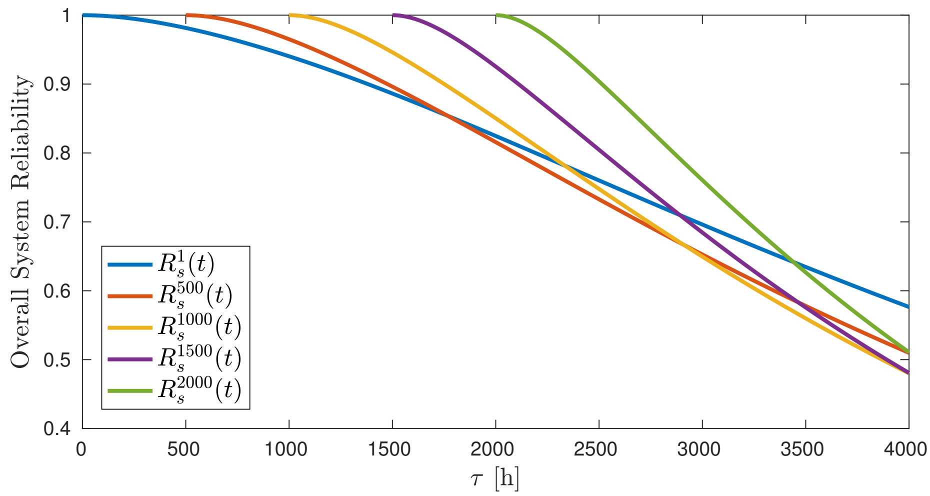

FIGURE 7.4: Expected overall system reliability profile evolution at different time instants with $\rho_i = 1$.

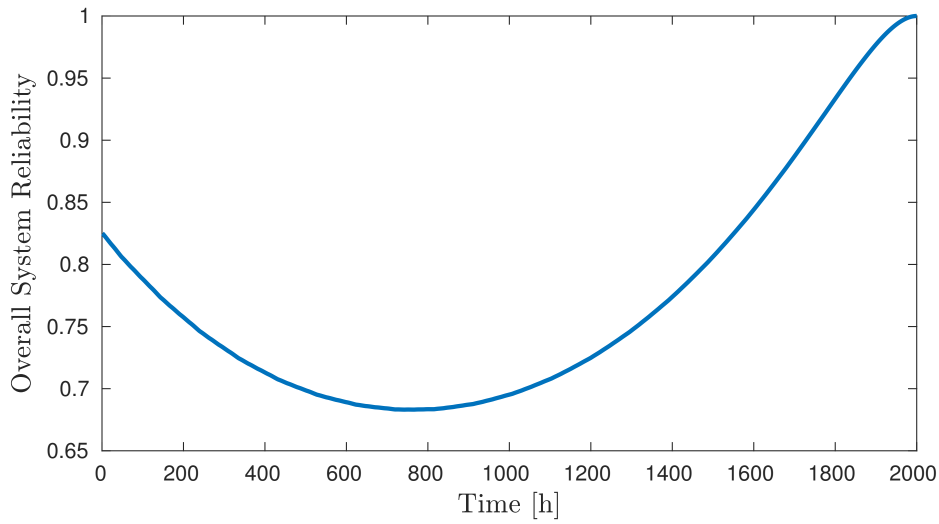

FIGURE 7.5: Expected system reliability at mission time $T_M = 2000h$ evolution with $\rho_i = 1$.

7.2.1 Reliabilities comparison

The five scenarios proposed in Section 7.1.2 have been considered in the MPC control of the DWN. All cases will be assessed under both cumulative reliability indices (7.10) and (7.11).

Figure 7.6 shows the instantaneous system reliability evolution for the five scenarios. Remark that the most suitable policies that improve system reliability are those based on the Birnbaum's measure.

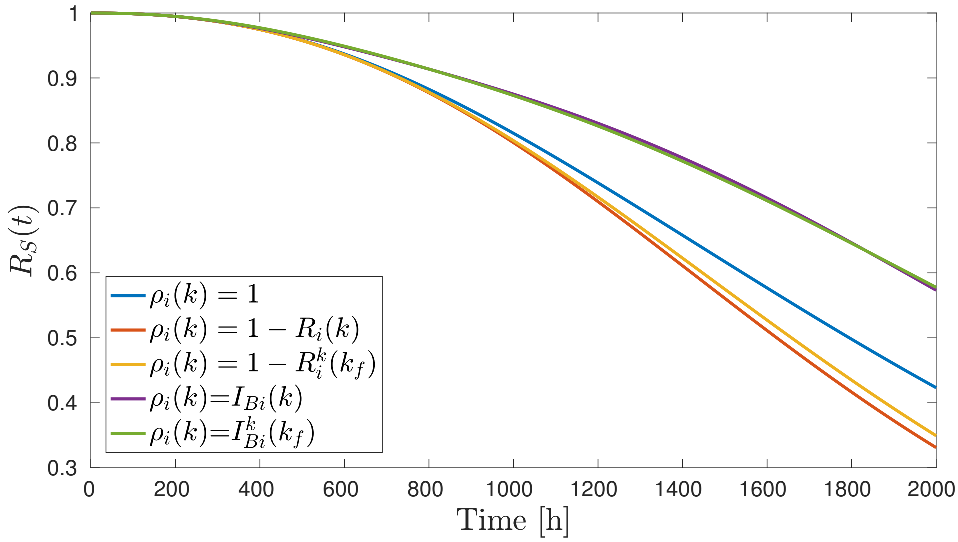

FIGURE 7.6: Instantaneous system reliability.

Figure 7.7 provides the expected system reliability at the end of the mission time T_M for the five scenarios. Again the best results correspond to those based on the Birnbaum's measure.

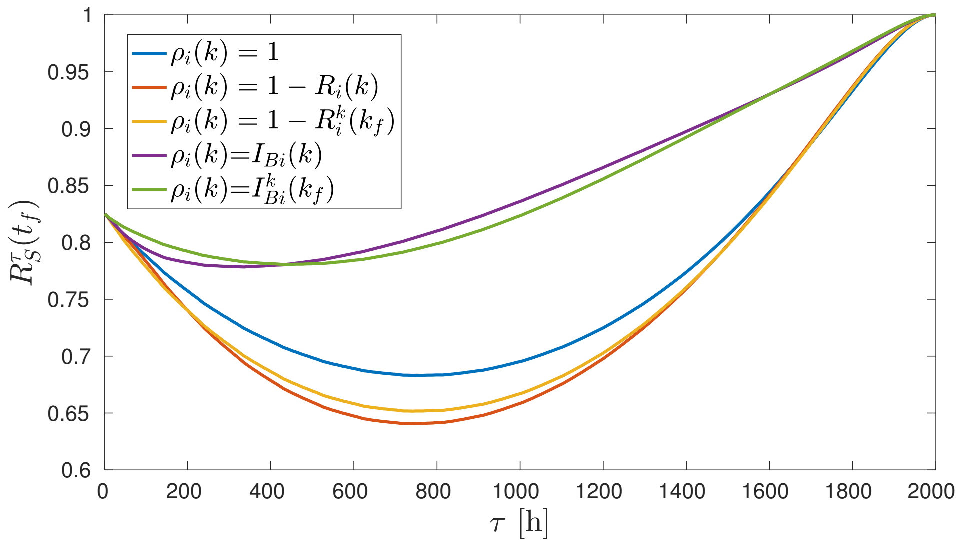

FIGURE 7.7: Expected system reliability at mission time t_f.

The reliability performance indices were also computed for each scenario and are presented in Table 7.2.

The performance indices confirm that the best reliability performance is attained when using a redistribution policy based on the Birnbaum's importance measure, i.e., (7.7) and

TABLE 7.2: Reliability performance indexes.

$\rho_i(k)$	$R_{S\text{cum}}$ $[\cdot 10^6]$	$R^{k_f}_{S\text{cum}}$ $[\cdot 10^6]$	U_{cum} $[\cdot 10^6]$
1	5.6131	5.5583	1.5370
$1 - R_i(k)$	5.4046	5.4054	1.9687
$1 - R_i^k(k_f)$	5.4525	5.4340	1.9002
$I_{Bi}(k)$	6.1006	6.1653	3.2158
$I^k_{Bi}(k_f)$	6.0915	6.1447	3.5040

(7.9), with a small improvement when the instantaneous reliability interpretation is followed, i.e., (7.7). Focusing on actuator reliability (i.e., (7.6) and (7.8)) does not optimize system reliability. However, targeting system reliability leads to a greater actuator energy expenditure.

To illustrate the performance of the control algorithm, tank volumes for the best redistribution policy, corresponding to (7.7), are presented in Figure 7.8. Note that, the DWN is able to supply the required water demand maintaining tank volumes within the specified bounds.

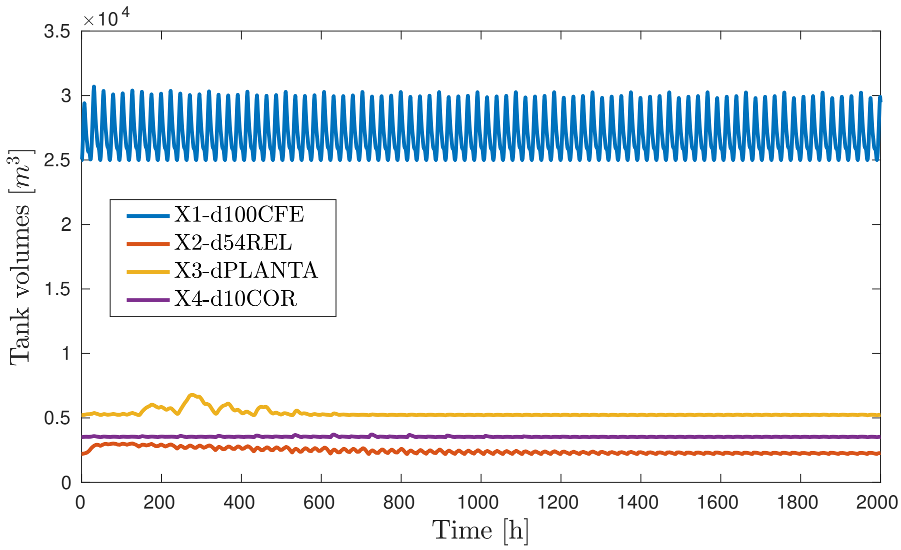

FIGURE 7.8: Tank volumes corresponding to $\rho_i(k) = \mathrm{I}_{Bi}(k)$.

And the pump control actions corresponding to the policy given in (7.7) are presented in Figure 7.9. Note that the control actions evolve in time according to the importance of each actuator, which change dynamically as their reliabilities change.

Remark that in this scenario, the cost function which computes the control actions does not take into account any tracking objective. Therefore, tank volumes freely evolve within

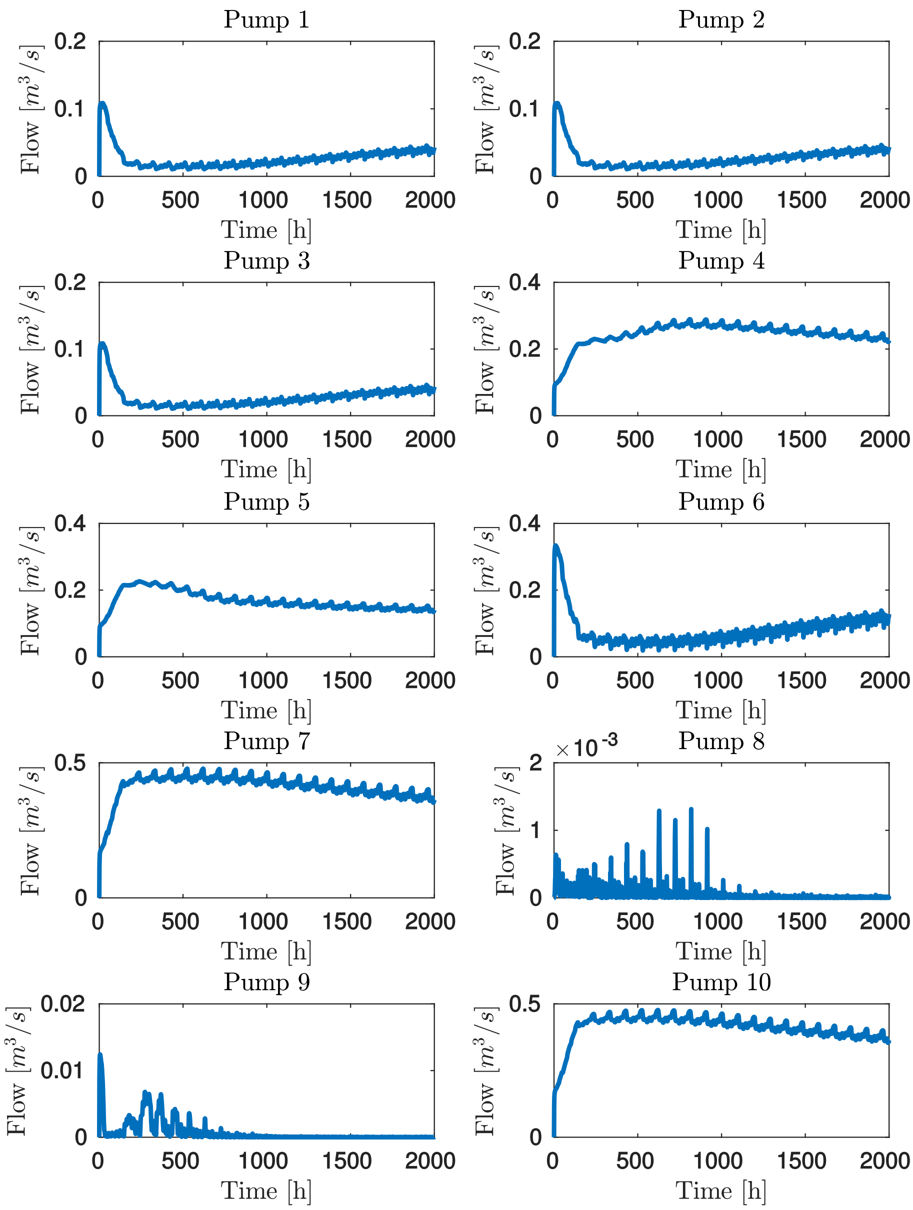

FIGURE 7.9: Pump commands corresponding to $\rho_i(k) = \mathrm{I}_{\mathrm{B}i}(k)$.

their bounds.

7.3 Conclusions

In this chapter, two reliability interpretations have been presented and illustrated using a DWN system. Both approaches have been applied to a Health-Aware Control scheme based on an MPC algorithm with the objective of improving system reliability.

The study of two different interpretations of reliability were presented. This study was done due to the need of clarify what is meant by reliability in both cases and what it is obtained by using each of those interpretations.

The results of the redistribution policy provide similar results in terms of reliability enhancement independently of the reliability interpretation. Thus, both interpretations are virtually equivalent.

This Chapter aims to illustrate another interpretation of the reliability. It is not intended to do the same experimentations done in the previous chapter where different weighting criteria were compared, and only one RIM was used in the experiment. Moreover, another RIMs or a mix of them can give better results in terms of reliability improvement, as it was demonstrated in the previous chapter.

Moreover, by applying both of them results coincide in determining that the Birnbaum's measure is the best approach to integrate the assets reliability into the control law.

Part III

Conclusions and perspectives

Chapter 8

Conclusions and future work

This thesis has proposed some contributions to the field of HAC systems based on MPC and LQR techniques. This chapter summarizes the contributions presented in this thesis, review the main conclusions, and explore the possibilities of further research.

8.1 Conclusions

PHM and HAC methodologies can be implemented on dynamical systems, allowing to improve the system safety and reduce costs in maintenance, shutdowns, and repairs. They have been studied during the last decades, and several results have been presented in the literature. However, there are still some aspects for further research, and this thesis has been devoted to the progress of the state-of-the-art in this field.

The key contributions of the research work in this thesis are:

- An overview on HAC methodologies and reliability modeling, contributes to clarify concepts like reliable control, FTC, HAC among others, which are often used indistinctly, sometimes in a wrong way.
- A design methodology of HAC schemes based on MPC and LQR techniques. It has been shown how the use of RIMs are valuable to identify the relative importance of each actuator with regarding the overall reliability of the system.

  This framework takes into account the usage of the actuators to preserve overall system reliability while maximizing control performance by means of tuning the cost function weights of an MPC. Two approaches have been compared, the first one, called "local approach" is focused on preserving only the actuators reliability, and the second one, called "global approach", uses the RIMs.

The results showed that the local approach, which considers an equivalent contribution of component reliability to system reliability is not the best method in terms of improving the overall system reliability, instead, the global approach results in better levels of reliability. This can be explained, to the fact that reliability has multiple dependencies, for instance, it depends on how much a particular actuator is used and also it has dependencies between actuators systems due to its localization within the system.

- Regarding the use of RIMs to tune the MPC algorithm, a comparison of them has been presented through an example in the DWN system. The results, provide better results by using combined RIMs.
- Also, a study of the multi-objective cost function has been presented. This study showed that a trade-off between the objectives has to be taken into account. To manage this trade-off, a methodology for selecting the optimal weights in the cost function has been presented.
- As a key contribution, the overall system reliability has been obtained by studying its link with the system controllability. An example on a UAV was presented, it stands that at least 4 rotors are required to assure the controllability of the system. Hence, the minimal path sets have been determined based on those 4-rotor configurations.
- A review of failure rate modeling used in the literature was done. As a result, a better-suited model of failure rate which considers the aggregated usage of the actuators and the time of life, was proposed.
- An study of two reliability interpretations have been presented and illustrated on a DWN system. Both approaches have been applied to the HAC scheme based on an MPC algorithm with the objective of improving system reliability presented in Chapter 6. Results show that both interpretations provide similar criteria concerning how MPC should be properly tuned in a HAC scheme.

8.2 Perspectives and future work

This research work can also be extended by exploring the following ideas:

- Explore other control methodologies to implement an HAC. In such a way, a feedback controller synthesizing approach based on Linear Matrix Inequalities (LIMs) could be considered as it was already proposed in [74].

- An open issue that requires further research is the procedure to obtain a cost function that can include other terms for its minimization and maintain its simplicity, due that nonlinear optimization cost function is computationally heavy and could lead to non-implementable control schemes. Therefore, it could be interesting to have an explicit system reliability expression into the MPC cost function, nevertheless, it would lead to a nonlinear MPC (NLMPC) implementation. Therefore, the NLMPC drawbacks should be taken into account.

- Special attention must be paid to the determination of the minimal path sets since their meaning depends on the system, and the objectives to be addressed. For instance, in DWNs a minimal path set is the set of actuators whose functioning satisfies the demands, i.e., they connect the demands with the sources. On the other hand, in the UAV system, a minimal path set is the set of actuators whose functioning guarantees the controllability of the system. Thus, further research should be done in studying different interpretation for the minimal path sets for other systems.

- The reliability analysis of the DWN systems can be extended to consider not only the topological reliability but also the hydraulic one. This can be a challenge because information of the availability of the water supplies is needed in advance and a precise forecast of the water consumption will be also required.

- The computation of the overall system reliability can result in an NP-hard problem in a complex system with high amount of components. This quantity of components could lead to a high amount of minimal path sets ($amps$) incrementing the amount of terms in the structure function by $2^{amps} - 1$. One solution could be the use of an approximation of the system reliability, such as the upper or lower reliability bounds [47]. Nevertheless, the use of this approach could not be the solution to this problem, and more research should be done.

- An open challenge is to apply the proposed methodology to real systems. Nevertheless, the slow decrease on reliability makes it difficult to obtain results in a reasonably fast way.

- Regarding the attempts to address the problem of HAC, a list of applications and control techniques used were given. However, the problem of how to include the system health information in the controller design in a systematic way is still an open research topic to explore and dedicate more research.

- The right health indicator to be used for reconfiguring/accommodating the controller is also a key issue. Some methodologies for the designer should be given in order to facilitate the design of the HAC reconfiguration/accommodation strategy.

- Other functions to model the failure rate could be used, e.g. the failure rate can be a function of the control effort variations. In that case, appropriate weights in the cost function can be used to improve the reliability by making those variations softer. Evidently, the modeling of the failure rate depends on the nature of the component to be modeled and the environment where it is used.

Bibliography

[1] M. Abdel-Geliel, E. Badreddin, and A. Gambier. "Application of model predictive control for fault tolerant system using dynamic safety margin". In: *Proceedings of the American Control Conference*. Minneapolis, USA, 2006, pages 5493–5498 (cit. on p. 28).

[2] M. Abdolhosseini, Y. M. Zhang, and C. A. Rabbath. "An efficient Model Predictive Control scheme for an unmanned quadrotor helicopter". In: *Journal of Intelligent & Robotic Systems* 70.1-4 (2013), pages 27–38 (cit. on p. 9).

[3] V. G. Adîr and A. M. Stoica. "Integral LQR control of a star-shaped octorotor". In: *INCAS BULLETIN* 4.2 (2012), pages 3–18 (cit. on p. 9).

[4] F. Ahmadzadeh and J. Lundberg. "Remaining useful life estimation: review". In: *International Journal of System Assurance Engineering and Management* 5.4 (2014), pages 461–474 (cit. on pp. 5, 19, 23).

[5] A. Amirat, A. Mohamed, and K. Chaoui. "Reliability assessment of underground pipelines under the combined effect of active corrosion and residual stress". In: *International Journal of Pressure Vessels and Piping* 83.2 (Feb. 2006), pages 107–117 (cit. on p. 78).

[6] Y. Bagul, I. Zeid, and S. Kamarthi. "Overview of remaining useful life methodologies". In: *Proceedings of the ASME 2008 International Design Engineering Technical Conferences & Computers and Information in Engineering Conference (IDETC/CIE 2008)*. Brooklyn, New York, USA, 2008, pages 1391–1400 (cit. on p. 22).

[7] D. M. Bates and D. G. Watts. *Nonlinear regression analysis and its applications*. New York: Wiley, 1988 (cit. on p. 45).

[8] A. Ben, A. Muller, and P. Weber. "Dynamic Bayesian Networks in system reliability analysis". In: *Proceedings of the 6th Fault Detection, Supervision and Safety of Technical Processes (SAFEPROCESS 2006)*. Beijing, China, 2006, pages 444–449 (cit. on pp. 54, 55).

[9] F. Bicking, P. Weber, D. Theilliol, and C. Aubrun. "Control Allocation Using Reliability Measures for Over-Actuated System". In: *Intelligent Systems in Technical and Medical Diagnostics*. Ed. by J. Korbicz and M. Kowal. Advances in Intelligent

Systems and Computing. Springer Berlin Heidelberg, 2014, pages 487–497 (cit. on pp. 3, 27, 28, 35).

[10] F. Bicking, P. Weber, and D. Theilliol. "Reliability importance measures for fault tolerant control allocation". In: *Proceedings of the 2nd International Conference on Control and Fault-Tolerant Systems (SysTol 2013)*. Nice, France, 2013, pages 104–109 (cit. on pp. 2, 3, 27).

[11] J. Birdwell, D. Castanon, and M. Athans. "On Reliable Control System Designs". In: *IEEE Transactions on Systems, Man and Cybernetics* 16.5 (1986), pages 703–711 (cit. on p. 24).

[12] Z. W. Birnbaum. "On the importance of different components in a multicomponent system". In: *Multivariate analysis*. Ed. by P. R. Krishnaiah. Vol. II. New York, NY, USA: Academic Press, 1969, pages 581–592 (cit. on pp. 62, 63).

[13] M. Blanke, M. Kinnaert, J. Lunze, and M. Staroswiecki. *Diagnosis and fault-tolerant control*. 2nd. Springer Berlin Heidelberg, 2006 (cit. on pp. 4, 15).

[14] W. R. Blischke. *Reliability: modeling, prediction, and optimization*. Wiley series in probability and statistics. Applied probability and statistics section. New York: Wiley, 2000 (cit. on pp. 30, 40, 43).

[15] A. Bobbio, L. Portinale, M. Minichino, and E. Ciancamerla. "Improving the analysis of dependable systems by mapping fault trees into Bayesian networks". In: *Reliability Engineering & System Safety* 71.3 (2001), pages 249–260 (cit. on p. 3).

[16] S. Borris. *Total Productive Maintenance*. McGraw-Hill Professional, 2005 (cit. on p. 1).

[17] C. Byington, M. Watson, D. Edwards, and P. Stoelting. "A model-based approach to prognostics and health management for flight control actuators". In: *2004 IEEE Aerospace Conference, 2004. Proceedings*. Vol. 6. Mar. 2004, pages 3551–3562 Vol.6 (cit. on p. 20).

[18] E. F. Camacho and C. Bordons. *Model predictive control*. 2nd. Advanced Textbooks in Control and Signal Processing. London ; New York: Springer, 2004 (cit. on pp. 68–70, 72).

[19] E. Çinlar. "On a generalization of Gamma processes". In: *Journal of Applied Probability* 17.2 (June 1980), pages 467–480 (cit. on p. 35).

[20] A. Chamseddine, D. Theilliol, I. Sadeghzadeh, Y. Zhang, and P. Weber. "Optimal reliability design for over-actuated systems based on the MIT rule: Application

to an octocopter helicopter testbed". In: *Reliability Engineering & System Safety* 132 (2014), pages 196–206 (cit. on pp. 26, 28, 122).

[21] C. Chen, G. Vachtsevanos, and M. E. Orchard. "Machine Remaining Useful Life Prediction Based on Adaptive Neuro-Fuzzy and High-Order Particle Filtering". In: *Proceedings of the Annual Conference of the Prognostics and Health Management Society*. Portland, 2010 (cit. on p. 23).

[22] J. Chen and R. H. Middleton. "New developments and applications in performance limitation of feedback control". In: *IEEE Trans. on Automatic Control* 48.8 (2003), pages 1297–1398 (cit. on p. 2).

[23] J. Chen and R. J. Patton. *Robust Model-Based Fault Diagnosis for Dynamic Systems*. Ed. by K. Cai. Vol. 3. The International Series on Asian Studies in Computer and Information Science. Boston, MA: Springer US, 1999 (cit. on p. 4).

[24] Z. Chen and S. Zheng. "Lifetime distribution based degradation analysis". In: *IEEE Transactions on Reliability* 54.1 (2005), pages 3–10 (cit. on p. 35).

[25] S. Cheng and M. Pecht. "A fusion prognostics method for remaining useful life prediction of electronic products". In: *2009 IEEE International Conference on Automation Science and Engineering*. 2009, pages 102–107 (cit. on p. 22).

[26] Y. J. Cho, Z. Bien, and B. K. Kim. "Reliable Control via Additive Redundant Adaptive Controller". In: *Proceedings of the American Control Conference*. 1989, pages 1899–1904 (cit. on p. 24).

[27] H. V. Christensen. "Modelling and Control of a Twin-Rotor MIMO System". In: *Report of Department of Control Engineering Institute of Electronic Systems of Aalborg University* (2006) (cit. on p. 110).

[28] M. Cocetti, A. Serrani, and L. Zaccarian. "Dynamic input allocation for uncertain linear over-actuated systems". In: *2016 American Control Conference (ACC)*. 2016, pages 2906–2911 (cit. on p. 9).

[29] J. T. Connor, R. D. Martin, and L. E. Atlas. "Recurrent neural networks and robust time series prediction". In: *IEEE Transactions on Neural Networks* 5.2 (Mar. 1994), pages 240–254 (cit. on p. 21).

[30] D. R. Cox. "Regression Models and Life-Tables". In: *Journal of the Royal Statistical Society. Series B (Methodological)* 34.2 (1972), pages 187–220 (cit. on pp. 38, 39, 46, 79).

[31] V. Dardinier-Maron, F. Hamelin, and H. Noura. "A fault-tolerant control design against major actuator failures: application to a three-tank system". In: *Proceedings*

of the 38th IEEE Conference on Decision and Control. Vol. 4. Phoenix, USA, 1999, pages 3569–3574 (cit. on pp. 26, 28).

[32] D. J. Davis. "An analysis of some failure data". In: *Journal of the American Statistical Association* 47.258 (June 1952), pages 113–150 (cit. on p. 33).

[33] E. Deloux, B. Castanier, and C. Bérenguer. "Predictive maintenance policy for a gradually deteriorating system subject to stress". In: *Reliability Engineering & System Safety* 94.2 (2009), pages 418–431 (cit. on p. 35).

[34] B. Dhillon. *Design Reliability: Fundamentals and Applications*. New York: CRC Press, 1999 (cit. on p. 36).

[35] O. Doguc and J. E. Ramirez-Marquez. "A generic method for estimating system reliability using Bayesian networks". In: *Reliability Engineering & System Safety* 94.2 (2009), pages 542–550 (cit. on p. 51).

[36] H. M. Elattar, H. K. Elminir, and A. M. Riad. "Prognostics: a literature review". In: *Complex & Intelligent Systems* 2.2 (2016), pages 125–154 (cit. on pp. 5, 17, 19, 20).

[37] J. Endrenyi and G. J. Anders. "Aging, maintenance, and reliability - approaches to preserving equipment health and extending equipment life". In: *IEEE Power and Energy Magazine* 4.3 (May 2006), pages 59–67 (cit. on p. 1).

[38] T. Escobet, V. Puig, and F. Nejjari. "Health Aware control and model-based Prognosis". In: *Proceedings of the 20th Mediterranean Conference on Control Automation (MED'12)*. 2012, pages 691–696 (cit. on pp. 26, 28).

[39] T. Escobet, V. Puig, J. Quevedo, and D. Garcia. "A methodology for incipient fault detection". In: *2014 IEEE Conference on Control Applications (CCA)*. Oct. 2014, pages 104–109 (cit. on p. 4).

[40] T. Escobet, J. Quevedo, V. Puig, and F. Nejjari. "Combining Health Monitoring and Control". In: *Diagnostics and Prognostics of Engineering Systems*. Ed. by S. Kadry. IGI Global, 2012, pages 230–255 (cit. on pp. 5, 6, 18).

[41] Y. Eun, C. Gokcek, P. T. Kabamba, and S. M. Meerkov. "Selecting the level of actuator saturation for small performance degradation of linear designs". In: *Proceedings of the 40th IEEE Conf. on Decision and Control*. 2001, pages 1769–1774 (cit. on p. 2).

[42] I. Fantoni and R. Lozano. *Non-Linear Control for Underactuated Mechanical Systems*. Secaucus, NJ, USA: Springer-Verlag New York, Inc., 2001 (cit. on p. 9).

[43] M. Finkelstein. “A note on some aging properties of the accelerated life model”. In: *Reliability Engineering & System Safety* 71.1 (2001), pages 109–112 (cit. on pp. 3, 35).

[44] P. Frank. “Fault diagnosis in dynamic systems using analytical and knowledge-based redundancy: A survey and some new results”. In: *Automatica* 26.3 (1990), pages 459–474 (cit. on p. 4).

[45] J. Fussell. “How to Hand-Calculate System Reliability and Safety Characteristics”. In: *IEEE Transactions on Reliability* R-24.3 (1975), pages 169–174 (cit. on p. 64).

[46] C. Gabriel. “Modelling, Simulation and Control of a Twin Rotor MIMO-System”. In: *Project Thesis at Department of Systems Engineering and Control of Universidad Politécnica de Valencia.* (2008) (cit. on p. 110).

[47] I. B. Gertsbakh. *Reliability theory: with applications to preventive maintenance*. 2nd. Berlin, New York: Springer, 2001 (cit. on pp. 33, 34, 135).

[48] A. Ginart, I. Barlas, J. L. Dorrity, P. Kalgren, and M. J. Roemer. “Self-Healing from a PHM Perspective”. In: *Proceedings of the IEEE Autotestcon*. Anaheim, CA, USA, 2006 (cit. on pp. 18, 28).

[49] F. Goba. “Bibliography on Thermal Aging of Electrical Insulation”. In: *IEEE Transactions on Electrical Insulation* EI-4.2 (1969), pages 31–58 (cit. on p. 44).

[50] K. Goebel, N. Eklund, and P. Bonanni. “Fusing competing prediction algorithms for prognostics”. In: *2006 IEEE Aerospace Conference*. 2006, pages 10 pp.– (cit. on p. 22).

[51] L. Gokdere, S. Chiu, K. Keller, and J. Vian. “Lifetime control of electromechanical actuators”. In: *Proceedings of the IEEE Aerospace Conference*. Big Sky, MT, USA, 2005, pages 3523–3531 (cit. on pp. 26, 28).

[52] N. Gorjian, L. Ma, M. Mittinty, P. Yarlagadda, and Y. Sun. “A review on degradation models in reliability analysis”. In: *Proceedings of the 4th World Congress on Engineering Asset Management, (WCEAM 2009)*. Engineering Asset Lifecycle Management. Athens, Greece, 2009, pages 369–384 (cit. on pp. 1, 31, 40).

[53] N. Gorjian, L. Ma, M. Mittinty, P. Yarlagadda, and Y. Sun. “A review on reliability models with covariates”. In: *Engineering Asset Lifecycle Management*. Ed. by D. Kiritsis, C. Emmanouilidis, A. Koronios, and J. Mathew. Springer London, 2010, pages 385–397 (cit. on pp. 37, 40, 45).

[54] J. M. Grosso, C. Ocampo, and V. Puig. “A service reliability model predictive control with dynamic safety stocks and actuators health monitoring for drinking water networks”. In: *Proceedings of the 51st IEEE Conference on Decision and Control (CDC)*. Maui, Hawaii, USA, 2012, pages 4568–4573 (cit. on pp. 26, 28, 35).

[55] J. M. Grosso. “A robust adaptive model predictive control to enhance the management of drinking water networks subject to demand uncertainty and actuators degradation”. Master thesis. Barcelona, Spain: Universitat Politècnica de Catalunya, Sept. 2012 (cit. on p. 79).

[56] F. Guenab, D. Theilliol, P. Weber, Y. M. Zhang, and D. Sauter. “Fault tolerant control system design: A reconfiguration strategy based on reliability analysis under dynamic behaviour constraints”. In: *6th IFAC Symposium Fault Detection, Supervision and Safety of Technical Processes, SAFEPROCESS 2006*. Beijing, P.R. China, 2006, pages 1312–1317 (cit. on pp. 2, 26).

[57] F. Guenab. “Contribution aux systèmes tolérants aux défauts : Synthèse d’une méthode de reconfiguration et/ou de restructuration intégrant la fiabilité des composants”. PhD thesis. Université Henri Poincaré - Nancy I, Feb. 2007 (cit. on p. 79).

[58] F. Guenab, P. Weber, D. Theilliol, and Y. Zhang. “Design of a fault tolerant control system incorporating reliability analysis and dynamic behaviour constraints”. In: *International Journal of Systems Science* 42.1 (2011), pages 219–233 (cit. on pp. 26–28, 35).

[59] W. Huang and R. Askin. “A generalized SSI reliability model considering stochastic loading and strength aging degradation”. In: *IEEE Transactions on Reliability* 53.1 (2004), pages 77–82 (cit. on p. 41).

[60] R. Isermann. *Fault-diagnosis systems: an introduction from fault detection to fault tolerance*. Berlin, New York: Springer, 2006 (cit. on pp. 2, 4, 47).

[61] R. Isermann. “Process fault detection based on modeling and estimation methods –A survey”. In: *Automatica* 20.4 (July 1984), pages 387–404 (cit. on p. 4).

[62] R. Isermann. “Supervision, fault-detection and fault-diagnosis methods – An introduction”. In: *Control Engineering Practice* 5.5 (May 1997), pages 639–652 (cit. on p. 4).

[63] A. K. S. Jardine, P. M. Anderson, and D. S. Mann. “Application of the Weibull proportional hazards model to aircraft and marine engine failure data”. In: *Quality and Reliability Engineering International* 3.2 (1987), pages 77–82 (cit. on p. 39).

[64] A. K. S. Jardine, D. Lin, and D. Banjevic. "A review on machinery diagnostics and prognostics implementing condition-based maintenance". In: *Mechanical Systems and Signal Processing* 20.7 (2006), pages 1483–1510 (cit. on pp. 18–21).

[65] F. V. Jensen. *An Introduction to Bayesian Networks*. London, UK: Editions UCL Press, 1996 (cit. on pp. 51, 53).

[66] F. V. Jensen and T. D. Nielsen. *Bayesian Networks and Decision Graphs*. Ed. by M. Jordan, J. Kleinberg, and B. Schölkopf. Information Science and Statistics. Springer New York, 2001 (cit. on p. 52).

[67] R. Jiang and A. K. S. Jardine. "Health state evaluation of an item: A general framework and graphical representation". In: *Reliability Engineering & System Safety* 93.1 (2008), pages 89–99 (cit. on pp. 3, 35, 41).

[68] S. Jiang, T. L. Landers, and T. Reed Rhoads. "Proportional Intensity Models Robustness with Overhaul Intervals". In: *Quality and Reliability Engineering International* 22.3 (2006), pages 251–263 (cit. on p. 39).

[69] R. Kaufman and J. Meador. "Dielectric Tests for EHV Transformers". In: *IEEE Transactions on Power Apparatus and Systems* PAS-87.1 (1968), pages 135–145 (cit. on p. 45).

[70] A. Z. Keller, A. R. R. Kamath, and U. D. Perera. "Reliability analysis of CNC machine tools". In: *Reliability Engineering* 3.6 (Nov. 1982), pages 449–473 (cit. on p. 22).

[71] J. P. Kharoufeh, C. J. Solo, and M. Y. Ulukus. "Semi-Markov models for degradation-based reliability". In: *IIE Transactions* 42.8 (2010), pages 599–612 (cit. on p. 43).

[72] A. Khelassi, J. Jiang, D. Theilliol, P. Weber, and Y. M. Zhang. "Reconfiguration of Control Inputs for Overactuated Systems Based on Actuators Health". In: *Proceedings of the 18th IFAC World Congress*. Milano, Italy, 2011, pages 13729–13734 (cit. on pp. 9, 24, 26–28, 35).

[73] A. Khelassi, D. Theilliol, P. Weber, and D. Sauter. "A novel active fault tolerant control design with respect to actuators reliability". In: *Proceedings of the 50th IEEE Conference on Decision and Control and European Control Conference (CDC-ECC)*. Orlando, USA, 2011, pages 2269–2274 (cit. on pp. 1, 26–28, 35).

[74] A. Khelassi, D. Theilliol, P. Weber, and J. Ponsart. "Fault-tolerant control design with respect to actuator health degradation: An LMI approach". In: *Proceedings of the IEEE International Conference on Control Applications (CCA)*. Denver, USA, 2011, pages 983–988 (cit. on pp. 2, 24, 26–28, 35, 79, 80, 134).

[75] A. Khelassi, D. Theilliol, and P. Weber. "Reconfigurability analysis for reliable fault-tolerant control design". In: *International Journal of Applied Mathematics and Computer Science* 21.3 (2011), pages 431–439 (cit. on pp. 2, 26–28, 35, 79, 80).

[76] J. Kiddy. "Remaining useful life prediction based on known usage data". In: *Proceedings SPIE 5046, Nondestructive Evaluation and Health Monitoring of Aerospace Materials and Composites II*. Vol. 5046. 2003, pages 11–18 (cit. on p. 22).

[77] D. Kumar and B. Klefsjö. "Proportional hazards model: a review". In: *Reliability Engineering and System Safety* 44 (1994), pages 177–188 (cit. on p. 38).

[78] W. Kuo. *Optimal reliability modeling: principles and applications*. Hoboken, N.J: John Wiley & Sons, 2003 (cit. on pp. 36, 50, 56).

[79] W. Kuo and X. Zhu. *Importance measures in reliability, risk, and optimization: principles and applications*. Hoboken, N.J: John Wiley & Sons, Ltd, 2012 (cit. on p. 123).

[80] H. J. Kwon and C.-E. Lee. "Reliability analysis of pipe network regarding transient flow". en. In: *KSCE Journal of Civil Engineering* 12.6 (Nov. 2008), pages 409–416 (cit. on p. 78).

[81] H. E. Lambert. "Fault tree for decision making in system analysis". PhD thesis. Lawrence Livermore Laboratory - University of California, 1975 (cit. on p. 63).

[82] Y. Langeron, A. Grall, and A. Barros. "Actuator Health Prognosis for Designing LQR Control in Feedback Systems". In: *Chemical Engineering Transactions* 33 (2013), pages 979–984 (cit. on pp. 26, 35).

[83] H. Lao and S. Zein-Sabatto. "Analysis of vibration signal's time-frequency patterns for prediction of bearing's remaining useful life". In: *Proceedings of the 33rd Southeastern Symposium on System Theory (Cat. No.01EX460)*. Mar. 2001, pages 25–29 (cit. on p. 22).

[84] J. Lawless and M. Crowder. "Covariates and Random Effects in a Gamma Process Model with Application to Degradation and Failure". In: *Lifetime Data Analysis* 10.3 (2004), pages 213–227 (cit. on pp. 3, 35).

[85] J. Lee, T. Kim, D. Kang, and D. Hyun. "A Control Method for Improvement of Reliability in Fault Tolerant NPC Inverter System". In: *Proceedings of the 37th IEEE Power Electronics Specialists Conference (PESC'06)*. Jeju, Korea, 2006, pages 1–5 (cit. on p. 28).

[86] G. Levitin, L. Podofillini, and E. Zio. "Generalised importance measures for multi-state elements based on performance level restrictions". In: *Reliability Engineering & System Safety* 82.3 (2003), pages 287–298 (cit. on p. 65).

[87] C. J. Li and H. Lee. “Gear fatigue crack prognosis using embedded model, gear dynamic model and fracture mechanics”. In: *Mechanical Systems and Signal Processing* 19.4 (July 2005), pages 836–846 (cit. on p. 20).

[88] H. LI, Q. Zhao, and Z. Yang. “Reliability Modeling of Fault Tolerant Control Systems”. English. In: *International Journal of Applied Mathematics and Computer Science* 17.4 (2007) (cit. on p. 28).

[89] N. Li, W. Xie, and R. Haas. “Reliability-based processing of Markov chains for modeling pavement network deterioration”. In: *Transportation research record: Journal of the Transportation Research Board* 1524.1 (1996), pages 203–213 (cit. on p. 43).

[90] Y. Li, S. Billington, C. Zhang, T. Kurfess, S. Danyluk, and S. Liang. “Adaptive prognostics for rolling element bearing condition”. In: *Mechanical Systems and Signal Processing* 13.1 (Jan. 1999), pages 103–113 (cit. on p. 20).

[91] F. Liao, J. L. Wang, and G. Yang. “Reliable robust flight tracking control: an LMI approach”. In: *IEEE Transactions on Control Systems Technology* 10.1 (2002), pages 76–89 (cit. on p. 27).

[92] H. Liao, W. Zhao, and H. Guo. “Predicting remaining useful life of an individual unit using proportional hazards model and logistic regression model”. In: *Proceedings of the Annual Reliability and Maintainability Symposium, (RAMS'06)*. Newport Beach, CA, USA, 2006, pages 127–132 (cit. on p. 40).

[93] D. Lin and Z. Ying. “Semiparametric Analysis of General Additive-Multiplicative Hazard Models for Counting Processes”. In: *The Annals of Statistics* 23.5 (1995), pages 1712–1734 (cit. on p. 38).

[94] C. Liu, W. Chen, and J. Andrews. “Tracking control of small-scale helicopters using explicit nonlinear MPC augmented with disturbance observers”. In: *Control Engineering Practice* 20.3 (2012), pages 258–268 (cit. on p. 9).

[95] C. J. Lu and W. Q. Meeker. “Using Degradation Measures to Estimate a Time-to-Failure Distribution”. In: *Technometrics* 35.2 (1993), pages 161–174 (cit. on pp. 3, 35, 41).

[96] S. Lu, H. Lu, and W. J. Kolarik. “Multivariate performance reliability prediction in real-time”. In: *Reliability Engineering & System Safety* 72.1 (2001), pages 39–45 (cit. on p. 43).

[97] D. Lugtigheid, A. K. S. Jardine, and X. Jiang. “Optimizing the performance of a repairable system under a maintenance and repair contract”. In: *Quality and Reliability Engineering International* 23.8 (2007), pages 943–960 (cit. on p. 39).

[98] L. Ma. “Condition monitoring in engineering asset management”. In: *Proceedings of the Asia Pacific Vibration Conference*. Sapporo, Japan, 2007 (cit. on p. 43).

[99] R. Mahony, V. Kumar, and P. Corke. “Multirotor Aerial Vehicles: Modeling, Estimation, and Control of Quadrotor”. In: *IEEE Robotics Automation Magazine* 19.3 (2012) (cit. on p. 96).

[100] A. Marks, J. Whidborne, and I. Yamamoto. “Control allocation for fault tolerant control of a VTOL octorotor”. In: *UKACC International Conference on Control (CONTROL)*. 2012, pages 357–362 (cit. on p. 9).

[101] K. Medjaher, D. A. Tobon-Mejia, and N. Zerhouni. “Remaining useful life estimation of critical components with application to bearings”. In: *IEEE Transactions on Reliability* 61.2 (2012), pages 292–302 (cit. on p. 23).

[102] K. Medjaher and N. Zerhouni. “Residual-based failure prognostic in dynamic systems”. In: *Proceedings of the 7th IFAC Symposium on Fault Detection, Supervision and Safety of Technical Processes*. Vol. 42. 2009, pages 716–721 (cit. on p. 20).

[103] W. Q. Meeker, L. A. Escobar, and C. J. Lu. “Accelerated degradation tests: Modeling and analysis”. In: *Technometrics* 40.2 (1998), pages 89–99 (cit. on pp. 35, 43, 44).

[104] K. P. Murphy. “The Bayes Net toolbox for MATLAB”. In: *Computing Science and Statistics* 33 (2001), pages 2001 (cit. on p. 52).

[105] D. N. P. Murthy and N. Jack. “System Degradation and Maintenance”. In: *Extended Warranties, Maintenance Service and Lease Contracts*. Springer Series in Reliability Engineering. Springer, London, 2014, pages 23–46 (cit. on pp. 1, 31).

[106] J. A. Nachlas. *Reliability engineering: probabilistic models and maintenance methods*. Boca Raton: Taylor & Francis, 2005 (cit. on p. 41).

[107] F. Nejjari, D. Rotondo, V. Puig, and M. Innocenti. “LPV modelling and control of a Twin Rotor MIMO System”. In: *19th Mediterranean Conference on Control Automation (MED)*. June 2011, pages 1082–1087 (cit. on p. 111).

[108] W. B. Nelson. *Accelerated Testing: Statistical Models, Test Plans, and Data Analysis*. Wiley series in probability and statistics. New Jersey: John Wiley & Sons, 1990 (cit. on p. 44).

[109] D. N. Nguyen, L. Dieulle, and A. Grall. “Feedback Control System with Stochastically Deteriorating Actuator: Remaining Useful Life Assessment”. In: *Proceedings of the 19th World Congress the International Federation of Automatic Control*. Cape Town, South Africa, 2014, pages 3244–3249 (cit. on pp. 26, 28).

[110] D. N. Nguyen, L. Dieulle, and A. Grall. “Remaining Useful Life Estimation of Stochastically Deteriorating Feedback Control Systems with a Random Environment and Impact of Prognostic Result on the Maintenance Process”. In: *Proceedings of the European Conference of the PHM Society*. Nantes, France: PHM Society, 2014 (cit. on pp. 26, 28).

[111] D. N. Nguyen, L. Dieulle, and A. Grall. “Remaining Useful Lifetime Prognosis of Controlled Systems: A Case of Stochastically Deteriorating Actuator”. In: *Mathematical Problems in Engineering* 2015 (2015), pages 1–16 (cit. on pp. 26, 28).

[112] J. M. van Noortwijk. “A survey of the application of gamma processes in maintenance”. In: *Reliability Engineering & System Safety* 94.1 (2009), pages 2–21 (cit. on pp. 3, 35, 43).

[113] S. Montes de Oca and V. Puig. “Reliable Fault-Tolerant Control Design for LPV Systems using Admissible Model Matching”. In: *Proceedings of the 18th IFAC World Congress*. Vol. 44. Milano, Italy, 2011, pages 13735–13740 (cit. on pp. 26–28).

[114] K. Ogata. *Discrete-time Control Systems*. 2nd ed. Prentice-Hall Inc., 1987 (cit. on p. 75).

[115] C. de Oliveira and T. Yoneyama. “Prognostics and Health Monitoring for an electro-hydraulic flight control actuator”. In: *Proceedings of the IEEE Aerospace conference*. Big Sky, MT, USA, 2009, pages 1–9 (cit. on p. 35).

[116] C. H. Oppenheimer and K. A. Loparo. “Physically based diagnosis and prognosis of cracked rotor shafts”. In: *Proceedings of SPIE 4733, Component and Systems Diagnostics, Prognostics, and Health Management II*. Vol. 4733. 2002, pages 122–132 (cit. on p. 20).

[117] S. Osaki and T. Nakagawa. “Bibliography for reliability and availability of stochastic systems”. In: *IEEE Transactions on Reliability* R-25.4 (1976), pages 284–287 (cit. on p. 3).

[118] C. I. Ossai, B. Boswell, and I. J. Davies. “A Markovian approach for modelling the effects of maintenance on downtime and failure risk of wind turbine components”. In: *Renewable Energy* 96, Part A (2016), pages 775–783 (cit. on p. 3).

[119] A. Ostfeld. “Reliability analysis of regional water distribution systems”. In: *Urban Water* 3.4 (Dec. 2001), pages 253–260 (cit. on p. 60).

[120] J. Pearl. *Probabilistic Reasoning in Intelligent Systems: Networks of Plausible Inference*. English. San Francisco, USA: Morgan Kaufmann Publishers Inc., 1988 (cit. on p. 53).

[121] M. Pecht. "Prognostics and health management of electronics". In: *Encyclopedia of Structural Health Monitoring*. Ed. by C. Boller. John Wiley & Sons, Ltd, 2009 (cit. on p. 17).

[122] M. Pecht and S. Kumar. "Data analysis approach for system reliability, diagnostics and prognostics". In: *Proceedings of the Pan pacific Microelectronics Symposium*. Kauai, USA, 2008, pages 22–24 (cit. on pp. 4, 5, 18).

[123] D. S. Peck and C. Zierdt. "The reliability of semiconductor devices in the bell system". In: *Proceedings of the IEEE* 62.2 (1974), pages 185–211 (cit. on p. 44).

[124] E. B. Pereira, R. K. H. Galvao, and T. Yoneyama. "Model Predictive Control using Prognosis and Health Monitoring of actuators". In: *Proceedings of the 2010 IEEE International Symposium on Industrial Electronics (ISIE)*. Bari, Italy, 2010, pages 237–243 (cit. on pp. 1, 2, 26–28, 106–109).

[125] E. B. Pereira, R. K. H. Galvao, and T. Yoneyama. "Model predictive control with constraints on accumulated degradation of actuators". In: *Proceedings of the ABCM Symposium Series in Mechatronics*. Vol. 4. Rio de Janeiro, Brazil, 2010, pages 394–402 (cit. on pp. 26, 28, 107).

[126] T. Perez, G. C. Goodwin, and M. M. Seron. "Performance degradation in feedback control due to constraints". In: *IEEE Trans. on Automatic Control* 48.8 (2003), pages 1381–1385 (cit. on p. 2).

[127] H. Pham. "System Reliability Concepts". In: *System Software Reliability*. London: Springer, 2006, pages 9–75 (cit. on p. 33).

[128] M. Pijnenburg. "Additive hazards models in repairable systems reliability". In: *Reliability Engineering & System Safety* 31.3 (1991), pages 369–390 (cit. on p. 43).

[129] G. V. Raffo, M. G. Ortega, and F. R. Rubio. "An integral predictive/nonlinear control structure for a quadrotor helicopter". In: *Automatica* 46.1 (2010), pages 29–39 (cit. on p. 9).

[130] A. Rahideh and M. H. Shaheed. "Mathematical Dynamic Modelling of a Twin-Rotor Multiple Input-Multiple Output System". In: *IMechE Journal of Systems and Control Engineering* 221.1 (2007), pages 89–101 (cit. on p. 110).

[131] F. Rinaldi, A. Gargioli, and F. Quagliotti. "PID and LQ regulation of a multirotor attitude: mathematical modelling, simulations and experimental results". In: *Journal of Intelligent & Robotic Systems* 73.1-4 (2014), pages 33–50 (cit. on p. 9).

[132] J. V. Ringwood and S. Simani. "Overview of modelling and control strategies for wind turbines and wave energy devices: Comparisons and contrasts". In: *Annual Reviews in Control* 40 (2015), pages 27–49 (cit. on p. 28).

[133] D. Robles, V. Puig, C. Ocampo-Martinez, and L. E. Garza-Castañón. "Reliable fault-tolerant model predictive control of drinking water transport networks". In: *Control Engineering Practice* 55 (2016), pages 197–211 (cit. on pp. 26, 28).

[134] M. J. Roemer, C. Hong, and S. H. Hesler. "Machine Health Monitoring and Life Management Using Finite-Element-Based Neural Networks". In: *Journal of Engineering for Gas Turbines and Power* 118.4 (1996), pages 830–835 (cit. on p. 21).

[135] D. Rotondo, F. Nejjari, and V. Puig. "Quasi-LPV modeling, identification and control of a twin rotor MIMO system". In: *Control Engineering Practice* 21.6 (2013), pages 829–846 (cit. on p. 110).

[136] J. C. Salazar, F. Nejjari, R. Sarrate, P. Weber, and D. Theilliol. "Reliability importance measures for a health-aware control of drinking water networks". In: *Proceedings of the 3rd Conference on Control and Fault-Tolerant Systems (SysTol'16)*. Barcelona, Spain, 2016, pages 572–578 (cit. on pp. 9, 11, 26, 28).

[137] J. C. Salazar, F. Nejjari, and R. Sarrate. "Reliable control of a twin rotor MIMO system using actuator health monitoring". In: *Proceedings of the 22nd Mediterranean Conference of Control and Automation (MED'14)*. Palermo, Italy, 2014, pages 481–486 (cit. on pp. 12, 26, 28).

[138] J. C. Salazar, A. Sanjuan, F. Nejjari, and R. Sarrate. "Health-Aware and Fault-Tolerant control of an octorotor UAV system based on actuator reliability". In: *To be submitted to International Journal of Applied Mathematics and Computer Science* (2018) (cit. on p. 11).

[139] J. C. Salazar, A. Sanjuan, F. Nejjari, and R. Sarrate. "Health-Aware Control of an octorotor UAV system based on actuator reliability". In: *Proceedings of the 4th International Conference on Control, Decision and Information Technologies (CoDIT'17)*. Barcelona, Spain, 2017 (cit. on pp. 2, 11, 80).

[140] J. C. Salazar, R. Sarrate, and F. Nejjari. "Health-Aware Control: A selective review and survey of current development". In: *To be submitted to Annual Reviews in Control* (2018) (cit. on p. 11).

[141] J. C. Salazar, R. Sarrate, F. Nejjari, P. Weber, and D. Theilliol. "Reliability computation within an MPC health-aware framework". In: *Proceedings of the 20th World Congress of the International Federation of Automatic Control (IFAC 2017)*. Toulouse, France, 2017, pages 12230–12235 (cit. on pp. 2, 11, 80, 121).

[142] J. C. Salazar, R. Sarrate, and F. Nejjari. “Upper bound system reliability assessment for health-aware control of complex systems”. In: *Proceedings of the 4th European Conference of the Prognostics and Health Management Society (PHME 2018)*. Utrecht, The Netherlands, 2018 (cit. on p. 11).

[143] J. C. Salazar, P. Weber, R. Sarrate, D. Theilliol, and F. Nejjari. “MPC design based on a DBN reliability model: Application to drinking water networks”. In: *Proceedings of the 9th IFAC Symposium on Fault Detection, Supervision and Safety for Technical Processes (SAFEPROCESS 2015)*. Vol. 48. 21. Paris, France: IFAC, 2015, pages 688–693 (cit. on pp. 2, 9, 11, 26, 28, 80).

[144] J. C. Salazar, P. Weber, F. Nejjari, D. Theilliol, and R. Sarrate. “MPC Framework for System Reliability Optimization”. In: *Advanced and Intelligent Computations in Diagnosis and Control*. Ed. by Z. Kowalczuk. Advances in Intelligent Systems and Computing 386. Springer International Publishing, 2015, pages 161–177 (cit. on pp. 2, 9, 11, 26, 28, 80, 84).

[145] J. C. Salazar, P. Weber, F. Nejjari, D. Theilliol, and R. Sarrate. “MPC Framework for System Reliability Optimization”. In: *Proceedings of the 12th Diagnosis of Processes and Systems (DPS 2015)*. Ustka, Poland, 2015, pages 386 (cit. on pp. 2, 12).

[146] J. C. Salazar, P. Weber, F. Nejjari, R. Sarrate, and D. Theilliol. “System reliability aware Model Predictive Control framework”. In: *Reliability Engineering & System Safety* 167 (2017). Special Section: Applications of Probabilistic Graphical Models in Dependability, Diagnosis and Prognosis, pages 663 –672 (cit. on pp. 2, 10, 80).

[147] A. Saxena, M. E. Orchard, B. Zhang, G. Vachtsevanos, L. Tang, Y. Lee, and Y. Wardi. “Automated Contingency Management for Propulsion Systems”. In: *Proceedings of the European Control Conference 2007 (ECC)*. July 2007, pages 3515–3522 (cit. on p. 14).

[148] S. Schuller, P. Schilinsky, J. Hauch, and C. Brabec. “Determination of the degradation constant of bulk heterojunction solar cells by accelerated lifetime measurements”. In: *Applied Physics A* 79.1 (2004), pages 37–40 (cit. on p. 45).

[149] J. W. Sheppard and M. A. Kaufman. “Bayesian diagnosis and prognosis using instrument uncertainty”. In: *IEEE Autotestcon, 2005.* Sept. 2005, pages 417–423 (cit. on p. 21).

[150] J.-J. H. Shiau and H.-H. Lin. “Analyzing accelerated degradation data by nonparametric regression”. In: *IEEE Transactions on Reliability* 48.2 (1999), pages 149–158 (cit. on p. 43).

[151] H. Shyur, E. A. Elsayed, and J. T. Luxhøj. "A general model for accelerated life testing with time-dependent covariates". In: *Naval Research Logistics (NRL)* 46.3 (1999), pages 303–321 (cit. on p. 38).

[152] D. D. Siljak. "On reliability of control". In: *Proceedings of the IEEE Conference on Decision and Control including the 17th Symposium on Adaptive Processes*. San Diego, USA, 1979, pages 687–694 (cit. on p. 23).

[153] N. Singpurwalla. "Gamma processes and their generalizations: An overview". In: *Engineering probabilistic design and maintenance for flood protection*. Ed. by R. Cooke, M. Mendel, and H. Vrijling. Boston, MA: Springer US, 1997, pages 67–75 (cit. on p. 43).

[154] A. Soldevila, J. Cayero, J. C. Salazar, D. Rotondo, and V. Puig. "Control of a quadruple tank process using a mixed economic and standard MPC". In: *Actas de las XXXV Jornadas de Automática*. Valencia, Spain, 2014 (cit. on p. 12).

[155] R. Stetter and M. Witczak. "Degradation Modelling for Health Monitoring Systems". In: *Journal of Physics: Conference Series* 570.6 (2014), pages 062002 (cit. on p. 40).

[156] Y. Sun, L. Ma, J. Mathew, W. Wang, and S. Zhang. "Mechanical systems hazard estimation using condition monitoring". In: *Mechanical Systems and Signal Processing* 20.5 (2006), pages 1189–1201 (cit. on p. 39).

[157] E. Sutrisno, H. Oh, A. S. S. Vasan, and M. Pecht. "Estimation of remaining useful life of ball bearings using data driven methodologies". In: *2012 IEEE Conference on Prognostics and Health Management*. 2012, pages 1–7 (cit. on p. 23).

[158] A. L. Sweet. "On the hazard rate of the lognormal distribution". In: *IEEE Transactions on Reliability* 39.3 (1990), pages 325–328 (cit. on p. 41).

[159] L. Tang, G. J. Kacprzynski, K. Goebel, J. Reimann, M. E. Orchard, A. Saxena, and B. Saha. "Prognostics in the control loop". In: *Proceedings of the AAAI Fall Symposium: AI for Prognostics*. Arlington, USA, 2007, pages 128–135 (cit. on pp. 26, 28).

[160] L. Tang, G. J. Kacprzynski, K. Goebel, A. Saxena, B. Saha, and G. Vachtsevanos. "Prognostics-enhanced Automated Contingency Management for advanced autonomous systems". In: *Proceedings of the International Conference on Prognostics and Health Management (PHM 2008)*. Denver, USA, 2008, pages 1–9 (cit. on pp. 15, 26).

[161] L. C. Tang and D. S. Chang. "Reliability prediction using nondestructive accelerated-degradation data: case study on power supplies". In: *IEEE Transactions on Reliability* 44.4 (1995), pages 562–566 (cit. on p. 43).

[162] D. Theilliol, P. Weber, A. Chamseddine, and Y. Zhang. “Optimization-based reliable control allocation design for over-actuated systems”. In: *Proc. 2015 International Conference on Unmanned Aircraft Systems (ICUAS)*. Denver, USA, 2015 (cit. on p. 28).

[163] J. G. Torres-Toledano and L. E. Sucar. “Bayesian Networks for reliability analysis of complex systems”. In: *Progress in Artificial Intelligence - IBERAMIA 98*. Ed. by H. Coelho. Lecture Notes in Computer Science 1484. Springer Berlin Heidelberg, 1998, pages 195–206 (cit. on p. 2).

[164] R. Toscano and P. Lyonnet. “On-Line Reliability Prediction via Dynamic Failure Rate Model”. In: *IEEE Transactions on Reliability* 57.3 (2008), pages 452–457 (cit. on p. 35).

[165] K. L. Tsui, N. Chen, Q. Zhou, Y. Hai, and W. Wang. “Prognostics and Health Management: A Review on Data Driven Approaches”. In: *Mathematical Problems in Engineering* 2015 (2015), pages e793161 (cit. on p. 18).

[166] S. Uckun, K. Goebel, and P. J. F. Lucas. “Standardizing research methods for prognostics”. In: *Proceedings of the 2008 International Conference on Prognostics and Health Management*. 2008, pages 1–10 (cit. on p. 20).

[167] R. Veillette, J. Medanic, and W. R. Perkins. “Design of reliable control systems”. In: *IEEE Transactions on Automatic Control* 37.3 (1992), pages 290–304 (cit. on p. 24).

[168] W. E. Vesely. “A time-dependent methodology for fault tree evaluation”. In: *Nuclear Engineering and Design* 13.2 (1970), pages 337–360 (cit. on p. 64).

[169] M. Vidyasagar and N. Viswanadham. “Reliable stabilization using a multi-controller configuration”. In: *Automatica* 21.5 (1985), pages 599–602 (cit. on p. 24).

[170] G. W. Vogl, B. A. Weiss, and M. Helu. “A review of diagnostic and prognostic capabilities and best practices for manufacturing”. In: *Journal of Intelligent Manufacturing* (2016), pages 1–17 (cit. on p. 18).

[171] H. Wang. “A survey of maintenance policies of deteriorating systems”. In: *European Journal of Operational Research* 139.3 (2002), pages 469–489 (cit. on p. 3).

[172] P. Wang and D. Coit. “Reliability prediction based on degradation modeling for systems with multiple degradation measures”. In: *Proceedings of the Reliability and Maintainability, Annual Symposium (RAMS 2004)*. Los Angeles, USA, 2004, pages 302–307 (cit. on p. 40).

[173] S. Wang, M. Tomovic, and J. Shi. “Integrated reliability metrics to assess fault tolerant control system”. In: *Proceedings of the IEEE International Conference on Systems,*

Man and Cybernetics (ISIC 2007). Montreal, Canada, 2007, pages 1310–1315 (cit. on p. 26).

[174] P. Weber, G. Medina, C. Simon, and B. Iung. "Overview on Bayesian networks applications for dependability, risk analysis and maintenance areas". In: *Engineering Applications of Artificial Intelligence* 25.4 (2012), pages 671–682 (cit. on p. 2).

[175] P. Weber, B. Boussaid, A. Khelassi, D. Theilliol, and C. Aubrun. "Reconfigurable control design with integration of a reference governor and reliability indicators". In: *International Journal of Applied Mathematics and Computer Science* 22.1 (2012) (cit. on pp. 26, 28).

[176] P. Weber and L. Jouffe. "Complex system reliability modelling with Dynamic Object Oriented Bayesian Networks (DOOBN)". In: *Reliability Engineering & System Safety* 91.2 (2006), pages 149–162 (cit. on p. 54).

[177] P. Weber and L. Jouffe. "Reliability modelling with dynamic Bayesian networks". In: *Proceedings of the 5th IFAC Symposium on Fault Detection, Supervision and Safety for Technical Processes (SAFEPROCESS 2003)*. Washington D.C., USA, 2003, pages 57–62 (cit. on p. 57).

[178] P. Weber, C. Simon, D. Theilliol, and V. Puig. "Fault-Tolerant Control Design for Over-Actuated System Conditioned by Reliability: A Drinking Water Network Application". In: *Proceedings of the 8th IFAC Symposium on Fault Detection, Supervision and Safety of Technical Processes (SAFEPROCESS 2012)*. Mexico City, Mexico, 2012, pages 558–563 (cit. on pp. 2, 26, 28, 58, 60).

[179] W. Weibull. "A statistical distribution function of wide applicability". In: *Journal of Applied Mechanics* 18 (1951), pages 293–297 (cit. on p. 34).

[180] N. E. Wu. "Reliability of fault tolerant control systems: Part I". In: *Proceedings of the 40th IEEE Conference on Decision and Control*. Vol. 2. Orlando, USA, 2001, pages 1460–1465 (cit. on pp. 2, 24).

[181] N. E. Wu. "Reliability of fault tolerant control systems: Part II". In: *Proceedings of the 40th IEEE Conference on Decision and Control*. Vol. 2. Orlando, USA, 2001, pages 1466–1471 (cit. on pp. 2, 24).

[182] N. E. Wu, X. Wang, M. Sampath, and G. Kott. "An operational approach to budget constrained reliability allocation". In: *Proceedings of the 15th IFAC World Congress*. Barcelona, Spain, 2002, pages 748–748 (cit. on pp. 3, 35).

[183] J. Xue and K. Yang. “Upper and lower bounds of stress-strength interference reliability with random strength-degradation”. In: *IEEE Transactions on Reliability* 46.1 (1997), pages 142–145 (cit. on p. 41).

[184] K. Yang and J. Xue. “Continuous state reliability analysis”. In: *Proceedings of the Annual Reliability and Maintainability Symposium*. Las Vegas, USA, 1996, pages 251–257 (cit. on p. 42).

[185] K. Yang and G. Yang. “Degradation Reliability Assessment Using Severe Critical Values”. In: *International Journal of Reliability, Quality and Safety Engineering* 5.01 (1998), pages 85–95 (cit. on pp. 1, 43).

[186] L. Zaccarian. “Dynamic allocation for input redundant control systems”. In: *Automatica* 45.6 (2009), pages 1431 –1438 (cit. on p. 9).

[187] Q. Zhang, C. Hua, and G. Xu. “A mixture Weibull proportional hazard model for mechanical system failure prediction utilising lifetime and monitoring data”. In: *Mechanical Systems and Signal Processing* 43.1–2 (2014), pages 103–112 (cit. on p. 39).

[188] S. Zhang and R. Ganesan. “Multivariable Trend Analysis Using Neural Networks for Intelligent Diagnostics of Rotating Machinery”. In: *Journal of Engineering for Gas Turbines and Power* 119.2 (Apr. 1997), pages 378–384 (cit. on p. 21).

[189] Y. M. Zhang and J. Jiang. “Fault tolerant control system design with explicit consideration of performance degradation”. In: *IEEE Transactions on Aerospace and Electronic Systems* 39.3 (2003), pages 838–848 (cit. on p. 2).

[190] Y. Zhang and J. Jiang. “Bibliographical review on reconfigurable fault-tolerant control systems”. In: *Annual Reviews in Control* 32.2 (2008), pages 229–252 (cit. on pp. 4, 15).

[191] M. Zuo, R. Jiang, and R. Yam. “Approaches for reliability modeling of continuous state devices”. In: *IEEE Transactions on Reliability* 48.1 (1999), pages 9–18 (cit. on p. 43).